MASTER'S THESIS 2019:08

A living room for the evaluation of multiple auditory scenes.

Nikolaos Chrysovalantis Roumpakis

Department of Civil and Environmental Engineering
Division of Applied Acoustics
CHALMERS UNIVERSITY OF TECHNOLOGY
Göteborg, Sweden 2019

A living room for the evaluation of multiple auditory scenes.

Master's Thesis 2019:08

Department of Civil and Environmental Engineering
Division of Applied Acoustics
Chalmers University of Technology
SE-41296 Göteborg
Sweden

Tel. +46-(0)31 772 1000

Reproservice / Department of Civil and Environmental Engineering
Göteborg, Sweden 2019

A living room for the evaluation of multiple auditory scenes.
Master's Thesis in the Master's programme in Sound and Vibration
Nikolaos Chrysovalantis Roumpakis
Department of Civil and Environmental Engineering
Division of Applied Acoustics
Chalmers University of Technology

Abstract

The subjective evaluation of sound, demands adequate environments where, listening tests can be carried out. As the presence of multi modal stimuli always influences the perception of sound, there are two main solutions to handle this influence in an appropriate way. External stimuli beside the auditory stimuli could be eliminated as far as possible (e.g. dark rooms) or one creates environments close to the environment of interest. During autumn 2017, the transmission lab at Applied Acoustics has been redesigned as to two listening rooms. While one of the both will be used as standard listening room, the second is intended for research that concerns people in their home environment. Therefore, it was designed to resemble a living room, in which subjects are going to be exposed to varying auditory scenes.
The MSc thesis will mainly focus in the documentation of the acoustic properties of the two laboratories, with a greater focus in the second room, relating to the intended research. In more detail, since very low frequencies will be used in order to simulate some of the auditory scenes, their acoustic properties need to be adequately documented in that region, in order for the researchers to be able to properly adjust their experiments. Moreover, the electro-acoustic equipment featured in the rooms, will be measured. For these purposes, two methods for impulse response extraction will be examined, in order to provide a first insight in the properties of the acoustic systems involved. Finally, by using these impulse responses, the reverberation times of both rooms will be estimated, as well as their behavior in the low frequency region.
Summarizing, the goal of the MSc thesis is the documentation of the aforementioned listening rooms, their featured equipment and the corresponding methodology used in the measurements.

Keywords: room acoustics, building acoustics, acoustics measurements, impulse response, listening room, loudspeakers, spectral decay, modal reverberation time.

Contents

Abstract iii

Contents v

List of Figures vii

List of Tables xi

1. Introduction 1

2. Room Acoustics Considerations. 3
- 2.1. Rooms description. 3
  - 2.1.1. Preexisting Sound Insulation Suite. 3
  - 2.1.2. Redesigned Measurement Facilities. 4
- 2.2. Estimation of the Reverberation Time. 11
  - 2.2.1. Theoretical background. 12
  - 2.2.2. Implementation. 12

3. Low Frequency Region. 17
- 3.1. Modal Analysis. 17
- 3.2. Modal Reverberation Time. 18
- 3.3. Spectral Decay. 22

4. Measurements 27
- 4.1. Impulse Response extraction of an LTI system. 27
  - 4.1.1. Theoretical background. 27
- 4.2. Measurement setup. 32
  - 4.2.1. Measurement System. 32
  - 4.2.2. IR measurements. 33
  - 4.2.3. Reduction Index. 38
  - 4.2.4. Loudspeaker Measurements. 41

5. Results and discussion. 47
- 5.1. Loudspeaker Measurements. 47
  - 5.1.1. Results 47

5.1.2. Remarks on the intended use. 58
5.2. Room characteristics in the diffuse field. 60
5.2.1. Living Room Lab. 60
5.2.2. Audio Lab. 65
5.3. Room Characteristics in the low frequency region. 68
5.3.1. Living Room Lab. 68
5.3.2. Audio Lab. 87
5.4. Reduction Index. 90

6. Conclusion. 91

Bibliography 96

Appendices 97

A. Equipment settings. 99

B. Loudspeaker mounting and serial numbers. 101

C. Measurement files. 105

List of Figures

2.1. The redesigned laboratories. 4
2.2. Intermediate wall construction between the two labs (illustrative). 6
2.3. Sound reduction index of the intermediate walls. 7
2.4. New laboratories wall design. 8
2.5. Ceiling mounted loudspeaker grid. 9
2.6. LSGU 100 silencer. 9
2.7. Reduction index of the mounted window. 10
2.8. Effect of the upper integration limit to the *Schröder* curve. 13
2.9. Magnitude and phase of a 3^{rd} -order Butterworth band-pass filter. . . . 14
2.10. Roll-off, f_0, f_1 of 3^{rd} -order Butterworth band-pass filter. 15

3.1. Lorentz function. $I = 1$,$\gamma = 0.2$,$x_0 = 0$. 20
3.2. The 34.5 Hz and 57.0 Hz mode, measured with sweep and noise signals. Solid line - measurement, dashed line - fitted Lorentzian 21
3.3. The 87.0 Hz mode of the unfurnished room and the 55.5 Hz mode, of the furnished room. Measured with logarithmic sweep. Solid line - measurement, dashed line - fitted Lorentzian. 21
3.4. Black line - Apodized rectangular window, windowed IR. Gray line - Original IR. 23
3.5. Spectral decay - Gauss window, α=3.5, T_r=0.1, R=0.6, T_d=0.2. 25
3.6. Spectral decay - Gauss window, α=10, T_r=0.01, R=0.3, T_d=0.02. 25
3.7. Spectral decay - Gauss window, α=3, T_r=0.08, R=0.6, T_d=0.08. 26
3.8. Spectral decay - Gauss window, α=3.5, T_r=0.1, R=2.6, T_d=0.2. 26

4.1. Linear sweep. Up: time signal, Down: spectrogram (frame size = 2^{15} samples, 50% overlap) 28
4.2. Logarithmic sweep. Up: time signal, Down: spectrogram (frame size = 2^{15} samples, 50% overlap) 29
4.3. Deconvolution result prior to filtering. Top: frequency response, Bottom: IR 30
4.4. Deconvolution result after filtering. Top: frequency response, Bottom: IR 31
4.5. Harmonic distortion components, pushed to the end of the signal. 32
4.6. IR measurements: Microphone and loudspeaker positions, Living room lab. 37

4.7. IR measurements: Microphone and loudspeaker positions, Audio lab. . 37
4.8. RI measurements: Microphone and loudspeaker positions in Sending and Receiving rooms. 40

5.1. TF magnitude: Genelec8020B and 8030A. 48
5.2. TF phase: Genelec8020B and 8030A. 49
5.3. Coherence γ^2: Genelec8020B and 8030A. 49
5.4. Directivity patterns for Genelec 8020B 49
5.5. Directivity patterns for Genelec 8030A 50
5.6. TF magnitude for Genelec 8020B averaged, over 21 loudspeakers. The gray area indicates the 99.9% of the measurements. 50
5.7. TF magnitude: *B&K* Type 4295. 51
5.8. TF phase: *B&K* Type 4295. 52
5.9. Coherence γ^2: *B&K* Type 4295. 52
5.10. TF magnitude: KH80DSP 1 - 3297189744, 2 - 3297191291, 3 - 3297192147. 53
5.11. TF phase: KH80DSP 3297189744, 3297191291, 3297192147. 54
5.12. Coherence γ^2: KH80DSP 3297189744, 3297191291, 3297192147. 54
5.13. Directivity patterns for Neuman.BERLIN KH 80DSP 54
5.14. TF magnitude for Neuman.Berlin KH 80 DSP, averaged over 25 loudspeakers. The gray area indicated the 99.9% of the measurements. 55
5.15. TF magnitude: Genelec 7050B, KH 805. 56
5.16. TF phase: Genelec 7050B, KH 805. 57
5.17. Coherence γ^2: Genelec 7050B, KH 805. 57
5.18. Directivity patterns for Genelec 7050B 57
5.19. Frequency response of the ceiling louspeaker setup. 58
5.20. Frequency response of the room measurement loudspeaker setup. 59
5.21. Living room lab TF magnitude. Top without furniture, bottom with furniture. 62
5.22. Living room lab TF phase. 62
5.23. Living room lab γ^2. Top without furniture, bottom with furniture. 63
5.24. Living room lab IR. 63
5.25. Living room lab RT (T_{30}) and modal decays. With and without furniture. 64
5.26. Living room lab averaged RT (T_{30}). With and without furniture. 64
5.27. Audio Lab TF magnitude. 65
5.28. Audio Lab TF phase. 66
5.29. Audio Lab γ^2. 66
5.30. Audio Lab IR. 66
5.31. Audio lab RT (T_{30}) and modal decays. 67
5.32. Audio lab averaged RT (T_{30}). 67

5.33. Living Room Lab TF magnitude. KH 805. Top without furniture, bottom with furniture. 69
5.34. Living Room Lab TF phase. KH 805. 70
5.35. Living Room Lab IR. KH 805. Top without furniture, bottom with furniture. 71
5.36. Living Room Lab spectral decays - KH 805, without furniture, Gauss window, α=3.5, T_r =0.1, R=0.6, T_d =0.2. 76
5.37. Living Room Lab spectral decays - KH 805, with furniture, Gauss window, α=3.5, T_r =0.1, R=0.6, T_d =0.2. 76
5.38. Living Room lab RT (T_{30}) and modal decays. With and without furniture. KH 805. 77
5.39. Living Room lab averaged RT (T_{30}). With and without furniture. KH 805. 77
5.40. Living Room Lab TF magnitude. Genelec 7050B. Top without furniture, bottom with furniture. 79
5.41. Living Room Lab TF phase. Genelec 7050B. 79
5.42. Living Room Lab IR. Genelec 7050B. Top without furniture, bottom with furniture. 80
5.43. Living Room Lab spectral decays - Genelec 7050B, without furniture, Gauss window, α=3.5, T_r =0.1, R=0.6, T_d =0.2. 85
5.44. Living Room Lab spectral decays - Genelec 7050B, with furniture, Gauss window, α=3.5, T_r =0.1, R=0.6, T_d =0.2. 85
5.45. Living Room lab RT (T_{30}) and modal decays. With and without furniture. Genelec 7050B. 86
5.46. Living Room lab averaged RT (T_{30}). With and without furniture. Genelec 7050B. 86
5.47. Audio Lab TF magnitude. Genelec 7050B. 87
5.48. Audio Lab TF phase. Genelec 7050B. 88
5.49. Audio Lab IR. Genelec 7050B. 88
5.50. Audio Lab spectral decays - Genelec 7050B, Gauss window, α=3.5, T_r =0.1, R=0.2, T_d =0.1. 89
5.51. Audio lab averaged RT (T_{30}). With and without furniture. Genelec 7050B. 89
5.52. Reduction index of the window-wall between the two rooms. 90

B.1. Loudspeaker grid mounted on the ceiling of the Living Room Lab. . . . 102
B.2. Living Room Lab - Control Room breakout box grouping 102

List of Tables

2.1. Room volumes - preexisting laboratories. 4
2.2. Sound reduction index of the intermediate walls. 5
2.3. LSGU silencer. Top row - single. Bottom two silencers connected in series. 9

3.1. Resonance frequencies - Rectangular room with $L_x = 4.75\,\text{m}$, $L_y = 3.72\,\text{m}$, $L_z = 3.52\,\text{m}$. 18

4.1. IR measurements: Microphone input parameters. 34
4.2. IR measurements: White noise signal parameters. 35
4.3. IR measurements: Sinus sweep signal parameters. 35
4.4. IR measurements: Microphone coordinates, Living Room Lab. 38
4.5. IR measurements: Microphone coordinates, Audio Lab. 38
4.6. RI measurements: Microphone input parameters. 39
4.7. RI measurements: White noise signal parameters. 39
4.8. RI measurements: Microphone coordinates, Receiving and Sending rooms. 41
4.9. Loudspeaker measurements under test. 42
4.10. Loudspeaker IR measurements: Microphone input parameters. 42
4.11. Loudspeaker FRF on axis: White noise signal parameters. 43
4.12. Loudspeaker FRF on axis: Sinus sweep signal parameters. 43
4.13. Loudspeaker, FRF on varying angle: Initial settings - white noise. 44
4.14. Loudspeaker FRF on varying angle: Initial settings - sinus sweep. 44
4.15. Loudspeaker FRF on varying angle: Final settings. 45

5.1. Schröeder frequency and single value of RT - Living Room Lab. 61
5.2. Modal Decays - Lorentzian fit, Living Room Lab, Neuman.BERLIN KH 805, Without furniture. 72
5.3. Modal Decays - Lorentzian fit, Living Room Lab, Neuman.BERLIN KH 805, with furniture. 73
5.4. Modal Decays - Manual estimation, Living Room Lab, Neuman.BERLIN KH 805, Without furniture. 74
5.5. Modal Decays - Manual estimation, Living Room Lab, Neuman.BERLIN KH 805, with furniture. 75
5.6. Modal Decays - Lorentzian fit, Living Room Lab, Genelec 7050B, Without furniture. 81

5.7. Modal Decays - Lorentzian fit, Living Room Lab, Genelec 7050B, With furniture. 82
5.8. Modal Decays - Manual estimation, Living Room Lab, Genelec 7050B, Without furniture. 83
5.9. Modal Decays - Manual estimation, Living Room Lab, Genelec 7050B, With furniture. 84

A.1. Loudspeaker settings: Genelec 7050B. 99
A.2. Loudspeaker settings: Genelec 8030A and 8020B. 99
A.3. Loudspeaker settings: KH 805. 100
A.4. Loudspeaker settings: KH 80 DSP. 100
A.5. Amplifier settings: B&K Type 2735 2 x 35 Watt Measurement Power Amplifier. 100

B.1. Living Room Lab - Loudpeaker numbering and breakout box channels. 101
B.2. Living Room Lab - Cable lengths. 103
B.3. Neuman.BERLIN KH 80 DSP, serial numbers and corresponding calibration files. 103
B.4. Neuman.BERLIN KH 80 DSP, serial numbers and corresponding calibration files. 104

1. Introduction

Subjective evaluation of sound, is a very important part in research relating to the quality assessment of home environments, with respect to incoming noise. Whether the background noise under test is human related noise or traffic noise, the acoustical properties of the room where the experiment is conducted, will affect the resulting stimulus presented to the subject. Therefore, apart from fulfilling certain criteria, listening rooms need to be adequately documented, reducing uncertainties related to the room's sound field, as well as to enabling researchers to better design the listening test.

The purpose of this thesis is to investigate and implement measurement techniques, in order to document and evaluate the acoustical properties of the two rooms, located at the *Division of Applied Acoustics, Department of Civil and Environmental Engineering, of Chalmers University of Technology*, built during the fall of 2018. The first of the rooms is going to be used in research relating to traffic noise as well as impact noise coming from footsteps through the ceiling. Therefore, methods for investigating the room's reverberation time in frequencies lower than the specified limit of **ISO 3382-2:2008** [24] will be entertained. Both rooms will be examined in regard to their **Impulse response** and **Reverberation time**. Furthermore, the **Impulse response and the directivity** of the electro-acoustic equipment, featured in the rooms is going to be examined, as well as the **Reduction index** of the window and wall between them.

More specifically, in **Chapter 2: Room Acoustics Considerations**, the construction of the two rooms will be presented, along with the theory and the implementation, used in the estimation of the reverberation time, in the diffuse field. **Chapter 3: Low frequency region**, will introduce the methodology used, for the characterization of the room's sound field in the frequency region bellow the *Schröder* frequency. In **Chapter 4: Measurements**, both the theoretical background and the implementation of measurement methods, relating to linear time invariant systems used are presented. The results of the aforementioned measurements will be presented and commented in **Chapter 5: Results and discussion**. **Chapter 6: Conclusion**, will summarize the most important outcomes from the previous chapters.

Finally, the information regarding the hardware settings of the related electro-acoustic equipment, can be found in **Annex A**, the serial numbers and the cabling schematics in **Annex B**, while a description on the filing system used to store the acquired data, is given in **Annex C**.

2. Room Acoustics Considerations.

This chapter is intended as an initial examination of the two rooms and the methodology that can be used in order to acquire an overview for their acoustic behavior. Firstly, the description of the room's schematics as well as the rest of it's construction features, will be examined. Subsequently, an overview of the theoretical background and methodology for the estimation of reverberation time using *Schröder*'s method [23], will be presented.

2.1. Rooms description.

The two new laboratories are constructed inside the two reverberation chambers, that where being used as the main measurement facilities of the division's sound insulation suite. Therefore, a short description of the preexisting construction is necessary for the more accurate description of the facilities.

2.1.1. Preexisting Sound Insulation Suite.

The sound insulation suite was designed by **Kihlman and Svensk Akustikplanering** in 1967 and was built according to (((ask about the standard))) in 1969. It consists of 2 pairs of adjacent reverberation chambers built on top of each other. The two chambers located on the bottom floor of the building will be referred as the *Auxiliary Measurement Facilities*, while the pair located on the top floor of the building are referred as the *Main Measurement Facilities*. The total volume and dimensions of these facilities is displayed in table 2.1 . The rooms of each pair are identical, mirrored on their connecting wall, which serves as the mounting point for the element under test. The *main measurement facilities* have a $12.6\,\mathrm{m}^2$ opening between them, where a metal frame containing the wall under test can be inserted. The *auxiliary measurement facilities*, have a $2\,\mathrm{m}^2$ opening, used for testing windows and doors. Finally, each *main measurement facility* communicates with the *auxiliary measurement facility* directly below it through a $11.2\,\mathrm{m}^2$ removable concrete slab and can be used for measuring the characteristics of various floor constitutions.

Each room is mounted on 4 sets of steel springs, with each set comprised by 8 double springs. This design is chosen, in order to avoid flanking transmission between

Facility	Volume (m^3)	Dimensions (m^3)
Main	95	$5.5 \times 4.8 \times 3.6$
Auxiliary	103	$5.5 \times 4.8 \times 3.9$

Table 2.1.: Room volumes - preexisting laboratories.

the rooms, limiting the transmission path to the element under test. The resonance frequency of the mounted room is approximately 10 Hz. Furthermore, the temperature of one of the *main* rooms can be reduced by 7 °C, in order to reduce modal coupling. The ventilation of the rooms is connected to the ordinary ventilation system of the building, but plenum chamber sound attenuators have been used, in order to reduce background noise as much as possible. The background noise level is less than 39 dBA (less than 46 dBC).

2.1.2. Redesigned Measurement Facilities.

The two new measurement facilities were created inside the *main measurement facilities* of the sound insulation suite. More specifically, the chamber closest to the division's main building, was designed for conducting listening tests for various audio stimuli and will be referred in this document as the *Audio Lab*. The other chamber was redesigned and decorated as typical living room and will serve as a listening laboratory for auralization of impact sound. This room will be referred here as the *Living Room Lab*.

(a) Living room laboratory.

(b) Audio laboratory.

Figure 2.1.: The redesigned laboratories.

Intermediate Walls.

A triple gypsum, lightweight double wall, containing mineral wool and an air gap, was build in order to separate the two laboratories, as well as each laboratory and it's

f (Hz)	R (dB)	f (Hz)	R (dB)	f (Hz)	R (dB)
50	32.2	250	62.1	1250	83.0
63	32.5	315	66.2	1600	86.5
80	35.5	400	66.1	2000	87.3
100	40.5	500	70.3	2500	76.8
125	48.1	630	73.3	3150	75.6
160	53.7	800	76.9	4000	81.8
200	57.2	1000	80.3	5000	84.7

Table 2.2.: Sound reduction index of the intermediate walls.

corresponding control room. A cross-section of the wall design is displayed in figure 2.4a. The construction, from left to right, consists of: three gypsum boards 13 mm thick, mineral wool 140 mm thick, air gap 5 mm wide and finally three gypsum boards 13 mm thick. The construction is supported by 70 mm long wooden studs, spaced by 600 mm intervals.

In the case of the intermediate wall between the two laboratories, the double wall construction was build inside a thick concrete frame, mounted on the removable steel frame of the sound insulation suite. A window was installed on the double wall construction, while the whole surface of the wall is finished with an exterior cover, for aesthetic purposes. An illustrative schematic of the concrete - metal frame, displayed in figure 2.2a, while figure 2.2b features the placement of the window, as well as the exterior wall cover. It should be noted that this schematics are relevant for both the *Living Room Lab* and the *Audio Lab*.

The sound reduction index, displayed in figure 2.3 and table 2.2 were calculated using **BASTIAN**'s database. The calculations used **SAU** with the **insulation database v 5.5** and was corrected against 30 laboratory measurements. The average error is one standard deviation (approximately 70 %). The double wall resonance is calculated at approximately 38 Hz, while the weighted sound reduction index R_w at 70 dB.

Side walls connected to the main building.

The remaining two side walls of the two rooms, were built directly on top the concrete walls, of the *Main measurement facilities* of the preexisting *Sound insulation suite*. A cross-section of the construction design can be seen in figure 2.4b. The materials shown in the figure are, from left to right: concrete, mineral wool 45 mm thick and two gypsum boards each 13 mm thick. The construction is supported by wooden studs of the same width as the mineral wool. No sound insulation calculations were conducted for this construction, since it was deemed unnecessary, due to the already high sound insulation of the preexisting building.

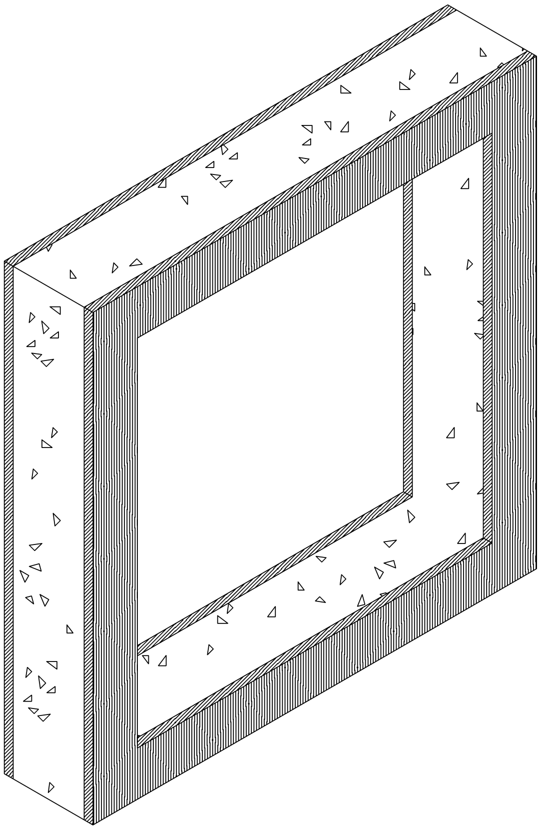

(a) Thick concrete construction, build inside the metal frame.

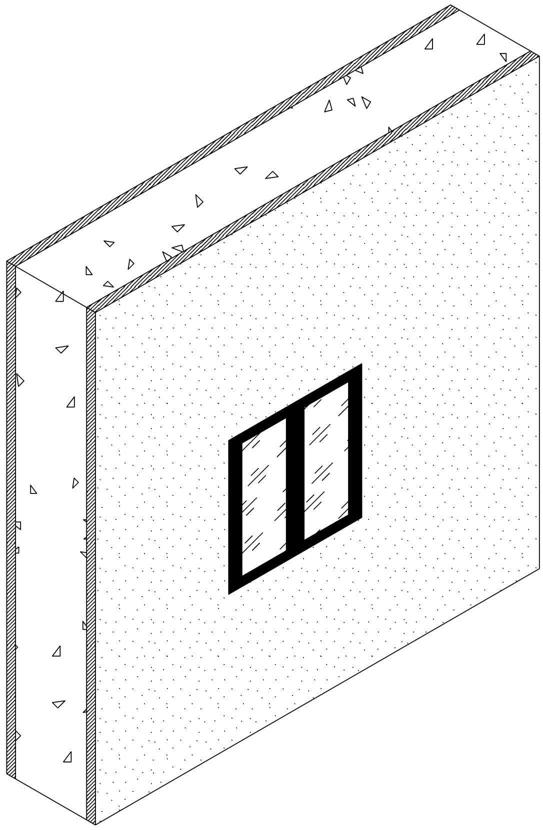

(b) Window mounting and exterior wall cover.

Figure 2.2.: Intermediate wall construction between the two labs (illustrative).

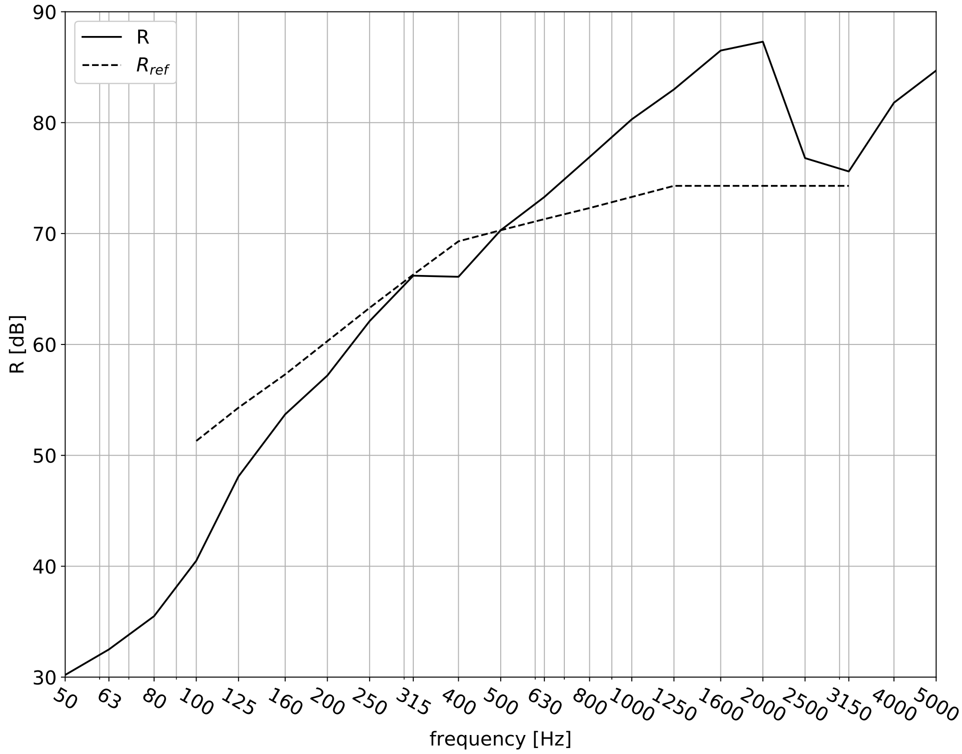

Figure 2.3.: Sound reduction index of the intermediate walls.

Ceiling and Floor - Living Room Lab.

The ceiling of the *Living Room Lab* was designed with the purpose of mounting a loudspeaker grid, that will be used to simulate the effect of impact sound on various floors. Apart from that, the ceiling height of the previous construction was reduced by placing a 0.63 m thick layer of mineral wool, on the concrete ceiling. At 0.81 m below the ceiling, an aluminum mounting construction is placed, along with a grid of twenty **Genelec 8020B** loudspeakers, four **NEUMANN KH 805** sub-woofers, as well as their connecting cables. The central axis of the sub-woofers' drivers are placed at 0.36 m below the ceiling. The grid was covered by an acoustically transparent fake ceiling, consisting of a light aluminum frames, covered with thin woven cotton fabric, with density $\rho = 0.265\,\mathrm{kg/m^2}$. Due to this design approach, the visible ceiling was lowered to a height of 2.46 m, which is similar to a typical Swedish apartment, while retaining acoustical transparency, due to the low density of the fabric.

The floor of the laboratory, is a floating floor construction, where a 3 mm elastic layer

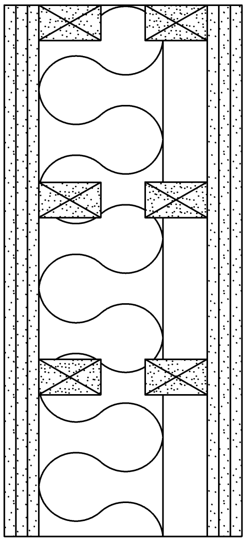

(a) Intermediate walls.

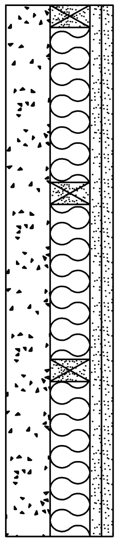

(b) Main building walls.

Figure 2.4.: New laboratories wall design.

is mounted directly on the concrete floor, of the preexisting construction. A wooden floor, with a thickness of 12 mm, is in turn placed on top of the elastic layer.

Ceiling and Floor - Audio Lab.

The ceiling of the *Audio Lab* consists of an approximately 1 m thick mineral wool layer, mounted directly on the concrete ceiling of the *Sound Insulation Suite*. A typical office fake ceiling is placed directly below. This construction effectively lowers the ceiling height to 2.6 m. A thick carpet is glued directly on the concrete floor, covering the entire area of the laboratory.

Ventilation.

In the preexisting ventilation system, fresh air was entering the room, through one of the floor corners of each of the new laboratories, while the air would exit the facility through one of the ceiling corners of the current control rooms. Due to the construction of the control rooms, this path was obstructed. Therefore, a new ventilation duct was installed, connecting each laboratory with it's control room. Two **LSGU 100** silencers in series, were placed on the top corner of the intermediate wall between each laboratory and it's control room, closer to the intermediate wall between the two labs. The length of the silencers, extended inside the laboratories, through the mineral wool on the ceiling. The dumping achieved from this duct is displayed in table 2.3. The first row in the table refers to a single silencer, while the second row refers to the two silencers in

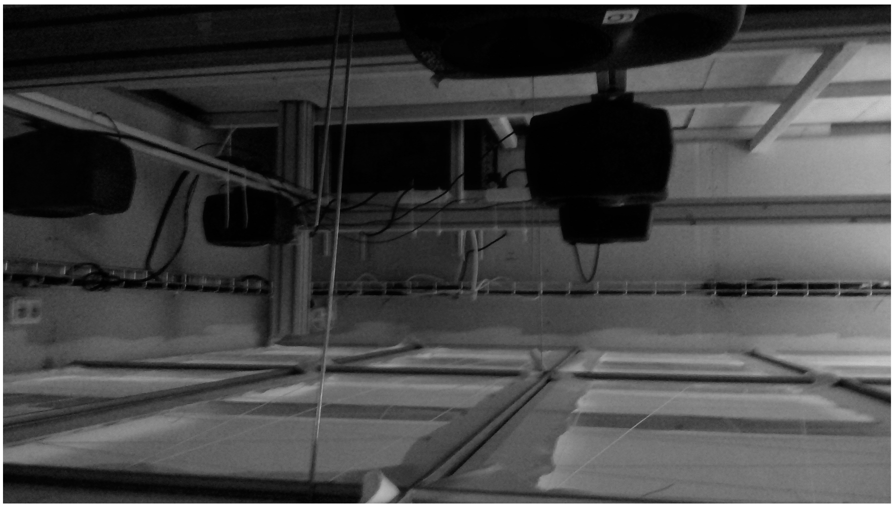

Figure 2.5.: Ceiling mounted loudspeaker grid.

$\varnothing\ d_{1nom}$ (mm)	I_{nom} (mm)	63	125	250	500	1k	2k	4k	8k	$\varnothing\ d_y$ (mm)	m (kg)
100	900	10	26	36	48	50	50	48	26	410	14.1
100	1800	20	52	72	96	100	100	96	52	410	26.2

Table 2.3.: LSGU silencer. Top row - single. Bottom two silencers connected in series.

series, used in the laboratory. The size specifications of each silencer is shown in figure 2.6.

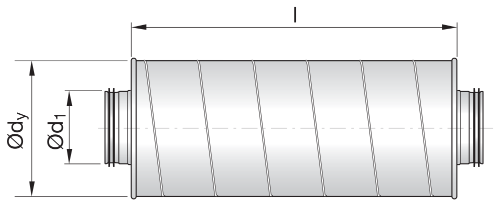

Figure 2.6.: LSGU 100 silencer.

Intermediate window.

The intermediate wall between the two laboratories, features an aluminum double glass window. The window is mounted on the gypsum double wall construction and has a weighted reduction index R_w of 38 dB, as provided by the manufacturer. The sound reduction data of the window are displayed in figure 2.7.

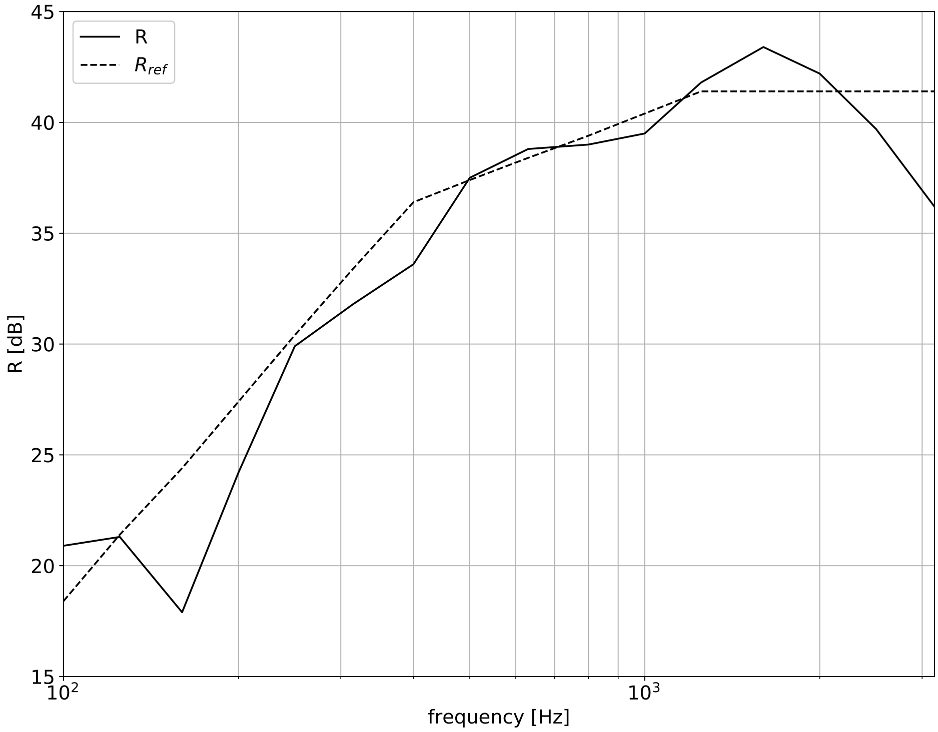

Figure 2.7.: Reduction index of the mounted window.

2.2. Estimation of the Reverberation Time.

Reverberation time is one of the most important and defining room characteristics in room acoustics. In relation with the volume of a room, RT can provide a rough estimate, as to how well the room is able to fulfill it's purpose. Unfortunately, a room as an acoustical system is far from simple, therefore the estimation of such an important parameter requires, extra care in terms of the limitations and assumptions taken into account.

According to theory, stopping the excitation of a room that has reached steady state conditions, the sound pressure level will decay exponentially until it reaches the background noise level. This applies in rectangular rooms consisting entirely of reflective surfaces and for frequencies above the room's *Schröder* frequency f_{sch}, given by:

$$f_{sch} = 2000 \cdot \sqrt{\frac{RT}{V}} Hz \tag{2.1}$$

In this region sound field is considered diffuse and the effect of individual modes is not visible in the decay. In this case and according to **ISO 3382-2:2008** [24], the RT can be calculated by:

$$RT = -\frac{60}{b} \tag{2.2}$$

where b corresponds to the slope of a line $L = b \cdot t + a$, fitted to the decay function, by means of a linear regression. This line is evaluated at 5 dB and at 25, 35 or 65 dB, below the steady state level, for the T_{20}, T_{30} and T_{60} estimations respectively. In the ideal, case described above the room's response will decay exponentially and therefore, the slope of the fitted line will be the same regardless the points chosen for the evaluation. Therefore, the following relation applies:

$$RT \approx T_{25} \approx T_{30} \approx T_{60} \tag{2.3}$$

The rooms under test, although fairly rectangular, have significantly higher absorption than the room described above and the measurement process unavoidably introduces a noise floor. As such the RT can differ, especially at the lower frequencies, depending on the dynamic range used for the evaluation of the linear regression. This should be taken into account when choosing the appropriate dynamic range. Finally, as stated in the standard, the second point used in the linear regression should be 5 dB above the noise floor, making the dynamic range required for the estimation of T_{20}, T_{30} and T_{60}, 30, 40 and 70 dB respectively.

The two methods for achieving the above, as described in the standard, are the **Interrupted noise** method and the **integrated impulse response** method. The later proved more suitable for the task at hand, for two main reasons. Firstly, impulse response measurements of the room were already available from the estimation of the modal reverberation time discussed in chapter 3. Lastly, this method does not require averaging over the same measurement position, in order to minimize the error introduced by the interrupted noise method, thus significantly decreasing the time required in the measurement process.

2.2.1. Theoretical background.

The estimation of reverberation time by means of the integrated impulse response was firstly introduced by *Schröder* in [23], while more information on the method can be found in chapter 8 in the book *Room Acoustics* from *Heinrich Kuttruff* [17]. As shown by *Schröder*, the following relation can be established between a room's squared impulse $r^2(x)$ response and the ensemble average of decaying noise in it $\langle s^2(t) \rangle$:

$$\langle s^2(t) \rangle = \int_t^\infty r^2(x) dx \tag{2.4}$$

The above relation allows for the estimation of an average of any possible decay curve produced by the room, by performing only one impulse response measurement. It is due to this fact, that the main advantage of this method is realized, providing with increased accuracy, by omitting errors introduced by random factors in the measured signal, such as background noise, without the need for averaging.

The most prominent practical limitation, comes from the fact that equation (2.4) involves an integral ranging form the time the excitation stops, to infinity. In reality, background noise is always present and therefore the integration needs to be calculated until $r^2(x)$ reaches the background noise level. Choosing an appropriate upper limit for the integration is very important, as failing to do so can result in integrating over background noise which can lead to erroneous slopes produced by the linear regression. This can be seen in figure 2.8, where the time limit for the integration has been set to $\tau_1 = 0.95$, $\tau_2 = 2.07$ and τ_3 0.51 s. In the case of τ_2 a lot of noise is included in the integration, while in the case of τ_3 the decay curve is cut abruptly.

2.2.2. Implementation.

Reverberation times were calculated using the rooms' impulse responses, the measurement details of which can be found in section 4.2.2. It should be noted that the measurements were conducted according the requirements specified in **ISO 3382-2:2008** [24] apart from section 4.3 "Measurement positions". This deviation was due to the fact that this document focuses mostly at the low frequency behavior of the rooms and therefore the positioning of the loudspeaker used for excitation, as well as the microphones in the corners of the room, as described in section 4.2 was preferable.

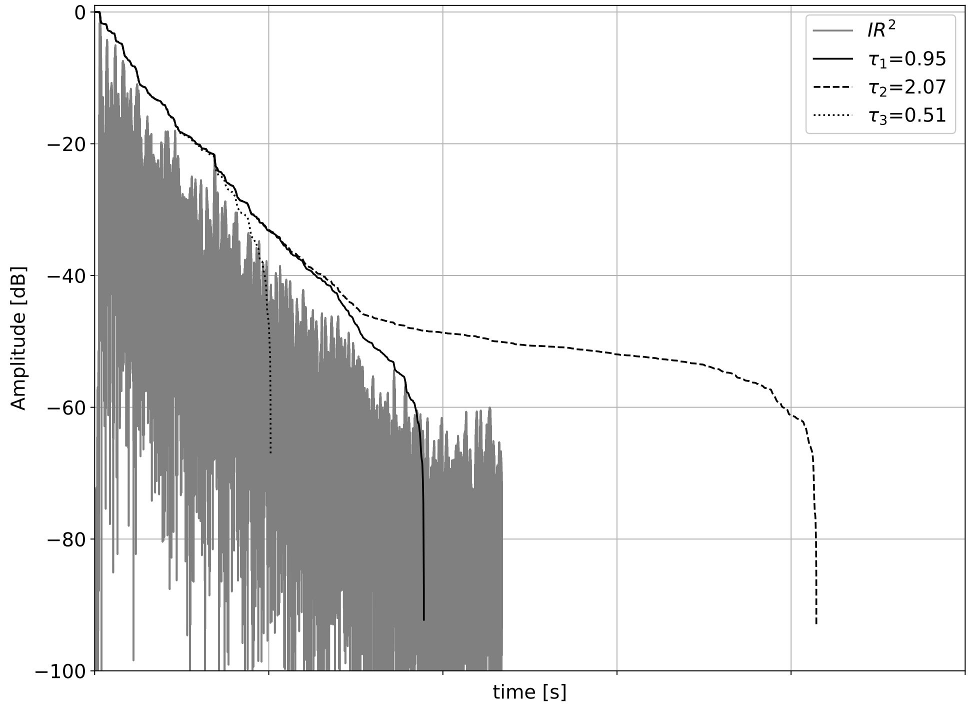

Figure 2.8.: Effect of the upper integration limit to the *Schröder* curve.

The calculations were carried out by the room acoustics module of the **nidaqmx-Aio** [21] measurement system, that uses the *Python* modules *Scipy* and *Numpy*, for calculating integrals, linear regressions and filter design. The project is hosted at the *Division of Applied Acoustics github* page and was developed for the purposes of this document. The procedure followed by the algorithm is presented in the steps bellow.

Filter bank.

Firstly, the measured IR is passed through a filter bank consisting of band-pass filters whose critical frequencies are calculated as:

$$f_0 = f_c * 2^{-\frac{1}{2*n}} \quad (2.5) \qquad f_1 = f_c * 2^{\frac{1}{2*n}} \quad (2.6)$$

where f_c corresponds to the center frequency of each of the octave or third-octave bands, as specified in *IEC 61260:1995* [3] . The bandwidth is determined by the factor n. This will result into a series of band limited impulse responses, each representing the room's behavior in the corresponding frequency band.

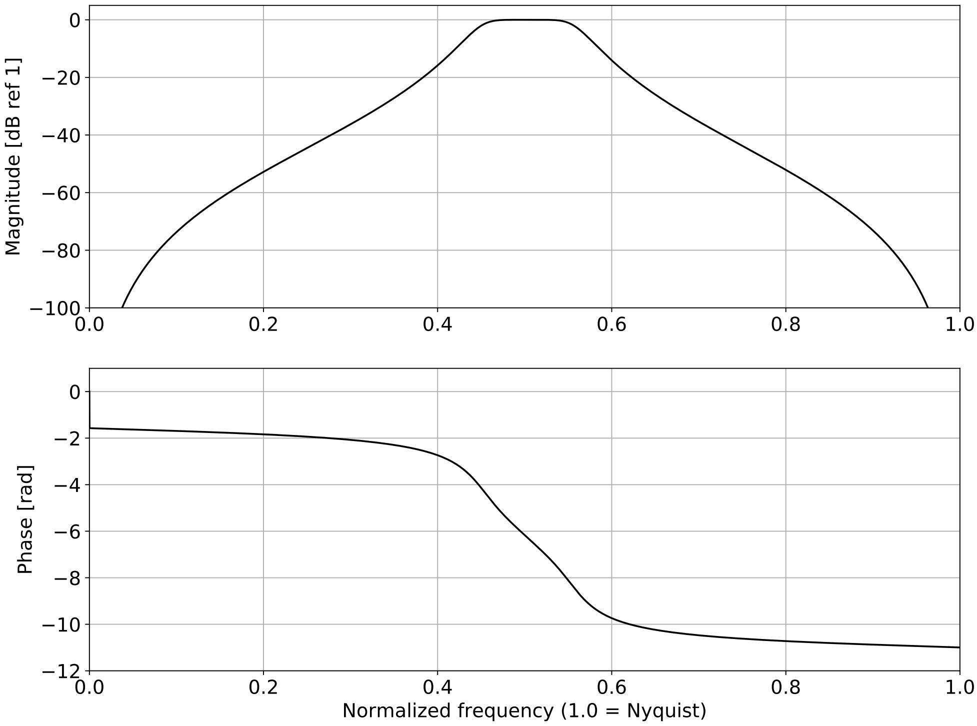

Figure 2.9.: Magnitude and phase of a 3^{rd} -order Butterworth band-pass filter.

Each individual filter is a $3^{rd}-$ order Butterworth, designed using the second order sections (sos) method. The magnitude and phase of the filter's transfer function are displayed in figure 2.9, for a 3^{rd}-octave band centered around one quarter of the sampling frequency. The x axes are being presented in normalized frequencies, with the point $f_{nyq} = 1.0$ representing the *Nyquist* frequency.

The 3^{rd}-order filters were able adequately separate the relevant information in each frequency band, while minimizing the additional delay introduced in the measurement chain by the inclusion of the filters.

This filter design was chosen because it provides the flattest possible frequency response in the pass band, while it's attenuation at the roll-off region starts at -46 dB/Octave, immediately after the cutoff frequencies f_0, f_1, transitioning to a linear attenuation of -18 dB/Octave starting around $f = 0.1$, maintaining this slope until infinity. The above features are displayed in figure 2.10.

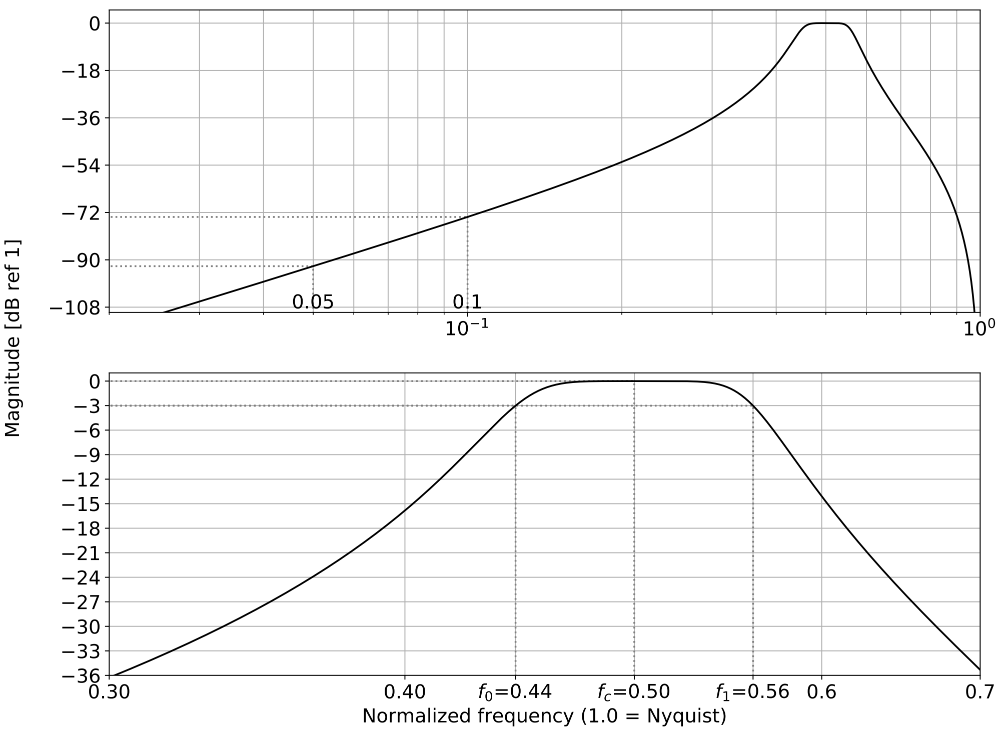

Figure 2.10.: Roll-off, f_0, f_1 of 3^{rd} -order Butterworth band-pass filter.

Calculation of RT in frequency bands.

Once the band limited IRs have been extracted, the method described in section 2.2.1 can followed, in order to calculate the integrated IR. The integration limit τ needs to be set manually for each individual frequency band, as the time where the level of the IR becomes equal to the noise level.

The resulting curves need to be converted into levels, relevant to the steady state level. Therefore, the maximum value of the signal is used as reference. As a result the integrated **IR** will always start at 0 dB, as shown in figure 2.8. This can be achieved by using:

$$Level_{norm} = 10 * \log_{10}\left(\frac{h^2(n)}{max(h^2(n))}\right) \tag{2.7}$$

where $h^2(n)$ represents the band limited squared **IR** at sample n.

Following the method described in Annex C of **ISO 3382-2** [24], three lines are fitted to the section of the integrated **IR** that lies between -5 and -25, -35, -65 dB. Finally, slopes b of the aforementioned lines can be used with equation (2.2), in order for the estimators T_{20}, T_{30} and T_{60}, to be calculated.

3. Low Frequency Region.

In large rooms, the *Schröder* frequency can be quite low, making the reverberation time, as described in chapter 2, an adequate measure for describing the decay of the sound field. Unfortunately, in small rectangular rooms, such as the two labs under test, the *Schröder* frequency can be around 350 HZ. Below that region the modal density is too small and the varying modal decays make the results of the method presented in section 2.2.1, inaccurate. In the region below the f_{Schr}, the decay of the sound field, would better be described in terms of individual modes, rather than frequency bands.

In this chapter a theoretical estimation of the modes occurring in a rectangular room, will be presented as well as a methodology for estimating the modal decays and viewing the time-frequency response of a room, using measured room impulse responses.

3.1. Modal Analysis.

Prior to measuring the sound field of a room, in the low frequency region, a theoretical calculation of the expected modes needs to be conducted. This will serve as a reference when relating a peak in the frequency response function, with a mode of the room. As presented in section 2.1, the two side walls and the floor of the laboratory, are built on top of a concrete construction and due to their design, can be considered as rigid boundaries. The rest of the boundaries are not rigid, but for the purpose of these calculations will be considered as such, since the correction for non-rigid boundaries as presented in chapter 3.3 of *Kuttruff* [17], would require the measurement of the damping factor ζ, and the correction it would provide, would not greatly affect the center frequency of the mode. As presented in chapter 3 of [17], using this approximation the *Helmholtz* equation can be separated into three ordinary differential equations such as

$$\frac{d^2 p_i}{di^2} + k_i^2 p_i = 0, \text{ where } i = x, y, z \tag{3.1}$$

and can be solved using the boundary conditions:

$$\frac{dp_i}{di} = 0, \text{ for } i = 0 \text{ and } i = L_i \tag{3.2}$$

the above will result into the following equation for calculating the frequency of a mode in a small rectangular room.

$$f_{n_x,n_y,n_z} = \frac{c}{2}\left[\left(\frac{n_x}{L_x}\right)^2 + \left(\frac{n_y}{L_y}\right)^2 + \left(\frac{n_z}{L_z}\right)^2\right]^{1/2} \tag{3.3}$$

The frequency of a room resonance, can then be calculated by substituting the dimensions L_x, L_x, L_x of the room in equation (3.3). The initial fifteen resonance frequencies of a rectangular room, with rigid walls and the same size as the *Living Room Lab*, are displayed in table 3.1. The dimensions of the room are L_x = 4.75 m, L_y = 3.72 m, L_z = 3.52 m.

mode	n_x	n_y	n_z	f_{xyz} (Hz)
1	1	0	0	36.5
2	0	1	0	46.0
3	0	0	1	48.7
4	1	1	0	58.5
5	1	0	1	60.6
6	0	1	1	67.0
7	2	0	0	72.1
8	1	1	1	76.1
9	2	1	0	85.5
10	2	0	1	87.0
11	0	2	0	92.0
12	0	0	2	97.4
13	2	1	1	98.4
14	1	2	0	98.9
15	1	0	2	103.9

Table 3.1.: Resonance frequencies - Rectangular room with L_x = 4.75 m, L_y = 3.72 m, L_z = 3.52 m.

3.2. Modal Reverberation Time.

When excitation is interrupted in a room, after having reached steady state conditions, the decay of the squared sound pressure, of a mode n will be related to it's damping constant δ_n as:

$$p^2(t) = p^2(0) \cdot e^{(-2\delta_n t)} \tag{3.4}$$

as the room is considered an linear time invariant system, the damping constant δ_n can be related with the quality factor Q of the system as:

$$Q = \frac{\omega_n}{2\delta_n} \tag{3.5}$$

while as described in chapter 2 of *Kuttruff* [17], Q is reciprocal to the relative 'half-width' $\Delta\omega/\omega_n$, which represents the bandwidth where pressure of the resonance has decreased by $\sqrt{2}$, divided by it's angular frequency. This pressure decrease corresponds to a -3 dB drop. Using the two previous relations the damping constant can be expressed in terms of the half bandwidth, using:

$$\Delta f_{-3dB} = \frac{\delta_n}{\pi} \tag{3.6}$$

Finally, by defining the modal reverberation time, as the time the pressure of a mode needs to decrease by 60 dB and by using equations (3.4),(3.6), the reverberation time of the mode T_n can be calculated by:

$$T_n = \frac{2.2}{\Delta f_{-3dB}}. \tag{3.7}$$

The calculation of the modal reverberation time using equation (3.7) is referred as the *indirect method* in [22], due to the fact that a frequency response of the room is needed, prior to it's calculation. Since the measurement techniques applied for obtaining said *FRF*s, result into a discrete function and taking into account that the fixed frequency resolution used, can provide limited measured values of the mode, additional measures should be taken, in order to increase the accuracy of the results. As suggested by the paper [22], a *Lorentzian* function can be fitted to each of the modes in question, by minimizing the normalized residual sum of squares.

The *Lorentzian* function, also called the *standard Cauchy distribution* is defined by:

$$f_{x_o,\gamma,I}(x) = I\left[\frac{\gamma^2}{(x-x_0)^2+\gamma^2}\right] \tag{3.8}$$

where I corresponds to the maximum value, located at x_0 and γ is the scale parameter. The shape of this function with $I = 1$, $\gamma = 0.2$ and $x_0 = 0$ is presented in figure 3.1. The scale parameter γ, if doubled, is equal to the width of the curve when the function is at half it's maximum value. This practically means that, $\Delta f_{-3dB} = 2 \cdot \gamma$, since the *FRF* and the corresponding *Lorentzian* fit are going to be presented in levels.

The authors of this method suggested the use of frequency responses measured using sweep signals, as a reference for the method. This was due to the fact that sweep signals provided with a more smooth result, that would allow for a more accurate fit of the *Lorentzian* function. As shown in figures 3.2a and 3.2b, the sweep measurement produces only a slightly smoother result, and the *Lorentzian* function is fitted quite well to both curves, for the 34.5 Hz mode. On the other hand, the 57.0 Hz mode is substantially more smooth when measured with a logarithmic sweep, as shown in figures 3.2c and 3.2d. This comes from the fact that using a sinus sweep signal, the signal to noise ratio is quite higher, providing with a better defined result. The 34.5 Hz mode is well defined for both signals due the fact that it has much more energy than the rest of the modes. As a result and in compliance with the authors of [22], the frequency response functions measured with logarithmic sinus sweep signals will be used as a reference for the estimation of the modal reverberation time, using this method.

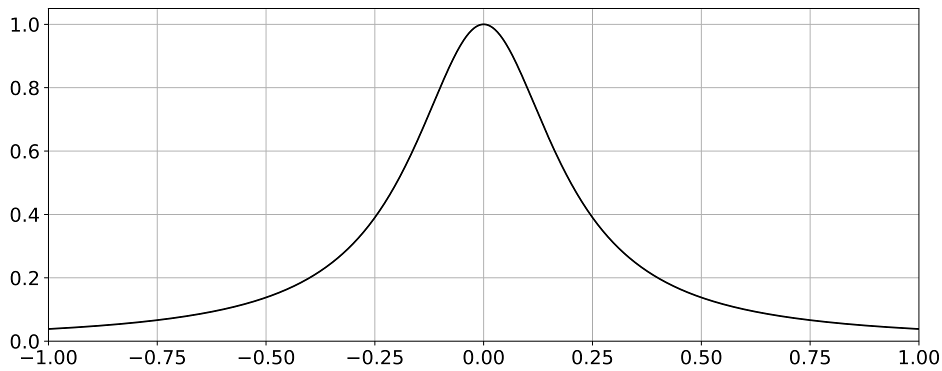

Figure 3.1.: Lorentz function. $I = 1, \gamma = 0.2, x_0 = 0$.

As described in [22], the above method is best deployed in rooms with low absorption. In the case that the room has significant damping due to furniture or other absorptive surfaces, the modal overlapping will increase and the *Lorentzian* fit will not be sufficient for the estimation of the half-widths. By comparing figures 3.2c and 3.3b, it's possible to see that the *Lorentzian* can be fitted adequately to the 2^{nd} mode and though the resonance has moved to the lower frequencies, it's still possible to produce an accurate value of the modal reverberation time. On the other hand, the 3^{rd} mode of the unfurnished room depicted in figure 3.3a, produces an asymmetrical shape, making the use of the half-bandwidth, for determining the modal reverberation time, ambiguous.

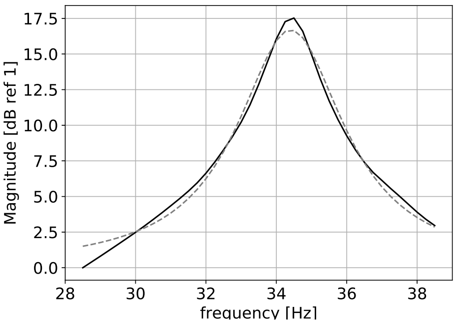

(a) Logarithmic sweep signal - 34.5 Hz

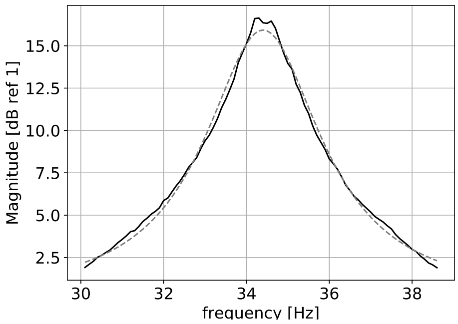

(b) White noise signal - 34.5 Hz

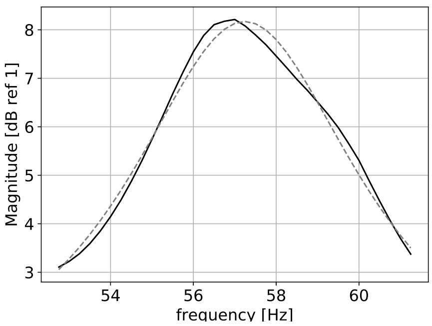

(c) Logarithmic sweep signal - 57.0 Hz

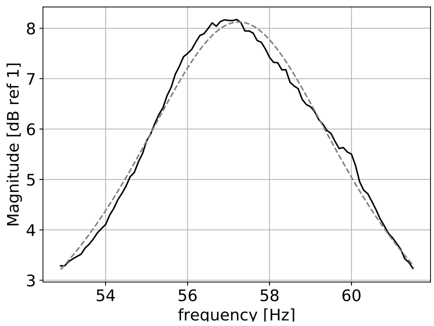

(d) White noise signal - 57.0 Hz

Figure 3.2.: The 34.5 Hz and 57.0 Hz mode, measured with sweep and noise signals. Solid line - measurement, dashed line - fitted Lorentzian

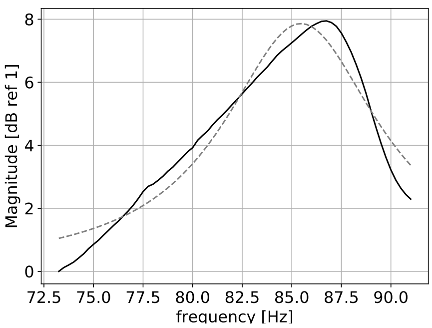

(a) No furniture - 87.0 Hz

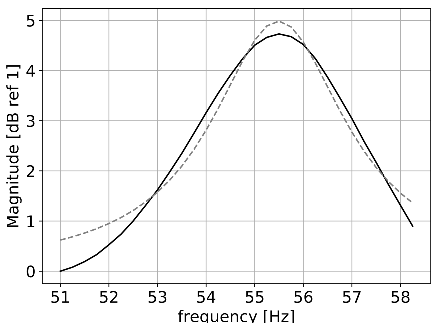

(b) With furniture - 55.5 Hz

Figure 3.3.: The 87.0 Hz mode of the unfurnished room and the 55.5 Hz mode, of the furnished room. Measured with logarithmic sweep. Solid line - measurement, dashed line - fitted Lorentzian.

3.3. Spectral Decay.

Further insight into the behavior of small rooms, as well as other linear time invariant systems, can be given by examining their decaying spectra, using waterfall plots. While this method has significant limitations, due to the relation between the time and the frequency resolution, an intuitive inspection of the simultaneous decay of the modes can be had, using this presentation, due to the low modal density of the room at low frequencies. From the variety of ways, that such a plot can be produced from, the extraction through the room's IR will be used here, for consistency between the rest of the methods used to describe the sound field.

The extraction of the spectral decay $S_\tau(\omega)$, from an impulse response $h(t)$, can be achieved by calculating the *Fourier* transform of the product of $h(t)$, with a window w. This can be written in the form of a mathematical expression as:

$$S_\tau(\omega) = \int_{-\infty}^{\infty} h(t)w(t-\tau)e^{-j\omega t}dt \tag{3.9}$$

As shown in equation (3.9), the window w can moved by a time step of τ, creating a series of spectrum slices each representing the frequency content of $h(t)$, after τ seconds has passed. The length and the type of the window used, is crucial for correctly detecting the modes of the room.

The simplest window that can be used for this purpose is a rectangular window, that is zero everywhere except for a flat portion of R seconds, where it has the value one. This window creates a discontinuity to the signal, by abruptly changing from zero to one. This discontinuity introduces a lot of noise especially on the higher frequencies, covering much of the details of the decaying modes. A method of resolving this is suggested in [2], which uses a special formulation of rectangular windows, called *"apodization"*. This method employs a set of functions with varying rise and decay times, to remove the discontinuity introduced by the rectangular window. The resulting apodized window, for each time step τ, can be defined by four time values namely t_0, t_1, t_2, t_3 as well as the rise time T_r, the flat portion R and the decay time T_d as:

$$w(t) = \begin{cases} 0, & t < t_0, \quad t_0 = \tau \\ f(t), & t_0 \leq t \leq t_1, \quad t_1 = t_0 + T_r \\ 1, & t_1 < t < t_2, \quad t_2 = t_1 + R \\ f(T_r + R + T_d - t), & t_2 < t < t_3, \quad t_3 = t_2 + T_d \\ 0, & t > t_3 \end{cases} \tag{3.10}$$

where the function $f(t)$ can be any of the functions presented in the appendix A2 of [2]. The functions are presented in analytical form and while this makes their implementation significantly simpler, it also affixes their rise or decay time to a specific value. Therefore, if a longer decay time is needed the function needs to be normalized with it's maximum value, in order to result to the value of one, at it's peak. This is not the case for the *Gaussian* apodized window. This window works similarly to a *Bessel* filter whose order can be increased by increasing the value of α in:

$$f_T(t) = \frac{\rho\left(\alpha\left(\frac{2t-T}{T}\right)\right) - \rho(-\alpha)}{\rho(\alpha) - \rho(-a)} \tag{3.11}$$

resulting to a steeper slope and reducing the rise or decay time. The function $\rho(x)$ is given by:

$$\rho(x) = \frac{1}{(2\pi)^{1/2}} \int_{-\inf}^{x} e^{-t^2/2} dt \tag{3.12}$$

and can be easily implemented digitally, by modern software. An apodized rectangular window featuring a *Gaussian* function with $\alpha = 3.5$, T_r = 0.1 s, T_d = 0.2 s and R = 0.6 s is displayed in figure 3.4.

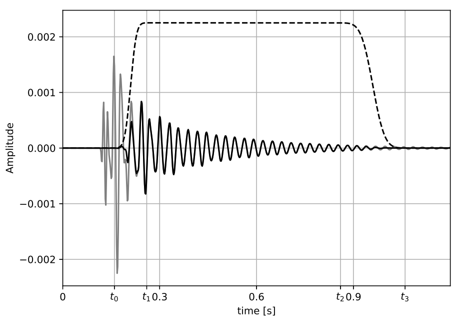

(a) Correct window, T_r=0.1, R=0.6, T_d=0.2.

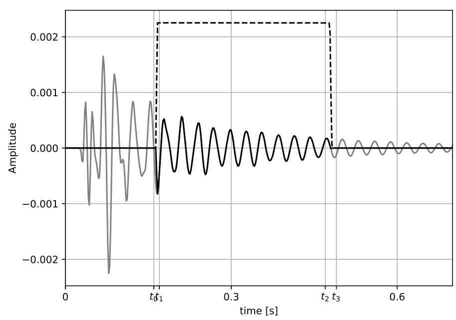

(b) Short window, T_r=0.01, R=0.3, T_d=0.02

Figure 3.4.: Black line - Apodized rectangular window, windowed IR. Gray line - Original IR.

Apart form the appropriate apodization function, choosing the correct T_r, T_d and R play a crucial part. A too short window will not be able to detect the behavior of the system in the very low frequencies, while a short rise and decay time will decrease the resulting signal to noise ratio, especially in the higher frequencies. Such a window is displayed in figure 3.4b, while the resulting waterfall plot is shown in figure 3.6. A too long rise and decay time will result to smoothing the spectral decays to much and therefore exclude important information from the result. This behavior can be observed in figure 3.7, where the waterfall plot was created using a *Gaussian* window of α=3, T_r, T_d=0.8 s and R=0.8 s. Finally, the waterfall featured in figure 3.8, was created using the same window displayed in figure 3.4a, but with a much larger value for R, at 2.6 s. By comparing figure 3.5 with 3.8, it's possible to see that using a very long window, results into including an unnecessarily long part of the IR into the calculation, which in turn, creates the undesired effect of reducing the signal to noise ratio.

The implementation of the method poses a few challenges, related to hardware restrictions. Although the calculation of the windows is quite simple for the present computers, displaying a waterfall plot, that has a very large resolution in both time and frequency, can be very demanding in terms of memory. Two main steps can be taken in the implementation of the method, in order to address this issue. Usually, a room's IR will contain all the information relating to the behavior of the room in it's first seconds, followed by a few seconds where the IR falls bellow the noise floor. In this case, it is safe to window and plot only the first part of the IR, without sacrificing any important information. Another way to reduce computational demand, is by re-sampling the IR to a sampling frequency that is at least two times larger than the highest frequency of interest.

The re-sampling method used here, is the *resample* function from *scipy.signal* module, that employs the *Fourier* method. In this method the *Fourier* transform is employed in order to acquire the signal's frequency response, before removing a number of frequency bins and finally reverting back to the time domain using the inverse *Fourier* transform. Removing frequency bins from the signal will remove energy from it, which needs to be compensated for. This can be done by multiplying the resulting frequency response by a factor b_{scale} given by:

$$b_{scale} = \frac{f_{s,target}}{f_{s,original}} \tag{3.13}$$

In conclusion, while this method can provide significant insight about the behavior of small rooms, the computational cost significantly limits either the frequency or the time resolution. While this limitation is easy to overcome in the low frequency region it's almost impossible for higher frequencies, where a high sampling frequency is required. Apart from the computational limitations, ordinary small rooms are usually very damped in the higher frequencies while the modal density increases substantially. Therefore, in that region the modes decay very fast and are quite close to each other, making their detection require a substantial and simultaneous increase in both time and frequency resolution.

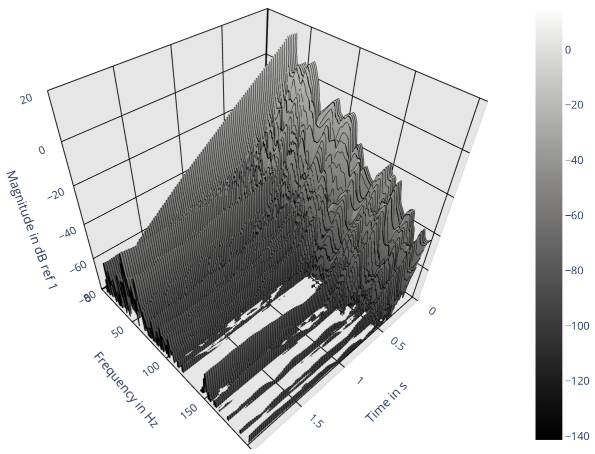

Figure 3.5.: Spectral decay - Gauss window, α=3.5, T_r=0.1, R=0.6, T_d=0.2.

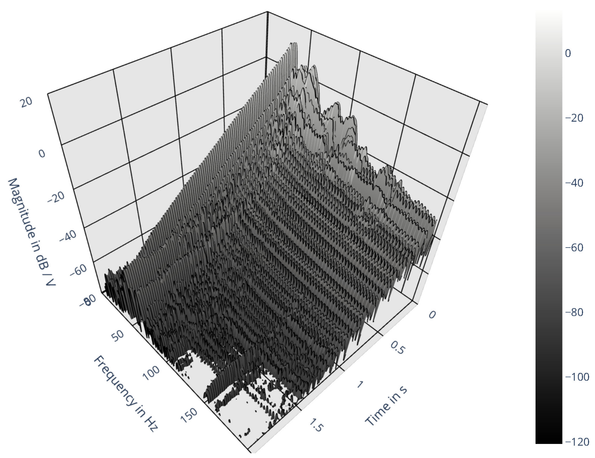

Figure 3.6.: Spectral decay - Gauss window, α=10, T_r=0.01, R=0.3, T_d=0.02.

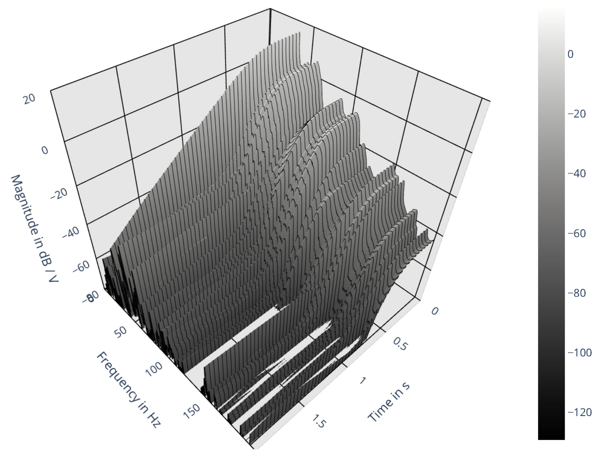

Figure 3.7.: Spectral decay - Gauss window, α=3, T_r=0.08, R=0.6, T_d=0.08.

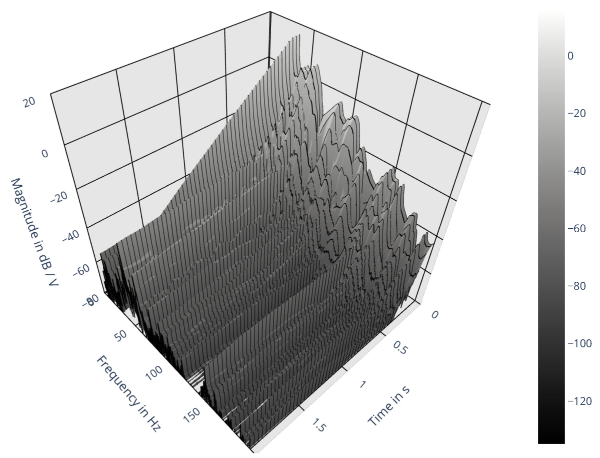

Figure 3.8.: Spectral decay - Gauss window, α=3.5, T_r=0.1, R=2.6, T_d=0.2.

4. Measurements

4.1. Impulse Response extraction of an LTI system.

4.1.1. Theoretical background.

For the purpose of validating the results of the measurement system, two different excitation signals were used, for the IR extraction. Firstly, the systems were measured using noise signals and secondly using logarithmically increasing sinusoidal sweep signals.

In order to eliminate the delay introduced by the audio interface, the excitation signal was recorded directly from the sound card's output, which will be referred here as the *reference channel*, noted with x. Likewise, the channel for the recording microphone will be referred to as the *input channel*.

IR extraction using noise signals.

The extraction of IRs, using noise signals, was conducted using the H1 estimator, by first calculating the Transfer Function (TF) of the system and then converting it to the Impulse Response function (IR), by means of the inverse *Fourier Transform* (ifft). The procedure followed for the calculation of the H1 estimator can be found in the *SVM lab 4 instructions* document [1].

IR extraction using sinus sweep signals.

The time signal of a linear increasing sinusoidal sweep is given by:

$$s(t) = A \sin\left[\phi_0 + 2\pi\left(f_0 t + \frac{k}{2}t^2\right)\right] \tag{4.1}$$

where f_0 corresponds to the frequency at $t = 0$ and k to the rate of frequency change, given by:

$$k = \frac{f_1 - f_0}{T} \tag{4.2}$$

where T is the length of the sweep in seconds and f_1 the instantaneous frequency, when the sweep is completed. The instantaneous frequency of the signal as a function of time can be calculated by:

$$f(t) = f_0 + kt \tag{4.3}$$

A linear sinus sweep ranging from 20 Hz to 2 kHz can be seen in figure 4.1.

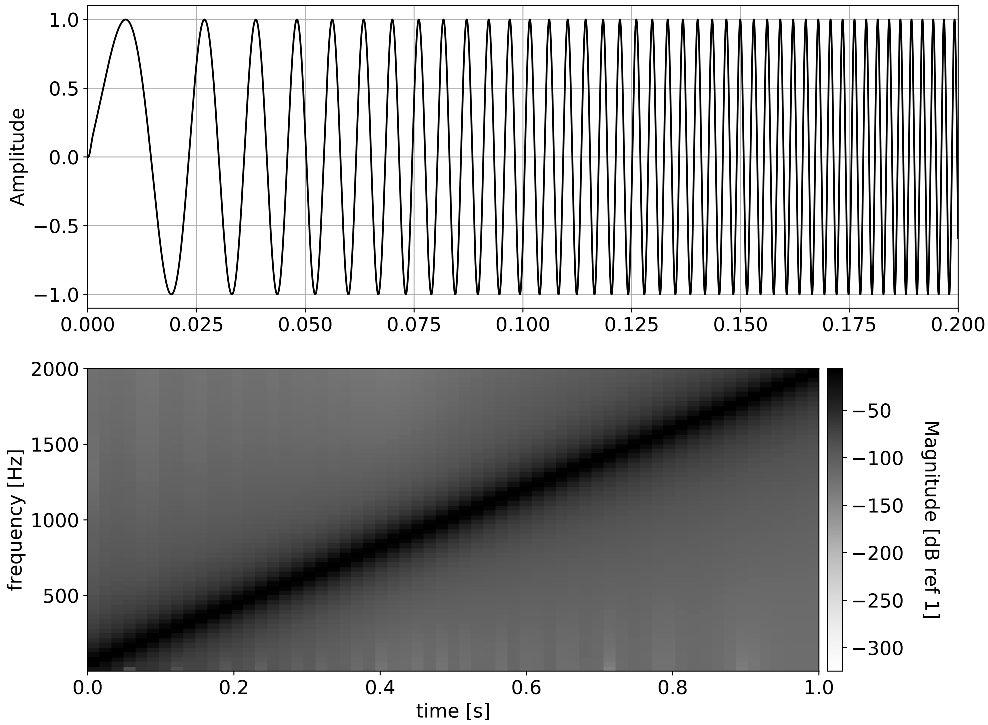

Figure 4.1.: Linear sweep. Up: time signal, Down: spectrogram (frame size = 2^{15} samples, 50% overlap)

Similarly the time signal of a logarithmically increasing sinusoidal sweep is given by:

$$s(t) = \sin\left[\phi_0 + 2\pi f_0 \left(\frac{k^{(t)} - 1}{\ln(k)}\right)\right] \tag{4.4}$$

where the rate of frequency change k corresponds to:

$$k = \left(\frac{f_1}{f_0}\right)^{\frac{1}{T}} \tag{4.5}$$

and the instantaneous frequency as a function of time is given by:

$$f(t) = f_0 k^t \tag{4.6}$$

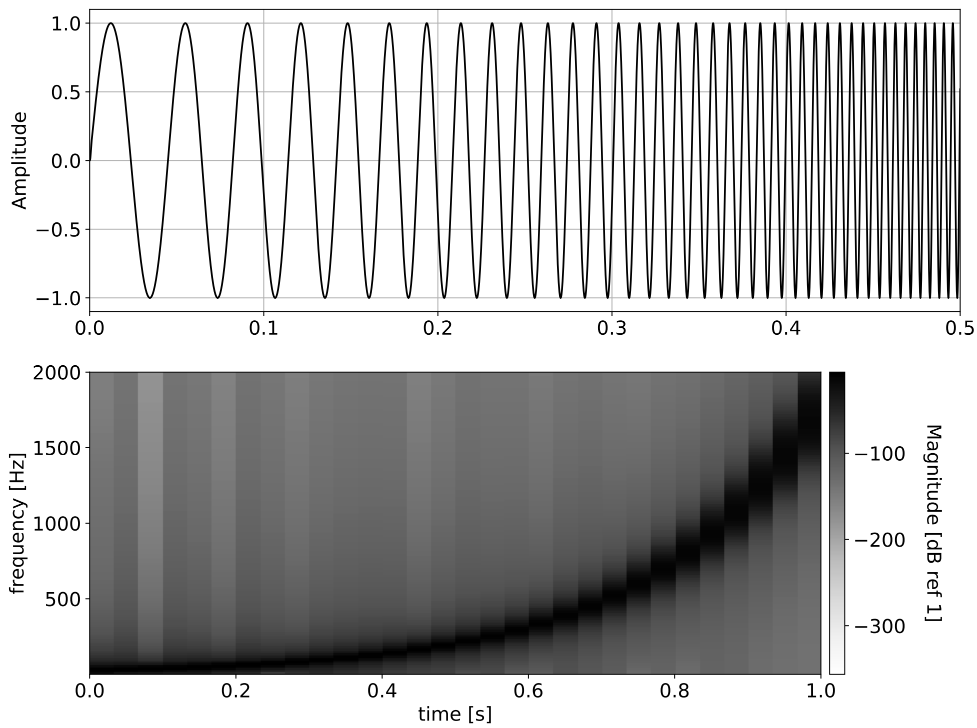

Figure 4.2.: Logarithmic sweep. Up: time signal, Down: spectrogram (frame size = 2^{15} samples, 50% overlap)

A logarithmic sinus sweep, similar to the one presented in figure 4.1, is presented in figure 4.2. By comparing the two spectrograms, one can easily distinguish, that the logarithmic sweep takes a longer time to scale up in frequency. For this reason it is preferred over the linear sweep, for the purpose of exciting a system in the low frequency region.

Extracting the impulse response of a system, that has been excited using the signals defined above, requires a process called deconvolution. In the frequency domain this will yield the system's transfer function (TF) and can be achieved by dividing the input channel $Y(k)$ with the reference channel $X(k)$ as in:

$$H(k) = \frac{Y(k)}{X(k)} \tag{4.7}$$

The impulse response of the system can then be easily obtained from 4.7 simply by using the $ifft$. In order to improve the result, a few limitations need to be taken into

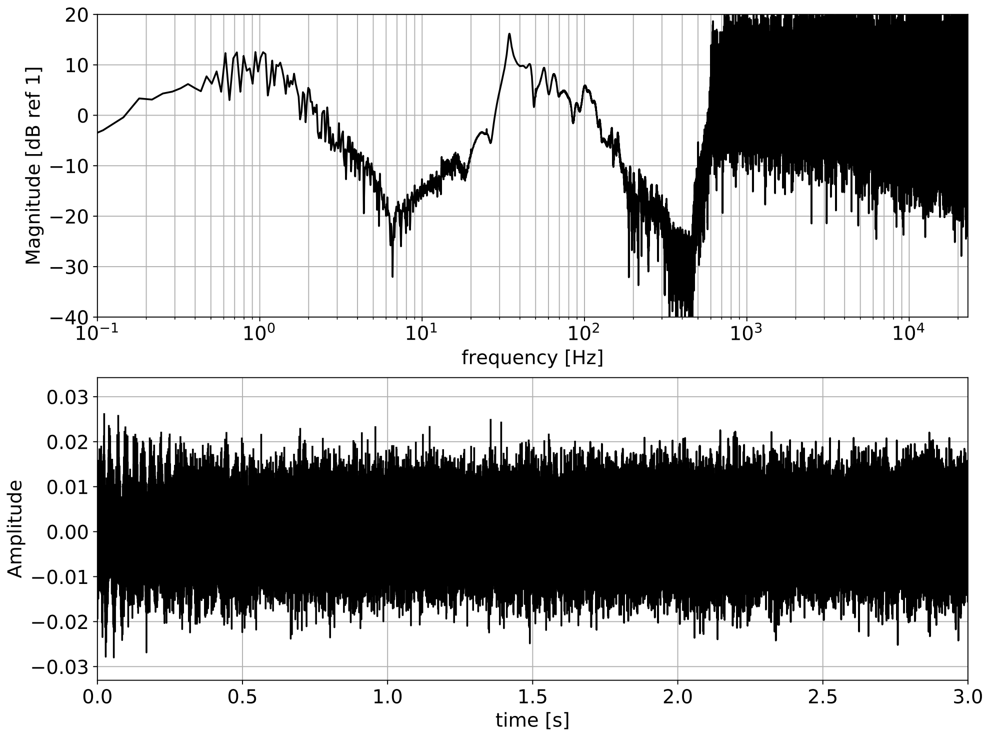

Figure 4.3.: Deconvolution result prior to filtering. Top: frequency response, Bottom: IR

account.

Initially, since the excitation signal has a very specific frequency content, ranging from f_0 to f_1. Therefore, both measured channels will have very low values outside that frequency range. As a result, their quotient will contain large numerical errors, due to the finite precision used in the fft algorithm. In turn, this numerical errors will introduce noise in the extracted impulse response.

For this reason it is crucial that the frequency range of the sweep starts at least one octave lower than the lowest frequency of interest and ends, one octave higher than the high frequency of interest. By following this methodology, the series of two filters can be implemented, without the risk of erroneous results in the frequency range of interest. The first filtering is done in the frequency domain by simply setting the values of the $Y(k)$ to zero, outside the frequency range of the sweep. The second filter, can then be applied in the resulting IR, further removing unwanted noise from the signal. In this step, a second order Butterworth band-pass filter is used, with a pass-band of

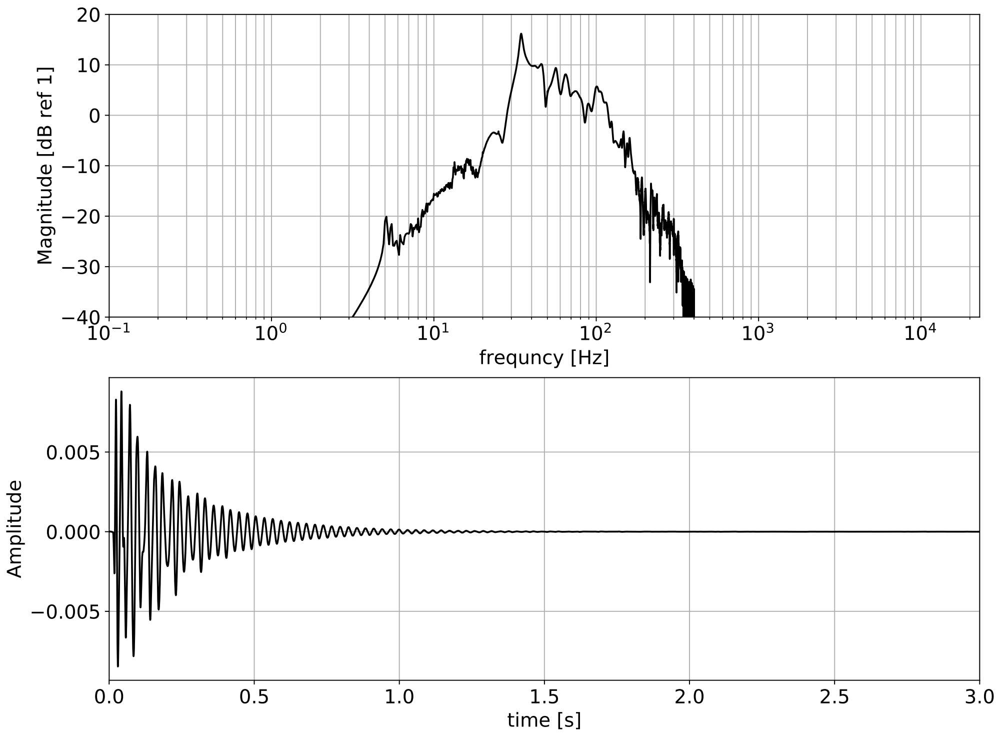

Figure 4.4.: Deconvolution result after filtering. Top: frequency response, Bottom: IR

$[f_0/2, f_1 * 2]$. The pass-band is chosen this way, in order to ensure that the signal will be sufficiently damped at the limits of the sweep range, while retaining a flat magnitude at the frequency range of interest. An example result can be seen in figures 4.3 and 4.4, featuring the resulting FRF and IR prior and after the application of the aforementioned filters.

Further noise can be removed from the resulting TF, simply by clipping it's IR at the end, when the signal has fallen into the noise floor. This is achieved because the harmonic noise components of the signal will be transferred to the negative times, due to the circular nature of the deconvolution process. These harmonic components can be seen in figure 4.5, for an IR, extracted using the deconvolution method.

For more detailed information on measurements using sweep signals please refer to [18].

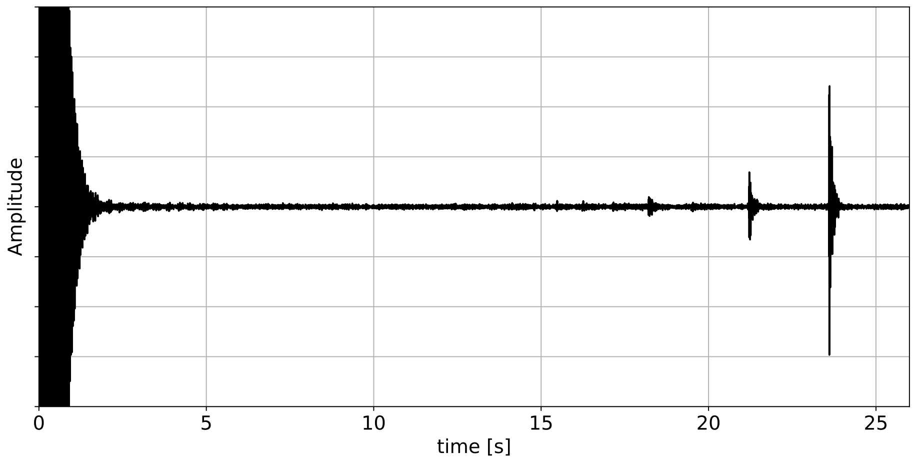

Figure 4.5.: Harmonic distortion components, pushed to the end of the signal.

4.2. Measurement setup.

4.2.1. Measurement System.

The audio interface used in all the following measurements consisted of the following **National Instruments** modules.

1. **NI** cDAQ^{TM} $-$ 9178 Eight-slot USB Chassis [7]
2. **NI 9234** 4-CH analog input module [8]
3. **NI 9260** 2-CH analog output module [9]

The above setup, was operated using the **nidaqmxAio** software, developed by the *Division of technical acoustics* and hosted at the division's *Github* page. The program handles the generation of the excitation signals as well as the settings of hardware. A complete description of the program's functionality can be found in the project's *README* file, although some parameters will be described below for quick reference.

1. **Sampling rate:** The sampling rate in Hz used by both the input and the output modules. Please refer to [8] for the available sample rates of the device.
2. **Measurement time:** The duration in seconds of the produced excitation signal. Please note, that this is not the total time of the recording, which is given by : *Measurement time + cutoff time + (initial zero-padding / sampling rate)*

3. **initial zero-padding:** The number of zeros, put before the excitation signal. The reason for this zero padding is to ensure that the initial value of the excitation signal is 0 V, rather the initial voltage of the signal generator.

4. **cutoff time:** The time in seconds, the measurement system will continue to record sound, after the reproduction of the excitation signal has finished. This is done in order to capture the decay of the sound field, after the excitation signal has stopped.

5. $\mathbf{V_{input}}$: The maximum input in Volts peak-to-peak, that the input module is set to measure.

6. $\mathbf{V_{output}}$: The voltage in Volts peak-to-peak, to which the excitation signal is scaled, in order for it's maximum absolute value to correspond to.

The use of this setup, allows for simultaneous generation of the excitation signal and capturing the voltage outputs of the connected microphones. Furthermore, the internal delay of the devise can be omitted (this is crucial during IR measurements), by simultaneously recording the output of the device, through one of it's inputs, during measurement. Finally, it should be noted here that the excitation signals are multiplied with a very short half-hanning window (0.1 % of the chosen sample rate) at the beginning and the end of their duration, in order to avoid abrupt changes in the signal. This needs to be avoided, not only to protect the equipment, but due to the fact that these sudden changes in voltage, can significantly distort the recorded signal.

4.2.2. IR measurements.

Overview.

The measurement setup for the IR extraction, consisted of a single loudspeaker placed in one corner of the room, fed with an excitation signal and a microphone placed on ten different positions, displayed in figures 4.6 and 4.7, for the **Living Room Lab** and the **Audio Lab** respectively. The microphone was positioned on each corner of the rectangular room, at varying heights. The motivation behind the positioning of the loudspeaker and the microphone, comes from the fact that all the modes have their maximum at the corners of the room. In this way, all the modes of the room can be sufficiently excited and the possibility of putting a microphone at a modal node, is avoided. The microphone was calibrated using a **B&K Type 4231** sound calibrator and following the procedure described in [1] section 8, prior to each set of measurements.

Loudspeakers.

The loudspeakers used, in order to excite the lower frequency region of the room were one **NEUMANN.BERLIN KH 805** mounted on the ceiling and a **Genelec 7050B**, placed on the floor. These sub-woofers have both internal amplification systems and therefore, the excitation signal was fed directly to the loudspeakers from the signal generator (**NI 9260**). The **Genelec 7050B** has a flat frequency response between $30-80\,\text{Hz}$, while the flat part of the **KH 805** frequency response is between $20-80\,\text{Hz}$, as shown in figure 5.15. In the mid-high frequency region the room was excited using a **B&K Type 4295** omni-directional source driven by a **B&K Type 2735** Measurement power amplifier, connected to the signal generator. The loudspeaker settings used in the measurements are displayed in Annex A, tables A.1,A.3 and A.5.

Microphone.

The room was measured using a *B&K* Type 4190 Free-field Microphone [12] with a sensitivity of 47.1 mV/Pa, connected to a *B&K* Type 2669 microphone preamplifier [11], using a *B&K* Type 1708 Signal Conditioner [16]. The settings used in the measurements of the room IRs were common in both the noise and the sinus sweep measurements and are displayed in table 4.1, along with the maximum voltage input (in Volts peak to peak) that the measurement system was set to detect.

Parameter	Value
Sensitivity (mV/Pa)	47.1
Signal Conditioner Amplification	10
V_{input} (V_{pp})	5

Table 4.1.: IR measurements: Microphone input parameters.

Excitation signals.

The parameters used by the measurement system for the excitation signals, are displayed in tables 4.2 and 4.3, for the white noise and the sinus sweep respectively. For more details about the signal parameters listed here, please refer to section 4.2.1. The formulation of the signals can be found in section 4.1.1.

Parameter	Genelec 7050B	KH805	B&K Type 4295
Sampling rate (kHz)	51.2	51.2	51.2
Measurement time (s)	180	180	180
initial zero-padding (# samples)	5000	5000	5000
cutoff time (s)	0	0	0
V_{output} (V_{pp})	0.5	1.0	2.0

Table 4.2.: IR measurements: White noise signal parameters.

Parameter	Genelec 7050B	KH805	B&K Type 4295
Type	logarithmic	logarithmic	logarithmic
f_0 (Hz)	5	5	40
f_1 (Hz)	400	400	16000
initial phase (rads)	0	0	0
Sampling rate (kHz)	51.2	51.2	51.2
Measurement time (s)	30	30	30
initial zero-padding (# samples)	5000	5000	5000
cutoff time (s)	2	2	2
V_{output} (V_{pp})	0.05	0.1	0.2

Table 4.3.: IR measurements: Sinus sweep signal parameters.

Equipment list.

The complete list of the equipment used, as well as links to their corresponding manuals are listed bellow.

1. Loudspeakers
   a) **Genelec 7050B** sub-woofer [4]
   b) **B&K** *OmniSource*^{TM} **Type 4295** omni-directional source [13]
   c) **B&K Type 2735** 2 x 35 Watt Measurement Power Amplifier [14]
   d) **NEUMANN.BERLIN KH 805** sub-woofer [19]
2. Microphones
   a) **B&K Type 4190** 1\2″ Free-field Microphone [12]
   b) **B&K Type 2669** Falcon^{TM} Range 1\2″ Microphone Preamplifier [11]

c) **B&K Type 1708** Signal Conditioner [16]

d) **B&K Type 4231** Sound Calibrator [15]

Measurement positions

The sound field of the two labs was sampled at the positions displayed in figures 4.6 and 4.7, for the Living Room Lab and the Audio Lab respectively. The exact coordinates of the microphone are displayed in tables 4.4 and 4.5. The zero point of the axes for the coordinates referred in tables 4.4, 4.5 is located on the bottom left corner of the inner wall of each room.

The microphone positions 1-3 correspond to the three corners of the room at the approximate height of a sitting person, positions 4-6, (as well as, position 9 for the **KH 805**, in the Living Room Lab) to the three corners at floor height and positions 7-10, to the four corners of the room, at the height of the fake ceiling.

In the Living Room Lab, the position of the exciting loudspeaker, as displayed in figure 4.6, corresponds to the upper left corner of the room. The **Genelec 7050B** and the *B&K* **Type 4395** were positioned on the floor, as close as possible to the corner, with their drivers facing toward it. In this case, the microphone position number 9 was set to be directly above the loudspeaker. The **KH 805** sub-woofer was mounted on the ceiling at a height of 3 m from the floor, with its driver being 7.5 cm from the left wall and facing the upper wall at a 32 cm distance. In this case, the microphone position number 9 refers to the microphone being placed at the upper left corner of the room 2 cm above the floor.

In the Audio Lab, only the **Genelec 7050B** and the *B&K* **Type 4395** were used. The loudspeakers were placed on the floor, as close as possible, to the upper left corner of the room, with their drives facing toward it.

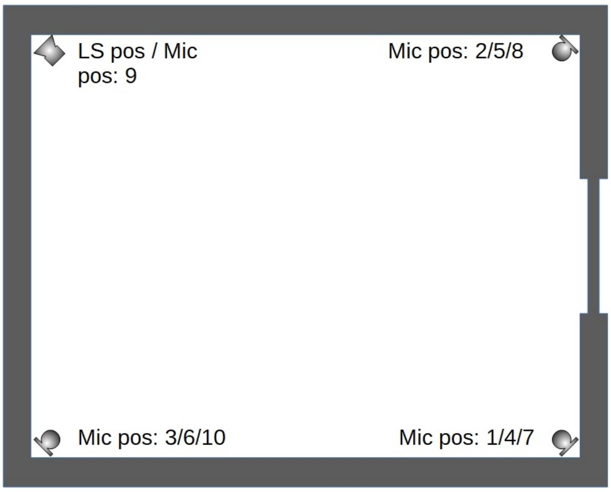

Figure 4.6.: IR measurements: Microphone and loudspeaker positions, Living room lab.

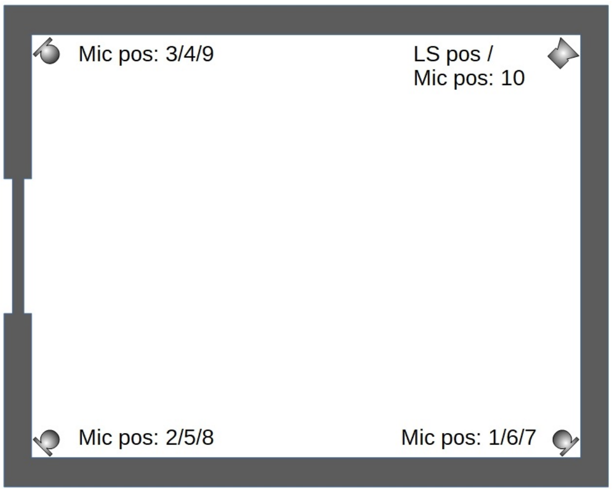

Figure 4.7.: IR measurements: Microphone and loudspeaker positions, Audio lab.

Mic position	x (m)	y (m)	h (m)
1	4.78	0.02	1.25
2	4.78	3.70	1.25
3	0.02	0.02	1.25
4	4.78	0.02	0.05
5	4.78	3.70	0.05
6	0.02	0.02	0.05
7	4.78	0.02	2.58
8	4.78	3.70	2.58
9	0.02	3.70	2.58
9 (KH805)	0.02	3.70	0.02
10	0.02	0.02	2.58

Table 4.4.: IR measurements: Microphone coordinates, Living Room Lab.

Mic position	x (m)	y (m)	h (m)
1	4.78	3.70	1.25
2	0.02	0.02	1.25
3	0.02	3.70	1.25
4	0.02	3.70	0.05
5	0.02	0.02	0.05
6	4.78	0.02	0.05
7	4.78	0.02	2.58
8	0.02	0.02	2.58
9	0.02	3.70	2.58
10	4.78	3.70	2.58

Table 4.5.: IR measurements: Microphone coordinates, Audio Lab.

4.2.3. Reduction Index.

Overview.

The measurement setup for the calculation of the Reduction Index (RI), of the window-wall between the two labs consisted of, a single loudspeaker, positioned on one of the corners of the **Sending Room** (**Audio Lab**) and two microphones, one placed in the **Sending Room** and one in the **Receiving Room** (**Living Room Lab**). The loudspeaker excited the **Sending room** using white noise and simultaneously the microphones measured the sound pressure levels, in their corresponding rooms. Background noise measurements were also taken at the end of the measurement session and each microphone was calibrated, prior to the measurement session, similarly to section 4.2.2.

Measurement equipment.

The equipment used for this measurement is nearly identical with the one listed in section 4.2.2 , excluding the **KH 805** sub-woofer from the loudspeaker section. Moreover, an additional set of microphone, preamplifier and signal conditioner was used.

For the same reasons as described in subsection 4.2.2 , the *B&K* **Type 4295** and the **Genelec 7050B** loudspeakers were used. The settings for the loudspeakers were kept identical as described in tables A.1 and A.5.

The microphone setup was kept the same as in subsection 4.2.2, with the addition of an extra microphone placed in **Sending room**, which had a sensitivity of 51.7 mV/Pa. The detailed parameters used, are displayed in table 4.6.

Parameter	Sending Room	Receiving Room
Sensitivity (mV/Pa)	47.1	51.7
Signal Conditioner Amplification (Genelec 7050B)	100	100
Signal Conditioner Amplification (*B&K* Type 4295)	10	100
V_{input} (V_{pp})	5	5

Table 4.6.: RI measurements: Microphone input parameters.

Excitation signals.

The excitation signal used for this measurement was white noise. The parameters used by the measurement system are displayed in table 4.7.

Parameter	Genelec 7050B	B&K Type 4295
Sampling rate (kHz)	51.2	51.2
Measurement time (s)	60	60
initial zero-padding (# samples)	5000	5000
cutoff time (s)	0	0
V_{output} (V_{pp})	1.0	2.0

Table 4.7.: RI measurements: White noise signal parameters.

Measurement positions.

The sound pressure levels of the **Sending** and the **Receiving Room**, were sampled at the positions displayed in figure 4.8. More specifically, for the receiving room, positions **a1 - a4** correspond to the four corners of the room at the height of a sitting person, positions **a5 - a8** to the four corners of the room at floor height, positions **a9 - a12** to the four corners right bellow the fake ceiling and finally, positions **a13 - a15** to three random positions at the height of a sitting person, fulfilling the requirements specified in section 4.2.2 of the ISO 10140-4:2010 standard [25].

In the **Sending Room**, the sound field was sampled only at the three corners of the room at floor height (positions **b1 - b3**), the three corners at a height just bellow the fake ceiling (positions **b4 - b6**) and at three random positions at the height of a sitting person similarly to positions **a13 - a15** above. The reason that the sound field was sampled at less points in the **Sending Room**, was that the sound pressure levels were much higher and there was very little variation between the floor, ceiling and mid plane heights. The positions directly above the exciting loudspeaker were also avoided, due to the interference caused by the direct wave. The complete list of coordinates for the measurement positions is displayed in table 4.8.

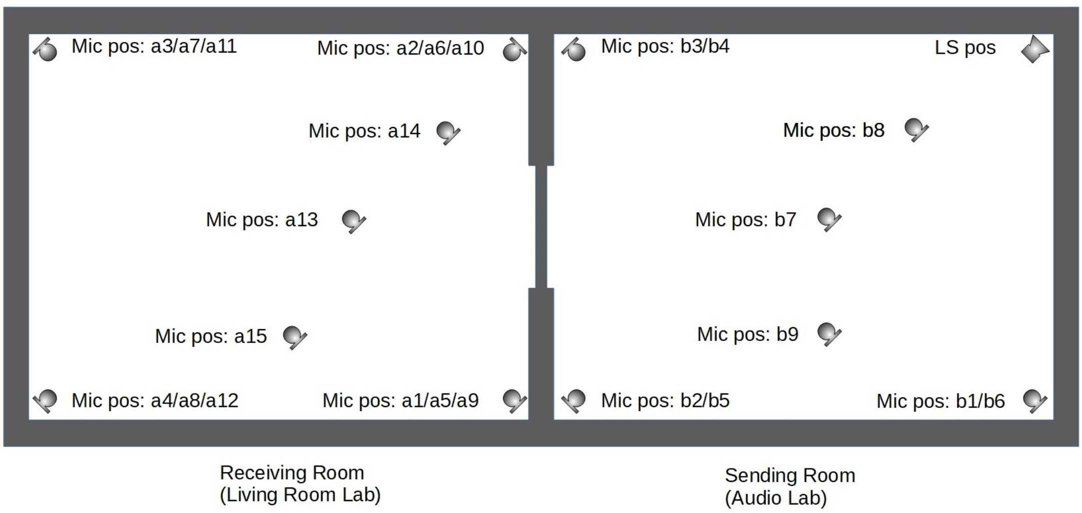

Figure 4.8.: RI measurements: Microphone and loudspeaker positions in Sending and Receiving rooms.

Mic position Receiving Room	x (m)	y (m)	h (m)	Mic position Sending Room	x (m)	y (m)	h (m)
a1	4.78	0.02	1.25	b1	4.78	0.02	0.05
a2	4.78	3.70	1.25	b2	0.02	0.02	0.05
a3	0.02	3.70	1.25	b3	0.02	3.70	0.05
a4	0.02	0.02	1.25	b4	0.02	3.70	2.58
a5	4.78	0.02	0.05	b5	0.02	0.02	2.58
a6	4.78	3.70	0.05	b6	4.78	0.02	2.58
a7	0.02	3.70	0.05	b7	2.30	1.94	1.25
a8	0.02	0.02	0.05	b8	3.98	2.91	1.25
a9	4.78	0.02	2.58	b9	1.35	0.83	1.25
a10	4.78	3.70	2.58				
a11	0.02	3.70	2.58				
a12	0.02	0.02	2.58				
a13	2.12	2.22	1.25				
a14	3.65	2.89	1.25				
a15	1.64	1.05	1.25				

Table 4.8.: RI measurements: Microphone coordinates, Receiving and Sending rooms.

4.2.4. Loudspeaker Measurements.

Overview.

The *Living Room Lab* would feature a loudspeaker grid mounted on it's ceiling, consisting of twenty **Genelec 8020B**. Furthermore, twenty five **NEUMAN.BERLIN KH 80 DSP**, were intended to be used in loudspeaker array setups In the *Audio Lab*. Therefore, the individual characteristics (frequency response and directivity) of each loudspeaker, were measured. These measurements were conducted using only sinus sweep signals, due to the substantially less time it requires. The loudspeakers used in this test are presented in Annex A, table B.3, for the **KH 80 DSP** and B.4, for the **Genelec 8020B**, along with their serial numbers.

Prior to conducting the above measurements the measurement procedure was validated, using the loudspeakers presented in table 4.9. More specifically, the frequency responses on axis as well as, on various angles, were extracted, using both white noise and sinus sweep signals. In this step the *B&K* **Type 4295** and the **KH 805** were only measured on axis. The former due to the fact that, it is an omni-directional source and the later due to the fact that it was too large to be put on a rotating table. Finally, only three of the **KH 80 DSP** were put under test using both the excitation signals.

All of the above measurements were conducted in accordance to the *IEC 60268-5:2003* standard [10] .

Brand	Model	S/N
Genelec	7050B	PM6007676 Dec10
Genelec	8030A	PM6030462 Jun 06
Genelec	8020B	PM6024250 Dec10
NEUMAN.BERLIN	805	3298358981
NEUMAN.BERLIN	KH 80 DSP	3297189744
NEUMAN.BERLIN	KH 80 DSP	3297191291
NEUMAN.BERLIN	KH 80 DSP	3297192147
B&K	*OmniSource*^{TM} Type 4295	-

Table 4.9.: Loudspeaker measurements under test.

Frequency response on axis.

During the validation tests, for the frequency response on axis, each loudspeaker presented in table 4.9, was placed in the center of the anechoic chamber. The microphone was mounted on a microphone stand, sitting on top of the metal net installed in the chamber. The two sub-woofers (**Genelec 7050B** and **KH 805**) were to big to be mounted on a conventional stand and therefore were placed directly on the wooden stand, that is permanently installed in the chamber. Reflections from the wooden base did not cause noticeable interference, since in frequency range of interest for the sub-woofers, $\lambda/2$ is quite larger, than the exposed wooden surface of the base. The rest of the loudspeakers were positioned on a stand 1.5 m above the wooden base, while the later was covered with absorptive material, to avoid the reflection interference.

The microphone was placed one meter away form the reference plane of the loudspeaker under test, on the same axis as it's reference axis. For more information on the reference plane and axis of each loudspeaker, please refer to the corresponding manufacturer manuals ([4], [5], [6], [13], [19], [20]).

The same microphone as in section 4.2.2 was used, while it's configuration is presented in table 4.10.

Parameter	Value
Sensitivity (mV/Pa)	47.1
Signal Conditioner Amplification	100
V_{input} (V_{pp})	5

Table 4.10.: Loudspeaker IR measurements: Microphone input parameters.

The configuration of the various loudspeaker's settings, can be found in Annex A, tables A.1, A.2, A.3, A.4 and A.5. Finally, the configuration for the excitation signals can be found in table 4.11 for the white noise and table 4.12 for the logarithmic sinus sweep.

Parameter	Genelec 7050B	Genelec 8030A	Genelec 8020B	KH805	KH80DSP	B&K Type4295
Sampling rate (kHz)	51.2	51.2	51.2	51.2	51.2	51.2
Measurement time (s)	180	180	180	180	180	180
initial zero-padding (# samples)	5000	5000	5000	5000	5000	5000
cutoff time (s)	0	0	0	0	0	0
V_{output} (V_{pp})	0.65	0.2	0.2	1.23	0.775	2.0

Table 4.11.: Loudspeaker FRF on axis: White noise signal parameters.

Parameter	Genelec 7050B	Genelec 8030A	Genelec 8020B	KH805	KH80DSP	B&K Type4295
Type	log	log	log	log	log	log
f_0 (Hz)	5	40	40	5	40	40
f_1 (Hz)	1000	20000	20000	1000	20000	20000
initial phase (rads)	0	0	0	0	0	0
Sampling rate (kHz)	51.2	51.2	51.2	51.2	51.2	51.2
Measurement time (s)	30	30	30	30	30	30
initial zero-padding (# samples)	5000	5000	5000	5000	5000	5000
cutoff time (s)	0	0	0	0	0	0
V_{output} (V_{pp})	0.065	0.02	0.02	0.123	0.0775	0.2

Table 4.12.: Loudspeaker FRF on axis: Sinus sweep signal parameters.

Frequency response on angle.

The measurement setup for the estimation of the FRF on various angles, was identical with the one described in section 4.2.4, except for the fact that the loudspeaker under test was mounted on top of a rotating table. The measurement started with the reference axis of the loudspeaker being in line with the microphone, at 1 m distance. After the measurement was conducted, the table would rotate by 5^o clockwise and repeat the measurement. This continued for a full circle, resulting in 72 FRF measurements. The settings for each measurement were kept the same as in section 4.2.4, except for the ones presented in table 4.13, for measurements conducted using white noise and table 4.14, using logarithmic sweep signals. Changing these parameters was necessary to ensure that the table would turn after each measurement had stopped, the recorded signal would never clip in any measurement of the full rotation and finally, the time of the measurement would be reduced as much as possible without risking a very poor signal to noise ratio in the result. Finally, the measurement settings were tweaked once more, in accordance to the criteria explained above, before the measurements of the 20 **Genelec 8020B** and the 25 **KH 80 DSP** were conducted. The final settings for these measurements are displayed in table 4.15.

Parameter	Genelec 7050B	Genelec 8030A	Genelec 8020B	KH80DSP
Measurement time (s)	30	30	30	30
cutoff time (s)	0	0	0	0
V_{output} (V_{pp})	0.65	0.3	0.3	0.775
Signal Conditioner Amplification	100	10	10	100

Table 4.13.: Loudspeaker, FRF on varying angle: Initial settings - white noise.

Parameter	Genelec 7050B	Genelec 8030A	Genelec 8020B	K80DSP
f_0 (Hz)	5	20	20	40
f_1 (Hz)	1000	24000	24000	24000
Measurement time (s)	4	4	4	4
cutoff time (s)	0	2	2	0
V_{output} (V_{pp})	0.065	0.03	0.03	0.0775
Signal Conditioner Amplification	100	10	10	100

Table 4.14.: Loudspeaker FRF on varying angle: Initial settings - sinus sweep.

Parameter	Genelec 8020B	KH 80 DSP
Type	logarithmic	logarithmic
f_0 (Hz)	40	40
f_1 (Hz)	24000	24000
initial phase (rads)	0	0
Sampling rate (kHz)	51.2	51.2
Measurement time (s)	4	4
initial zero-padding (# samples)	5000	5000
cutoff time (s)	1	1
V_{output} (V_{pp})	0.02	0.0775
Signal Conditioner Amplification	100	100

Table 4.15.: Loudspeaker FRF on varying angle: Final settings.

5. Results and discussion.

This chapter is going to include the results from all the measurements described in chapter 4 and will be divided in four sections. Section 5.1, will include the results of loudspeaker transfer functions and directivity measurements, as well as a discussion on their use in room acoustics measurements and their intended function for the rooms. Section 5.2 will feature the measured transfer functions and reverberation times of the two rooms, in the frequency region above the *Schröder* frequency. The equivalent results for the low frequency region will be presented in section 5.3, along with the corresponding modal decay times and the spectral decays, for the most prominent modes present in the rooms. Finally, the reduction index of the intermediate window and wall, separating the two rooms, will be presented in section 5.4.

5.1. Loudspeaker Measurements.

As was mentioned in section 4.2.4, the loudspeaker transfer functions were extracted using both white noise and sinusoidal sweep signals, as excitation. Since both methods produced very similar results, both can be used in order to extract meaningful information about the loudspeakers, without the need of displaying the same result twice. More specifically, the white noise measurements will be used to display the information regarding the transfer function of the loudspeaker, due to the fact that the coherence function (γ^2) can provide additional insight on the quality of the measurement. For consistency with the previous results, the white noise measurements are also chosen for examining the directivity. On the other hand, as mentioned in section 4.2.4, due to the shorter measurement duration, the sinus sweep measurements were chosen, for calculating the mean magnitude and the confidence intervals of the 21 *Genelec 8020B* and the 25 *Neuman.BERLIN KH 80 DSP*.

5.1.1. Results

Genelec 8020B & 8030A.

The transfer function magnitudes for the *Genelec 8020B* and *8030A* are presented in figure 5.1. Both loudspeakers have a fairly flat frequency response up to 20 kHz. The flat region for the *8020B* starts form 45 Hz and from 60 Hz for the *8030A*. The magnitude

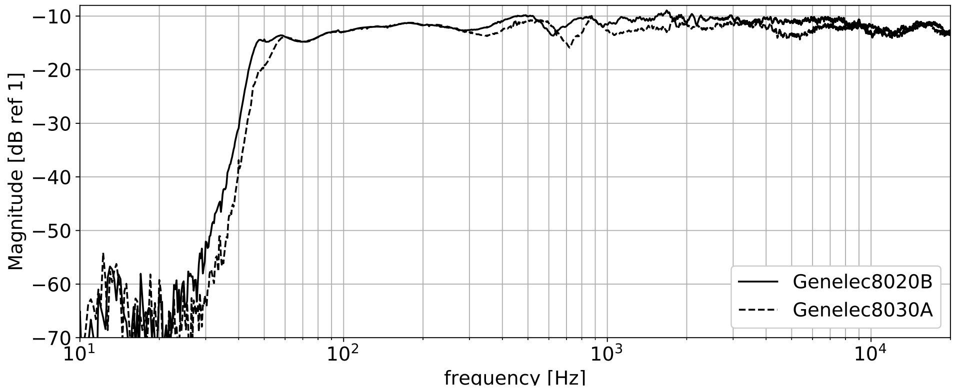

Figure 5.1.: TF magnitude: Genelec8020B and 8030A.

decreases very quickly bellow the lower limit. The response of the *8030A* shows a 5 dB decrease at 720 Hz, while similarly the *8020B* has a smaller decrease, about 3 dB in magnitude at 621 Hz.

The transfer function, for both loudspeakers shows a linear phase response, across the entire frequency range, as shown in figure 5.2.

The coherence is very high for both models, in almost the entire frequency range, as shown in figure 5.3. At the two deeps located at 40 and 50 Hz the value of γ^2, drops approximately at 0.49 and 0.77, for the *8020B* and at 0.23 and 0.81 for the *8030A*. The directivity patterns for the *8020B* and the *8030A* are displayed on figures 5.4 and 5.5 respectively. As expected both loudspeakers are omni-directional at 300 Hz, becoming increasingly directional at higher frequencies.

The mean of the frequency response for all the measured *Genelec 8020B*, is displayed in figure 5.6, along with the 99.9%, confidence interval. The response displays very small deviation across the measured loudspeakers in the entire frequency range.

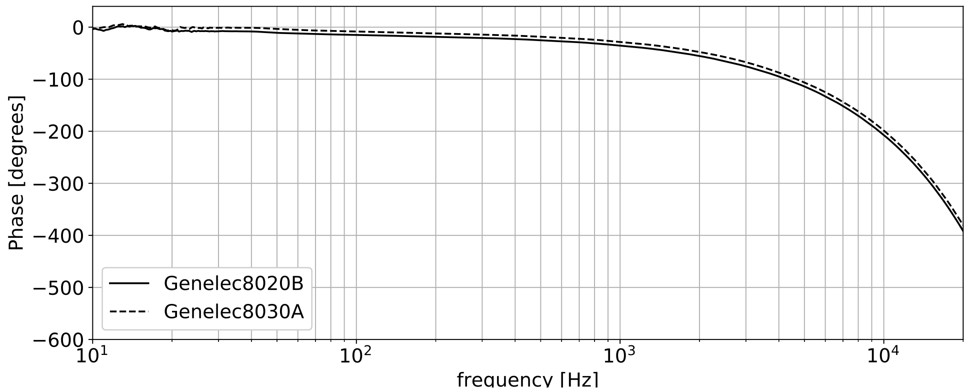

Figure 5.2.: TF phase: Genelec8020B and 8030A.

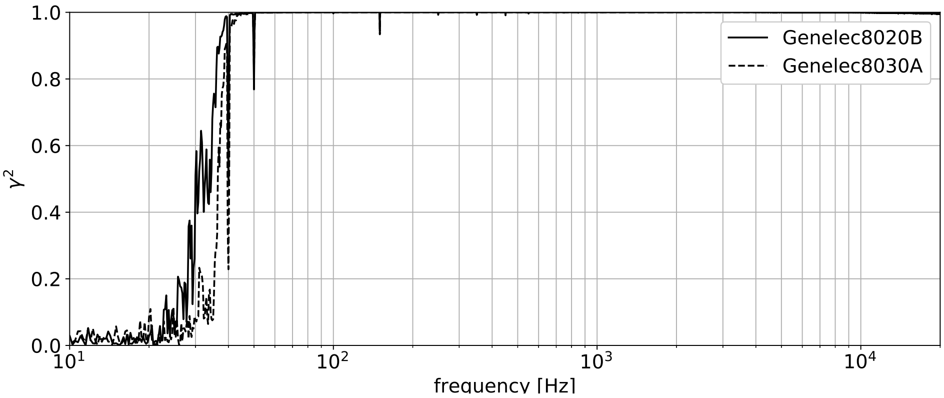

Figure 5.3.: Coherence γ^2: Genelec8020B and 8030A.

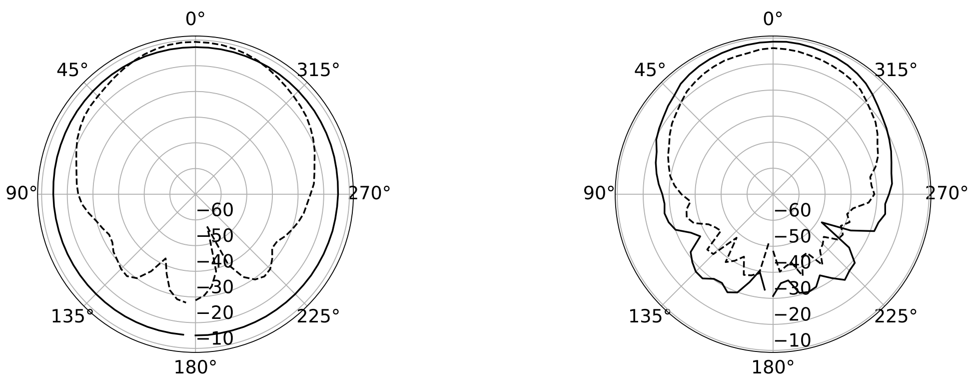

(a) Solid line 300 Hz, dashed line 3 kHz

(b) Solid line 6 kHz, dashed line 12 kHz

Figure 5.4.: Directivity patterns for Genelec 8020B

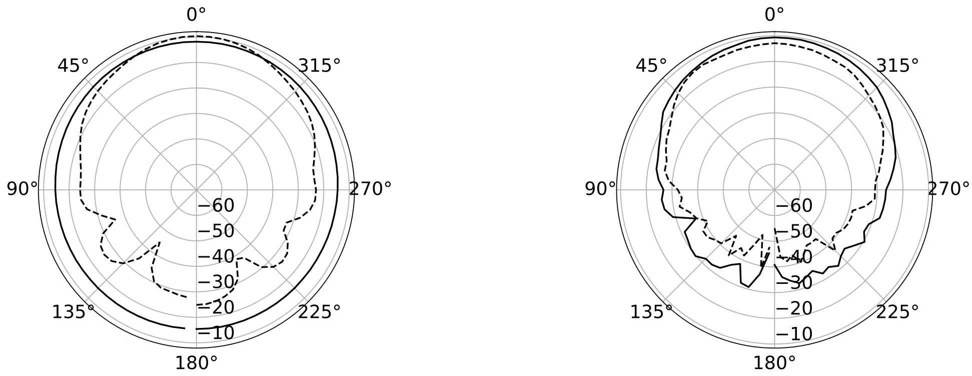

(a) Solid line 300 Hz, dashed line 3 kHz

(b) Solid line 6 kHz, dashed line 12 kHz

Figure 5.5.: Directivity patterns for Genelec 8030A

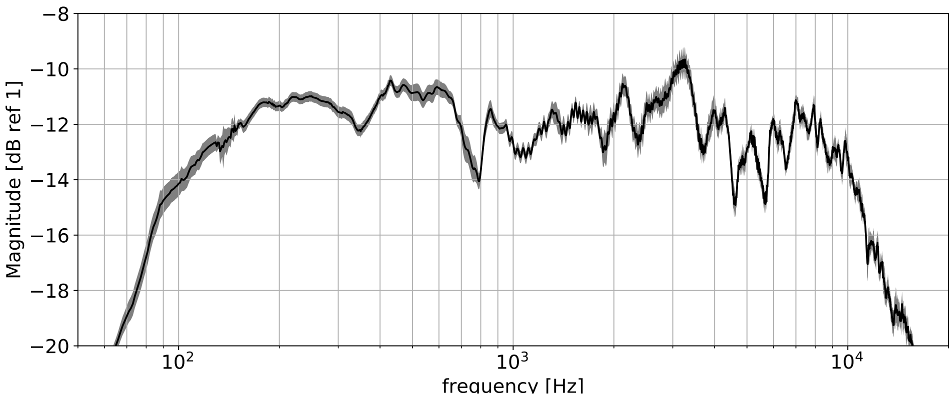

Figure 5.6.: TF magnitude for Genelec 8020B averaged, over 21 loudspeakers. The gray area indicates the 99.9% of the measurements.

Brüel & Kjær Type 4295.

The frequency response for the *B&K Type 4295* is displayed in figure 5.7. The response shows significant fluctuation across the entire frequency range. This however, is expected because the loudspeaker is designed for use in room and building acoustics measurements. Therefore, the design of the loudspeaker is more focused on delivering a flat response on n-octave bands and having an omni-directional directivity pattern.

The phase part of the transfer function shows that the loudspeaker's behavior is linear throughout it's frequency range, and is displayed in figure 5.8.

Examining figure 5.9, reveals several points, located in the region between 340 and 380 Hz, were the coherence drops significantly, with the lowest being 0.55 at 355 Hz. Apart form that region the coherence is very good in the usable frequency region of the loudspeaker, which after taking into consideration the figures 5.7, 5.8 and 5.9, can be considered to be between 80−10 kHz.

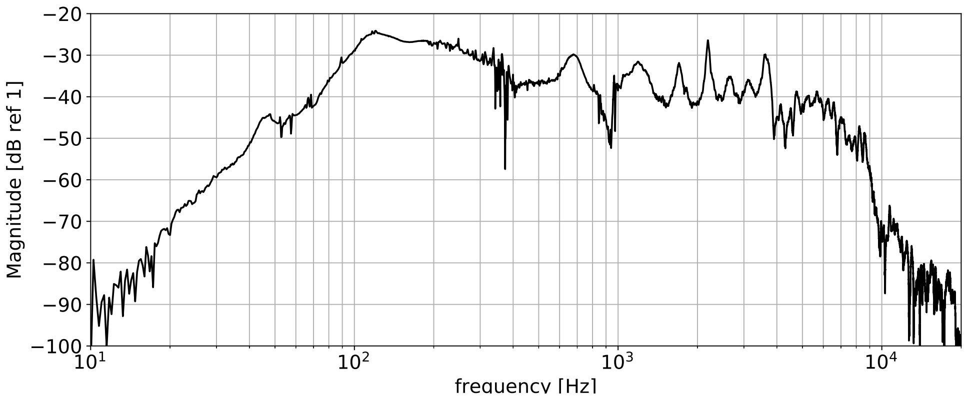

Figure 5.7.: TF magnitude: *B&K* Type 4295.

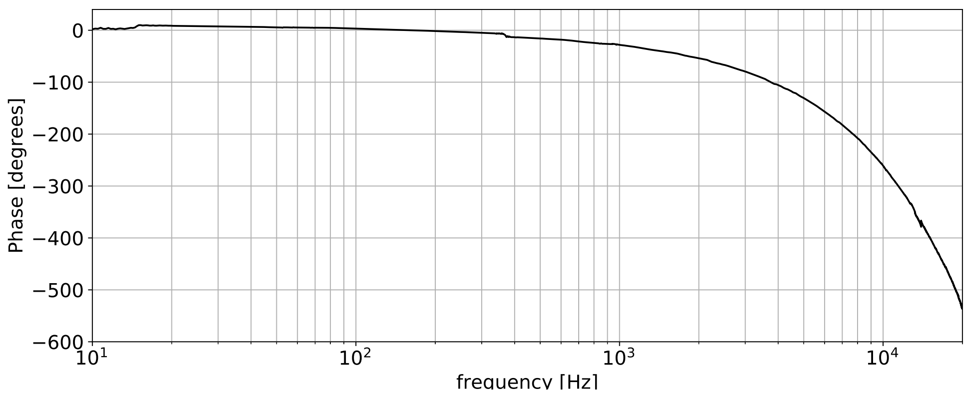

Figure 5.8.: TF phase: *B&K* Type 4295.

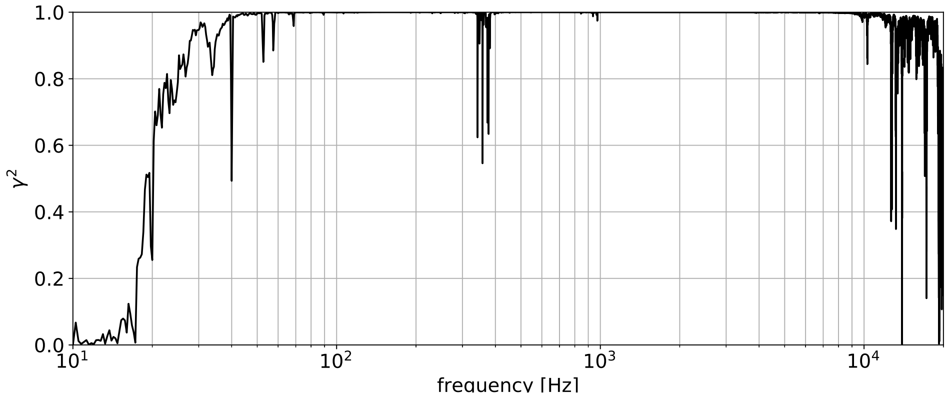

Figure 5.9.: Coherence γ^2: *B&K* Type 4295.

Neuman.BERLIN KH 80 DSP.

The frequency response functions of the three *Neuman.BERLIN KH 80 DSP* displayed in figure 5.10, show a fairly flat trend between 60−2 kHz. Below 60 Hz the magnitude drops significantly, approximately −35 dB per doubling of frequency. In the region between 2 KHz and 20 kHz the response shows multiple resonances, that make the response fluctuate between −30 and −40 dB. All the three loudspeakers have similar behavior across the entire spectrum, a fact that can be confirmed further by examining figure 5.6, where the mean value of 25 loudspeakers and it's 99.9% confidence interval, is displayed.

The phase response presented in figure 5.11 shows linear behavior, across the entire spectrum, for all three of the loudspeakers, while the coherence is very good above 60 Hz.

The *KH 80 DSP* have fairly good directivity as the patterns, displayed in figure 5.13, reveal. More specifically, on a 35 degrees angle the frequency response drops approximately by 5 dB at 3 and 6 kHz, while the loudspeaker is omni-directional at 300 Hz. As expected the loudspeaker becomes more directional, at higher frequencies, as shown by the dashed line in figure 5.13b displaying the FRF at 12 kHz.

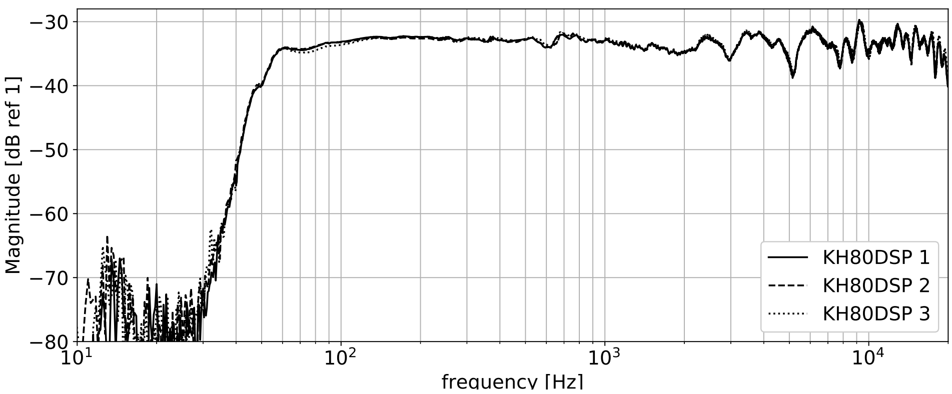

Figure 5.10.: TF magnitude: KH80DSP 1 - 3297189744, 2 - 3297191291, 3 - 3297192147.

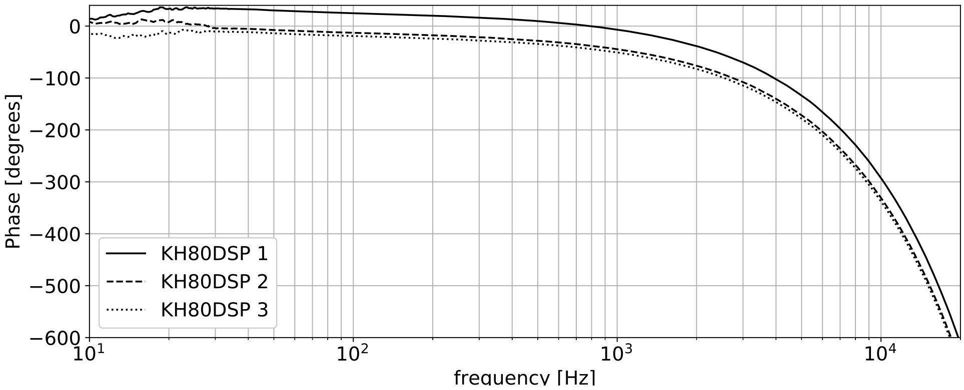

Figure 5.11.: TF phase: KH80DSP 3297189744, 3297191291, 3297192147.

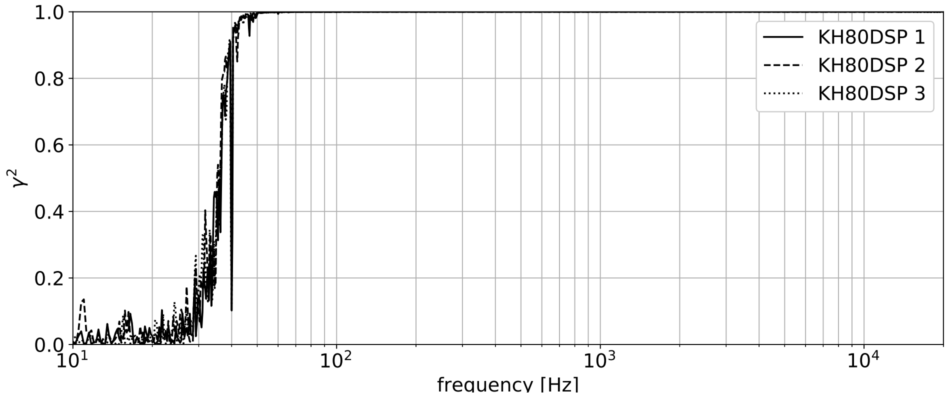

Figure 5.12.: Coherence γ^2: KH80DSP 3297189744, 3297191291, 3297192147.

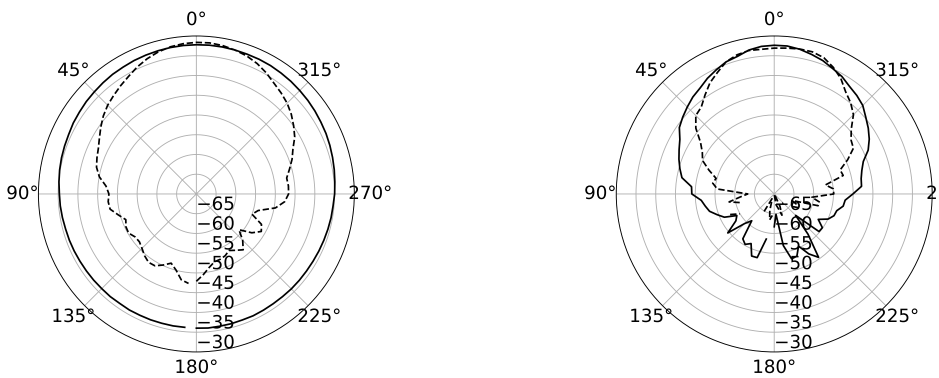

(a) Solid line 300 Hz, dashed line 3 kHz

(b) Solid line 6 kHz, dashed line 12 kHz

Figure 5.13.: Directivity patterns for Neuman.BERLIN KH 80DSP

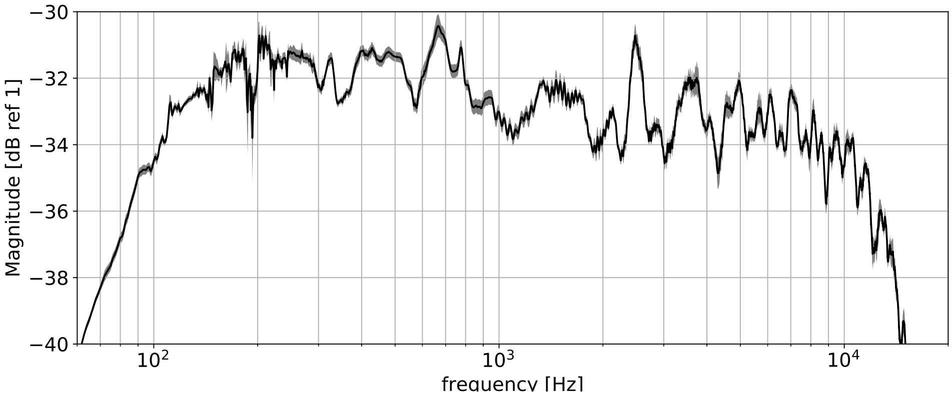

Figure 5.14.: TF magnitude for Neuman.Berlin KH 80 DSP, averaged over 25 loudspeakers. The gray area indicated the 99.9% of the measurements.

Genelec 7050B and Neuman.BERLIN K 805.

The frequency response of the two sub-woofers presented in figure 5.15 is far from flat, compared with the mid-range loudspeakers.

In more detail, the *Genelec 7050B* can be considered having a flat frequency response only between 30 and 80 Hz, where the response drops by approximately 4 dB, apart from a peak centered at 45 Hz where the response increases by approximately 5 dB. Outside of that range, the magnitude decays by 40 dB, until the highest usable frequency for the loudspeaker at 180 Hz. The response decays faster towards the lower usable frequency, reaching a 40 dB decrease at 18 Hz.

The *Neuman.Berlin KH 805*, shows similar overall behavior, but with it's flat portion ranging between 20 and 80 Hz. A similar peak is located at 45 Hz. The response decays much slower, towards both the highest frequency of use, located approximately at 250 Hz, and the lowest frequency at approximately 11 Hz.

The phase response, shown in figure 5.2 reveals linear behavior for both the loudspeakers, in their frequency range of use, while the corresponding coherence is also very good in that region, as figure 5.17 reveals. As expected, the directivity patterns for the *Genelec 7050B*, reveal that the sub-woofer is indeed omni-directional.

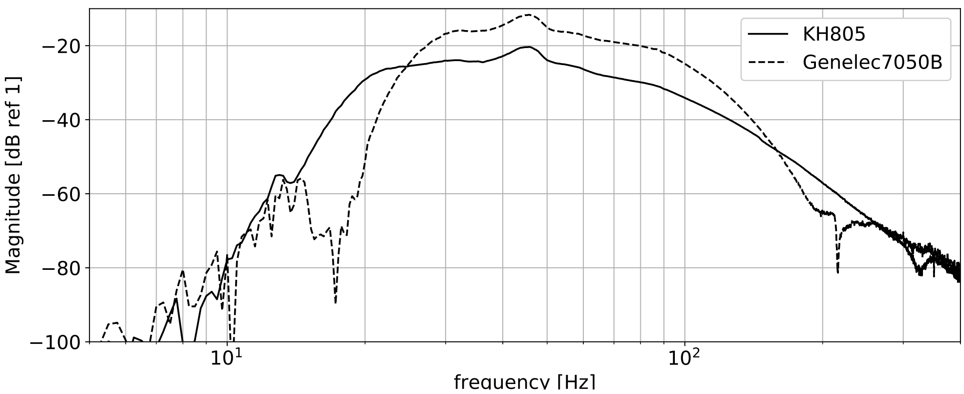

Figure 5.15.: TF magnitude: Genelec 7050B, KH 805.

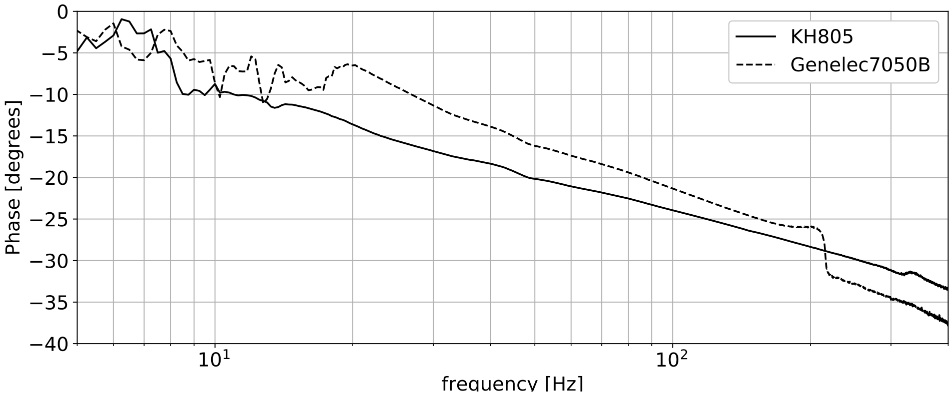

Figure 5.16.: TF phase: Genelec 7050B, KH 805.

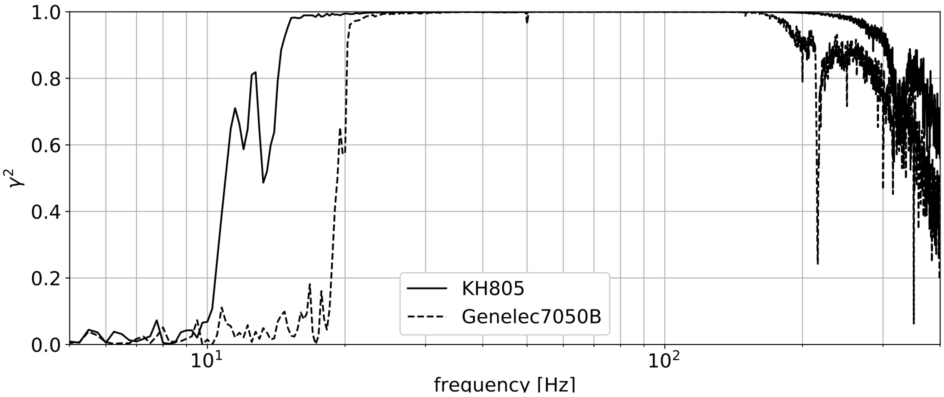

Figure 5.17.: Coherence γ^2: Genelec 7050B, KH 805.

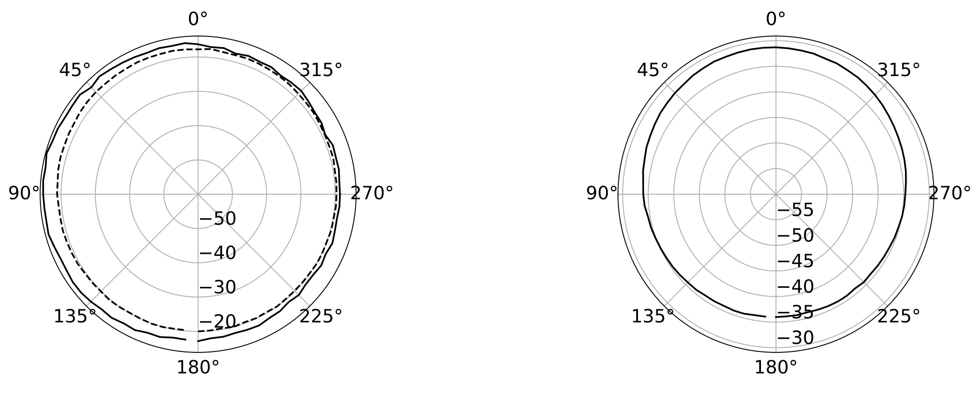

(a) Solid line 30 Hz, dashed line 60 Hz

(b) Solid line 120 Hz, dashed line 240 Hz

Figure 5.18.: Directivity patterns for Genelec 7050B

5.1.2. Remarks on the intended use.

According to the results presented in the previous section, the loudspeaker setup on the ceiling of the *Living room laboratory*, that consists of four *KH 805* and twenty *Genelec 8030A*, will feature a frequency response, capable of reproducing signals in a frequency range between 20 Hz and 20 kHz, as indicated by figure 5.19. Furthermore, the fact that the FRF of the *Genelec 8030A* is very consistent across all the measured loudspeakers, makes using them suitable for use in a grid setup. Finally, their directivity can render them useful in grids were the loudspeakers are far form each other, as long as the frequency range if interest is bellow 3 kHz.

The *K 80 DSP* and *Genelec 8020B* feature a flat enough frequency response, a wide frequency range and a directivity pastern that renders them suitable for use, in the presentation of auditory stimuli in listening test experiments, as long as the signals do not contain very low frequency content. Moreover, the *K 80 DSP* similarly with the *Genelec8030A* are suitable for use in loudspeaker grid setups.

Finally, as figure 5.20 reveals, combining either the *KH 805* or the *Genelec 7050B* with the *B & K Type 4295* can excite a small room sufficiently enough, in order to determine it's behavior both above and bellow the *Schröder* frequency.

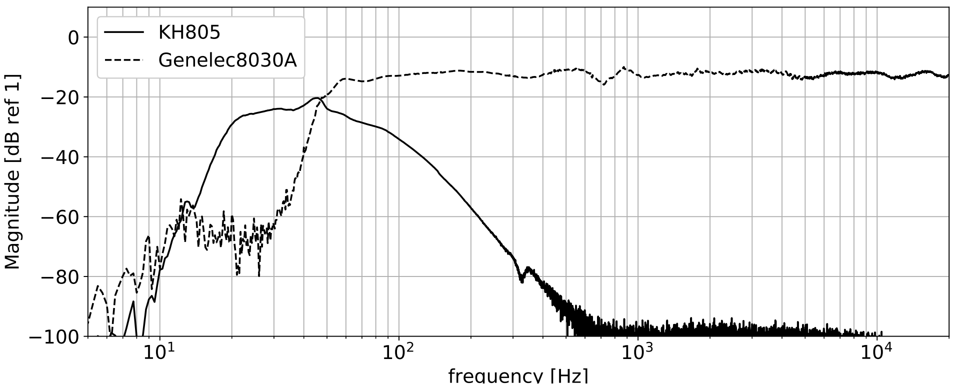

Figure 5.19.: Frequency response of the ceiling louspeaker setup.

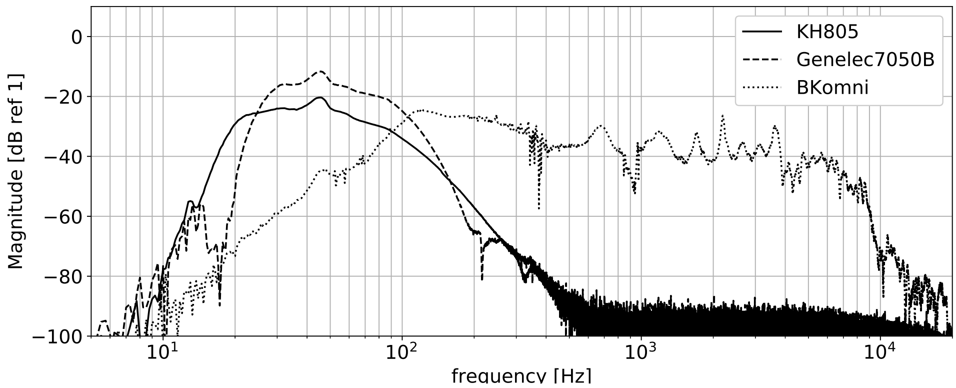

Figure 5.20.: Frequency response of the room measurement loudspeaker setup.

5.2. Room characteristics in the diffuse field.

The two rooms under investigation are very small, having a volume of 62.2 m3 for the *Living Room Lab* and 46 m3 for the *Audio Lab*. Taking into account the expected absorption of the rooms, as well as their volume, it is safe to assume that their *Schröder* frequency will be in the range of $250-350$ Hz. According to the loudspeaker magnitude responses presented in figure 5.20, exciting the rooms using the *B & K Type 4295* will result into impulse responses for the rooms, that fully describe their behavior in the diffuse field region, as well as some part of the low frequency modes.

The extraction of the room impulse responses and the subsequent calculation of the reverberation time using the reverse integration method, was carried out using both white noise and sinus sweep signals. After considering the results, it was deemed unnecessary to display the results for both signals, since they were equivalent in most ways. Therefore, for this part, only the IRs extracted using white noise will be presented, since the coherence can provide additional information about the damping of the rooms, in higher frequencies.

Finally, while the room IRs were extracted for ten measurement positions, displaying all of them here would not provide with much additional information. Therefore, for the sake of simplicity, microphone position 4 from figure 4.6, was chosen, for the *Living Room Lab*. This position corresponds to the height of a sitting person, on the corner diagonally opposite from the source. Similarly, microphone position 5, displayed in figure 4.7, was chosen for the *Audio Lab*.

5.2.1. Living Room Lab.

Since the *Living Room Lab* was measured prior and after the installation of furniture, the figures presented in this section will be grouped, in order to allow for a quick comparison between the two states of the room.

The frequency response function is displayed in figure 5.21. As shown in the top figure, no individual modes are distinguishable from as low as 250 Hz, while including the furniture has a very visible effect shown in the bottom part of the figure. With increased damping more modes are distinguishable, while lots of the anti-resonances disappear.

The phase response of the room, presented in figure 5.22 shows that the system is linear, while the introduction of the furniture and therefore, increase in damping lowers it's slope.

Similar conclusions can be drawn by examining figure 5.23, displaying the coherence function γ^2 of the room. The coherence is quite good in the lower frequencies, where there are less anti-resonances, while it worsens as the amount of anti-resonances increases. The increased damping significantly improves coherence, as displayed in the lower part of the figure.

The impulse responses presented in figure 5.24, are drawn using a decibel scale, where the reference is the maximum value of the IR. Examining these figures, reveals that the dynamic range form steady state conditions, until the signal falls at the noise floor, is approximately 40 dB. Therefore, the use of the T_{30} estimator is advisable for the calculation of the reverberation time. The effect of the furniture is quite prominent here, making the slope drastically more steep.

The resulting reverberation times, estimated using the T_{30}, for this measurement position, is shown in figure 5.25. The mean RT values, averaged across all the ten measurement positions with the corresponding 95% confidence intervals, are presented in figure 5.26. Without furniture the room displays high reverberation values, ranging from 0.7 at 160 Hz to 1.3 s at 250 Hz. Moreover, the reverberation time varies substantially across the frequency bands. The furniture significantly improves the *RT* values of the room, which now ranges between $0.3-0.4$ s, with very little variation across the whole spectrum. These reverberation times, more closely resemble a room of that size, while the fact that there is deviation across the spectrum, makes the sound field of the room more similar to that of a living room, rather than a typical "dry" listening room. The confidence intervals, across the all the measurement positions is approximately 0.2 s for the unfurnished room, while it gets significantly smaller, around 0.05 s, with the presence of furniture.

After the extraction of the impulse responses, the same methodology presented in section 2.2 can be applied, without the use of the band filter, in order to extract a reverberation time that corresponds to the entire frequency range. This value can be used along with equation (2.1), in order to estimate the value of the *Schröder* frequency. These results are presented in table 5.1. The *RT* represents the mean value, averaged across all measurement positions, along with the 95% confidence intervals. As shown by these values the initial assumption for the value of f_{Schr} was correct, only for the unfurnished lab. The increased damping included by the furniture, lowers both the *RT* and the f_{Schr} significantly, but not enough to make the frequency range of the *B & K Type 4295* inadequate for the excitation of the room at the diffuse field.

	RT [s]	$f_{Schr} [Hz]$
Unfurnished	1.03 ± 0.03	257
Furnished	0.36 ± 0.03	152

Table 5.1.: Schröeder frequency and single value of RT - Living Room Lab.

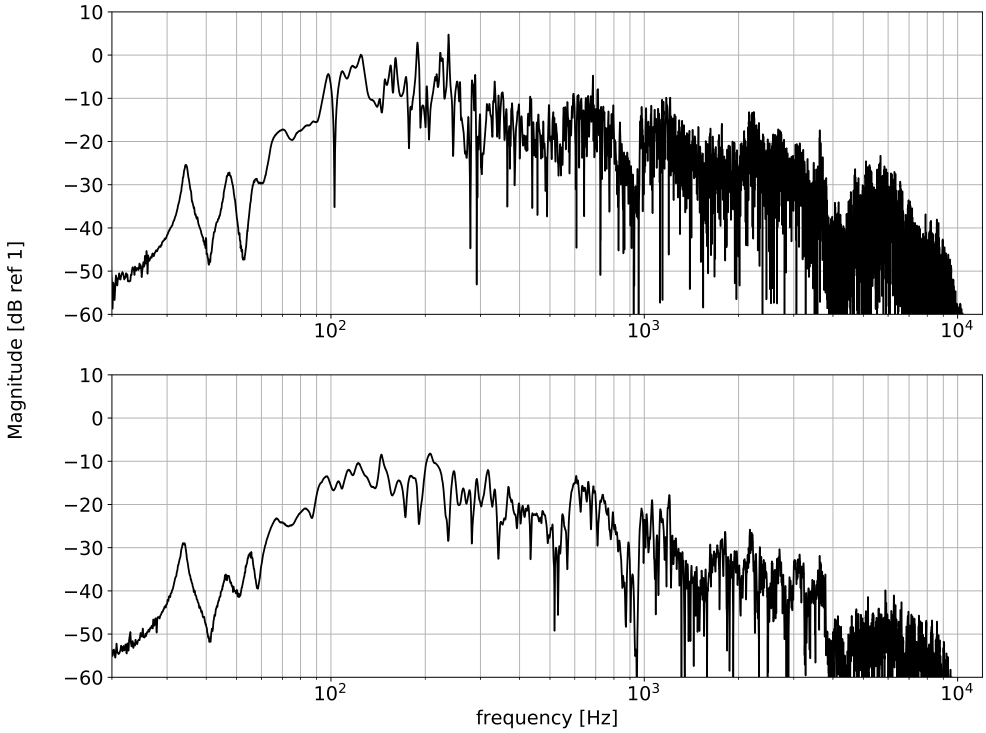

Figure 5.21.: Living room lab TF magnitude. Top without furniture, bottom with furniture.

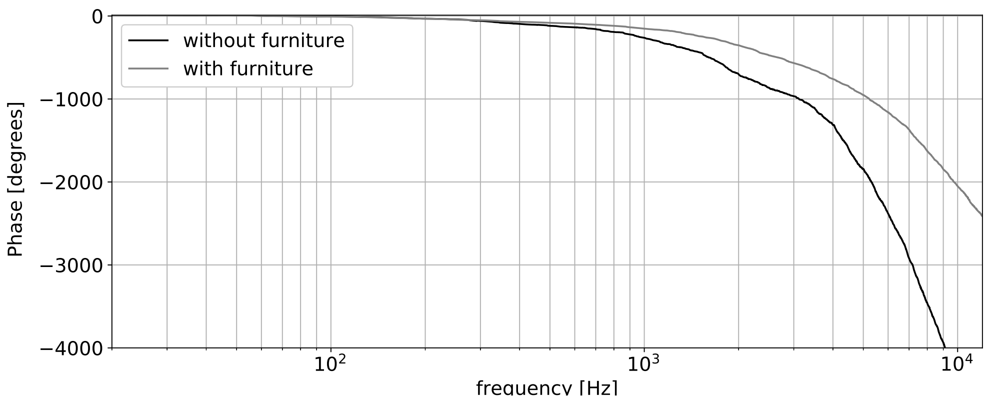

Figure 5.22.: Living room lab TF phase.

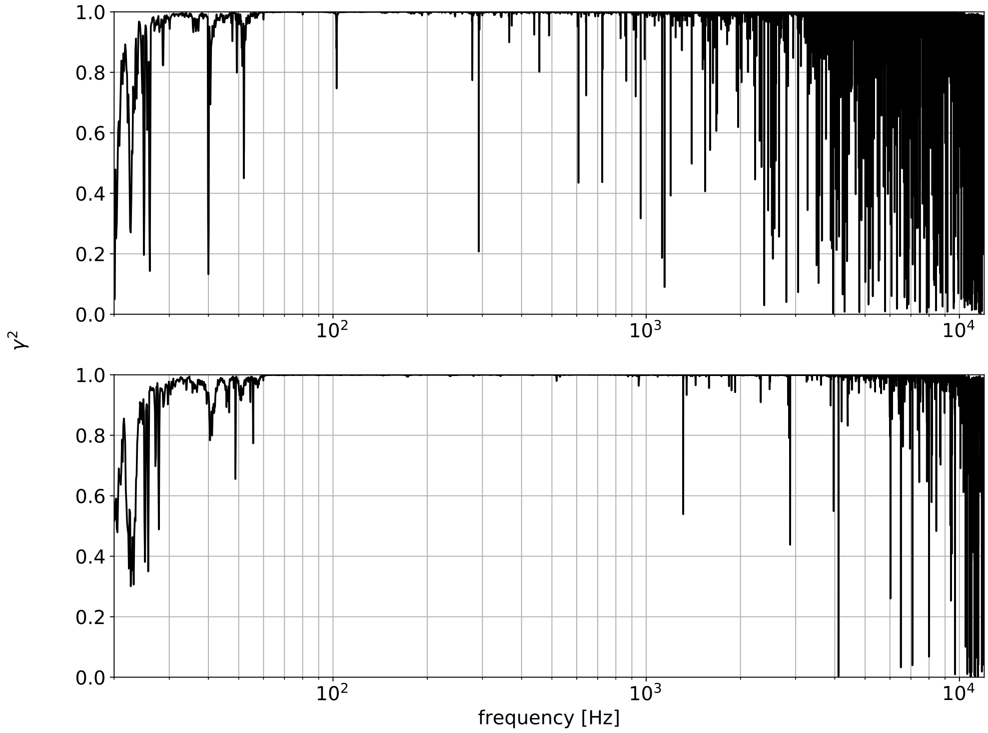

Figure 5.23.: Living room lab γ^2. Top without furniture, bottom with furniture.

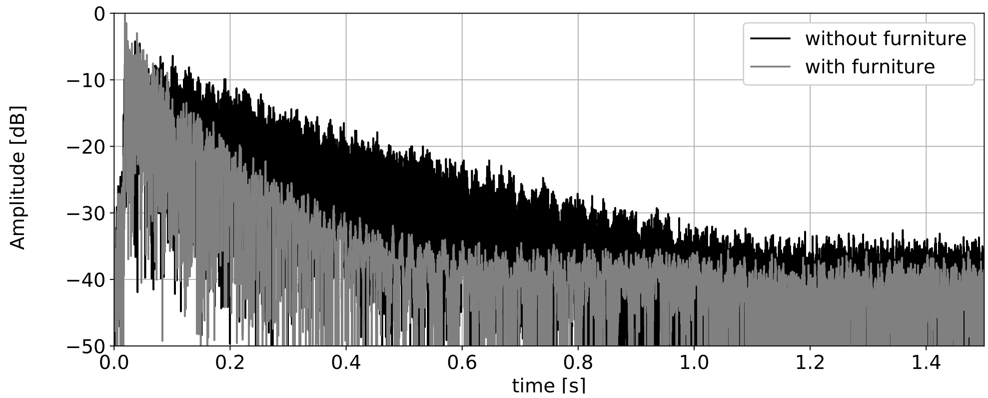

Figure 5.24.: Living room lab IR.

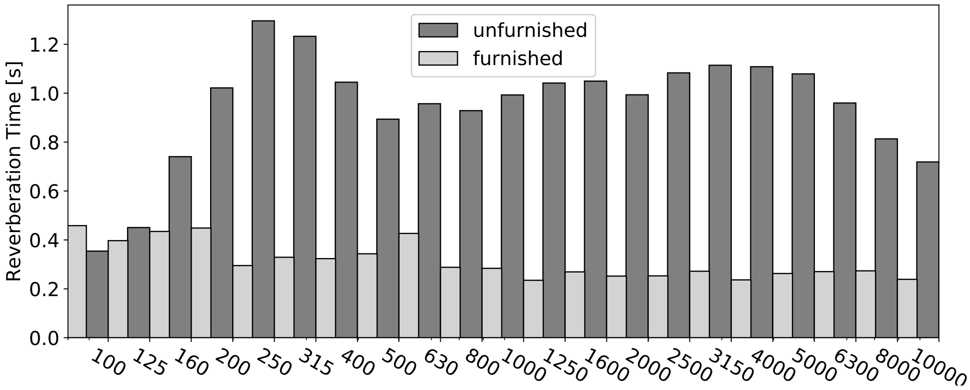

Figure 5.25.: Living room lab RT (T_{30}) and modal decays. With and without furniture.

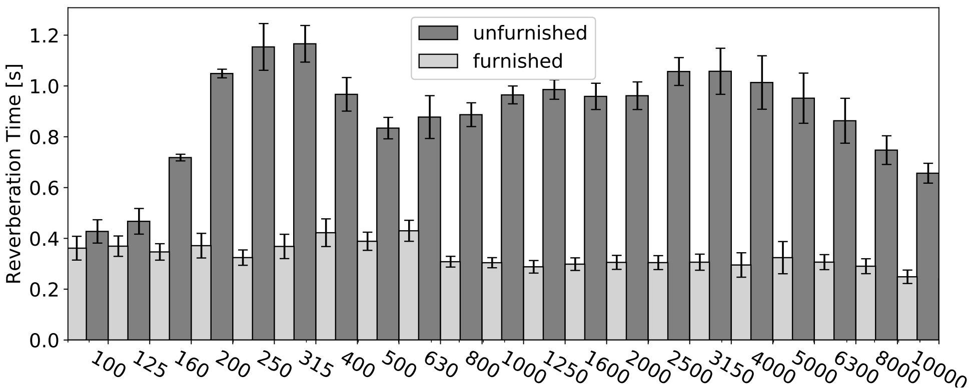

Figure 5.26.: Living room lab averaged RT (T_{30}). With and without furniture.

5.2.2. Audio Lab.

The *Audio Lab* shows very similar results with the *Living Room Lab*, since as described in section 2.1, prior to their redesign, the rooms were identical. The main difference between the two is that the *Audio Lab* has a thicker absorber on the ceiling and it's floor is covered with carpet. This introduces additional damping, which affects the entire spectrum, reducing the *RT* by approximately 0.2 s, compared with the unfurnished *Living Room Lab*, as shown in figures 5.31, 5.32. Apart from that, the additional damping greatly affects the 800 and 1250 Hz frequency bands. The frequency and phase response for the room are displayed in figures 5.27, 5.28, while the corresponding coherence function γ^2 and the impulse response are shown in figures 5.29 , 5.30. Similarly with the *Living Room Lab*, the single value *RT* is calculated at 0.87 ± 0.04 s, results into an f_{Schr} of 275 Hz, for the 46 m3 *Audio Lab*.

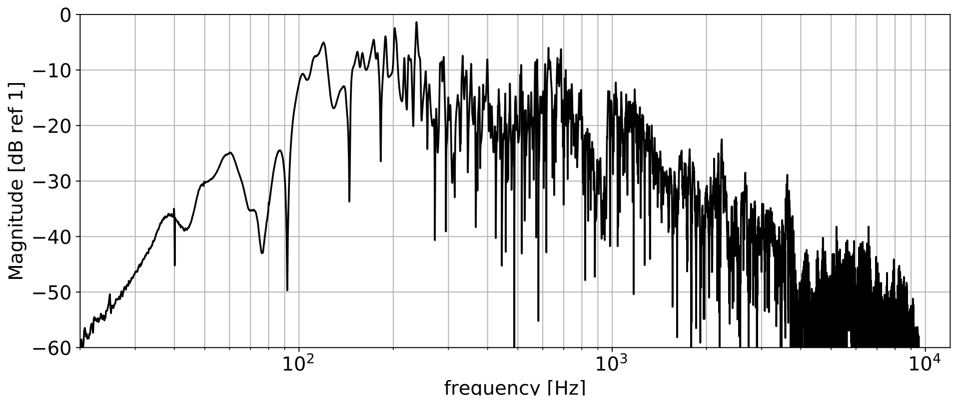

Figure 5.27.: Audio Lab TF magnitude.

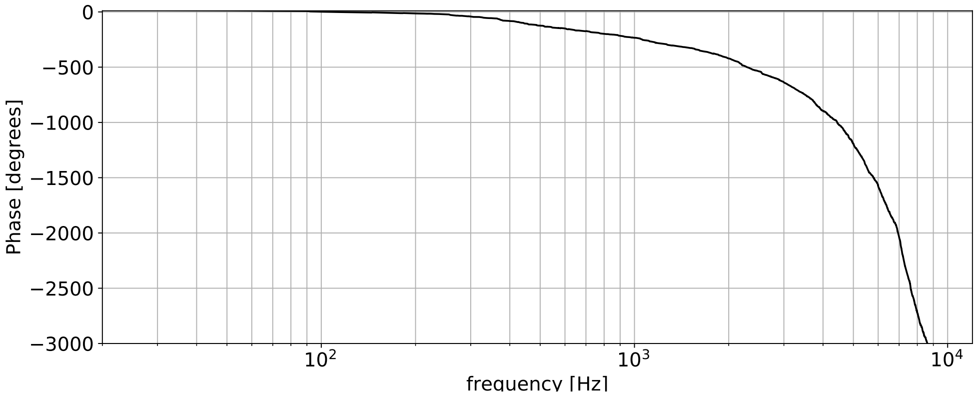

Figure 5.28.: Audio Lab TF phase.

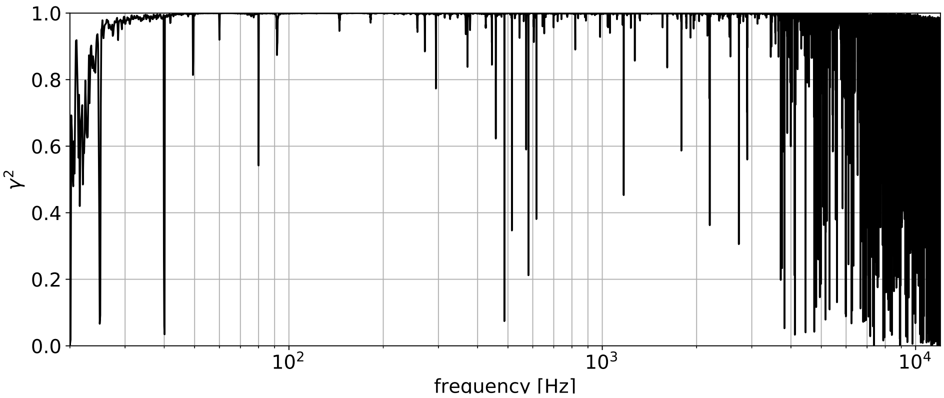

Figure 5.29.: Audio Lab γ^2.

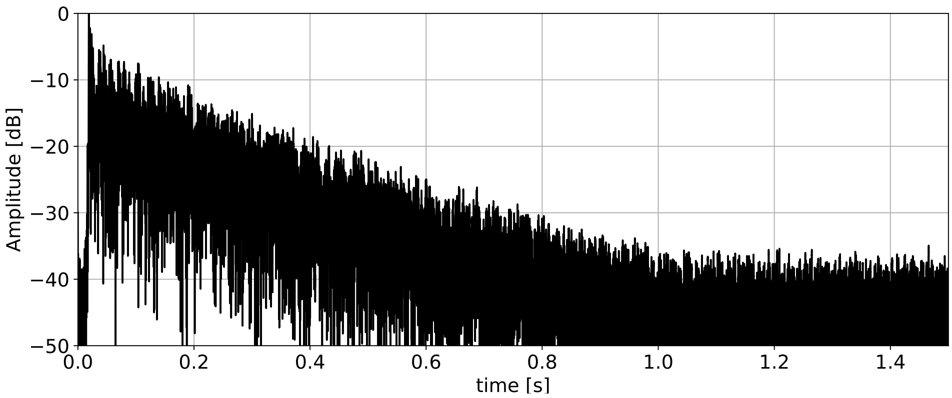

Figure 5.30.: Audio Lab IR.

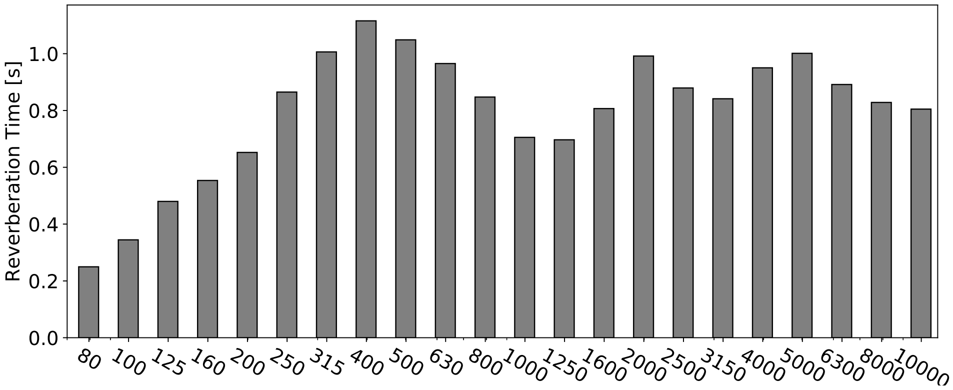

Figure 5.31.: Audio lab RT (T_{30}) and modal decays.

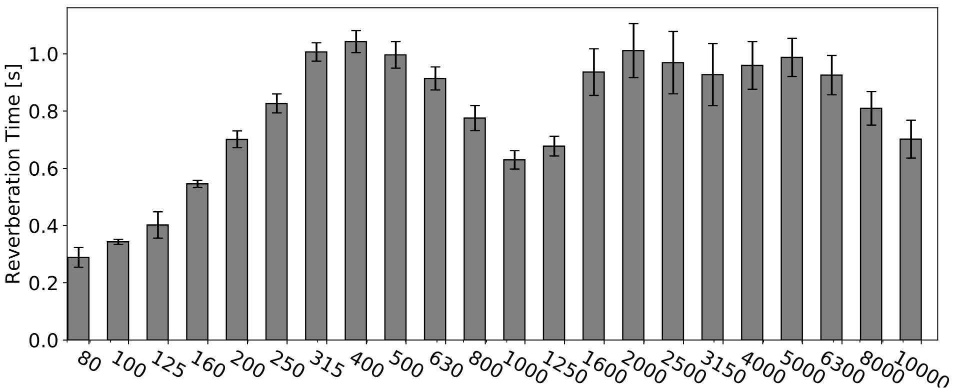

Figure 5.32.: Audio lab averaged RT (T_{30}).

5.3. Room Characteristics in the low frequency region.

This section will focus on the behavior of the rooms in the region below the *Schröder* frequency. For this reason the results of this section will correspond to the measurements conducted using the *Genelec 7050B* and the *Neuman.BERLIN KH 805* sub-woofers for the excitation of the *Living Room Lab*. In the *Audio Lab*, only the *Genelec 7050B* was employed in the room excitation. Similarly with the previous section, both white noise and sinusoidal sweep signals were used. This time however, the sinusoidal sweep proved more suitable for the task for a number of reasons. Firstly, since it provides smoother frequency response curves, the *Lorentzian* function used in the estimation of the modal decay time, is able to fit better to the result. Secondly, the smooth FRF results into clearer representation of the spectral decays in the waterfall plots. Finally, the sinus sweep can excite the room more efficiently, substantially increasing the signal to noise ratio.

Similarly to section 5.2, measurement position 4 was picked in order to display the results of the *Living Room Lab* and position 5 for the *Audio Lab*. However, all the evaluated modal decays are going to be presented in tables.

5.3.1. Living Room Lab.

Ceiling mounted KH 805

The magnitude response of the room, displayed in figure 5.33, was extracted using the *KH 805* sub-woofer, mounted on the ceiling, for room excitation. A first examination, easily reveals that the response of the room is governed, by a series of modes. The most prominent is the f_{100}=34.5 Hz, which is consistent across all the measurement positions. The rest of the modes are not easily distinguishable, either due to high modal overlapping, or due to high damping. There are however, a few more prominent modes, that vary with each measurement position, for example mode f_{110}=56.5 Hz for measurement position 4, as shown in figure 5.33. With the introduction of furniture, presented on the bottom figure 5.21, damping increases, especially above 60 Hz.

The transfer function shows linear behavior, as shown by the phase response presented in figure 5.34. The effect of the dumping can be seen in this graph, after 270 Hz, where the response shows significant non-linearities.

The impulse responses presented in figure 5.35, reveals an almost linear decay of the sound field. Comparing the response of the unfurnished room at the top, with it's furnished room counterpart at the bottom, however, reveals an odd behavior. The furnished room response seems to decay slower. While this may seem odd, after carefully re-examining figure 5.33, it's possible to discern that, while the introduction of the furniture increases the damping throughout the spectrum, the first three modes become

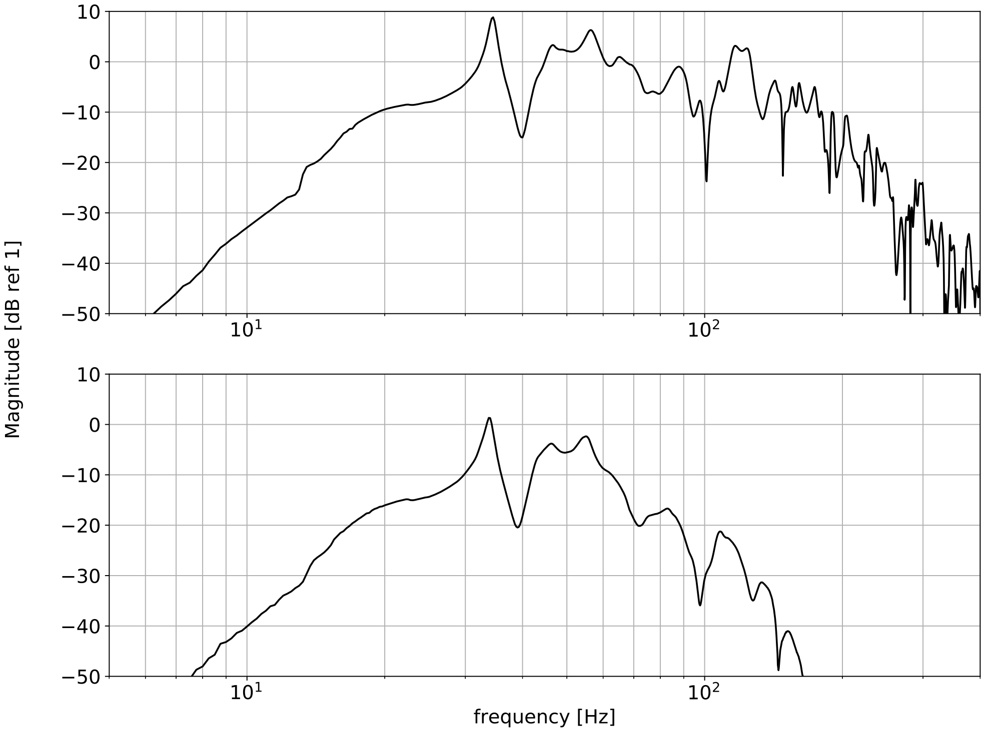

Figure 5.33.: Living Room Lab TF magnitude. KH 805. Top without furniture, bottom with furniture.

more prominent, in comparison with the rest of the response. Therefore, the overall decay of the IR might increase due to the energy added to the lower modes.

Tables 5.2 and 5.3 display the modes that were examined using the *Modal Reverberation Time* method presented in section 3.2. The tables present only the modes that were eligible for evaluation with the method. That means that a *Lorentzian* function fitted to the mode would provide with a meaningful result and that the mode's peak magnitude was at lest 3 dB higher than it's surroundings. The effect of the furniture can be seen more clearly here, where the $n_{xyz} = 100$ mode decays significantly slower in the furnished room, justifying further the behavior of the IR described above.

Figures 5.36 and 5.37 display the waterfall plots, generated using the methodology described in section 3.3. The window that was deemed appropriate for this analysis, was a rectangular window, apodized using a *Gauss* function with $\alpha = 3.5$, having a rise time T_r=0.1 s, a flat portion R=0.6 s and a decay time of T_d=0.2 s. Figure 5.36 clearly displays that the mode f_{100}=34.5 Hz is not attenuated and decays with a much different

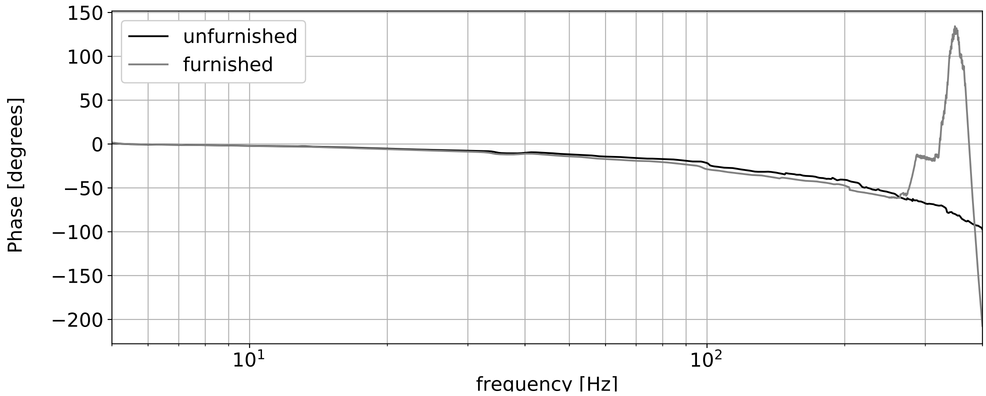

Figure 5.34.: Living Room Lab TF phase. KH 805.

rate than the rest of the FRF. The introduction of furniture makes the response decay much faster, throughout the spectrum, although it has little to no effect on the $n_{xyz} = 100$ mode.

The reverberation time, calculated using *Schröder*'s method, for this microphone position is displayed in figure 5.38. The evaluated modal reverberation times are plotted as points in the graphs as well. As shown in this figure, the introduction of furniture, has little effect to the reverberation time. The effect of the 34.5 Hz mode is visible on the 31.5 Hz 3^{rd}-octave band. Examining figures 5.36, 5.37 as well as their corresponding magnitude responses, it's possible to determine that the 34.5 Hz mode is the only factor that governs the 31.5 Hz 3^{rd}-octave band. Therefore, it's modal reverberation time should correspond better to the result of the *RT*. However, the resulting *RT* is almost double the modal reverberation time, in the unfurnished room, while the difference becomes smaller in the furnished room case.

Due to this inconsistency, an additional evaluation of the modal reverberation times was conducted, using the same methodology as before, but instead of relying in the *Lorentzian* fit, the half-widths were calculated by hand. The results of this investigation are presented in tables 5.4 and 5.5, for the unfurnished and furnished room, respectively. The modal reverberation times on these tables, correspond very well to the RT calculated with the reverse integration method. This indicates that the *Lorentzian* fit can be unreliable when used to determine the modal RT of modes that have a very narrow half-width.

Finally, the averaged RT across all the measurement positions, are shown in figure 5.39, along with the 95% confidence intervals. The CI are very small down to the 31.5 Hz frequency band, showing little variation of the RT between measurement positions. Below the 31.5 Hz band the CI gets very high, an effect that was to be expected, since the signal to noise ratio is a very small such low frequencies.

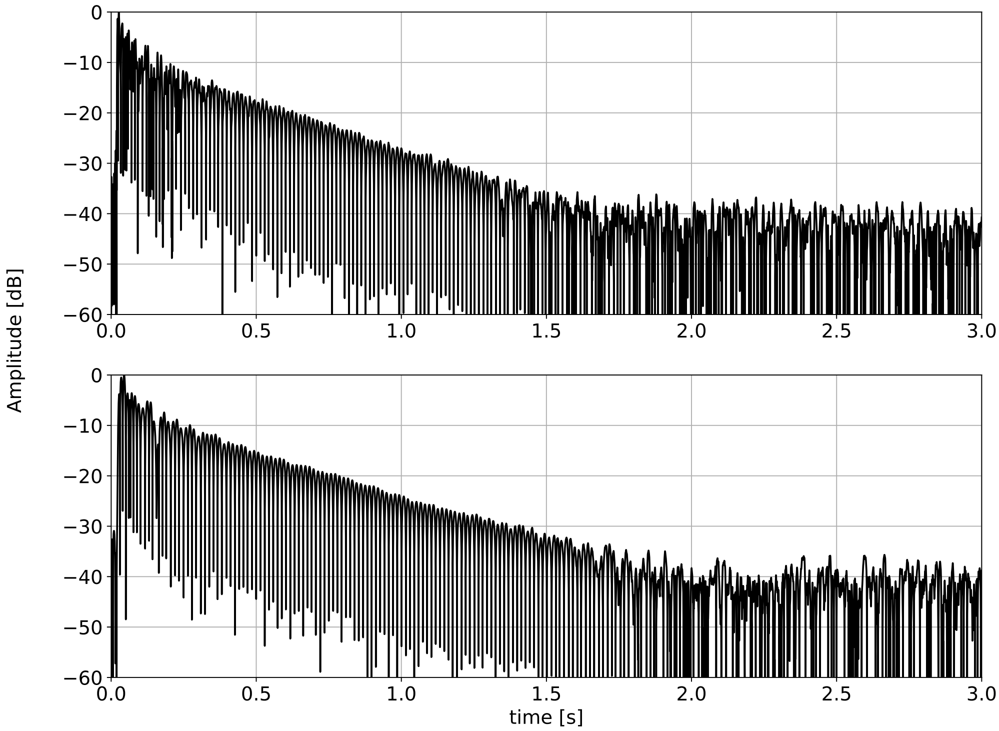

Figure 5.35.: Living Room Lab IR. KH 805. Top without furniture, bottom with furniture.

Mic Position	Mode	100	001	110
1	f [Hz]	34.5	-	56.5
	T_n [s]	0.78	-	0.65
2	f [Hz]	34.5	46.5	57.0
	T_n [s]	0.68	0.93	0.43
3	f [Hz]	34.5	-	-
	T_n [s]	0.88	-	-
4	f [Hz]	34.5	-	56.5
	T_n [s]	0.76	-	0.3
5	f [Hz]	34.5	47.0	57.25
	T_n [s]	0.61	0.47	0.48
6	f [Hz]	34.5	-	-
	T_n [s]	1.16	-	-
7	f [Hz]	34.5	46.75	56.5
	T_n [s]	0.67	0.59	0.61
8	f [Hz]	34.5	-	56.5
	T_n [s]	0.78	-	0.59
9	f [Hz]	34.5	46.75	-
	T_n [s]	0.78	0.42	-
10	f [Hz]	34.5	-	56.5
	T_n [s]	1.0	-	0.31

Table 5.2.: Modal Decays - Lorentzian fit, Living Room Lab, Neuman.BERLIN KH 805, Without furniture.

Mic Position	Mode	100	001	110
1	f [Hz]	33.75	-	-
	T_n [s]	0.96	-	-
2	f [Hz]	34.0	-	55.75
	T_n [s]	0.61	-	0.5
3	f [Hz]	34.0	-	56.0
	T_n [s]	0.88	-	0.32
4	f [Hz]	33.75	-	-
	T_n [s]	1.37	-	-
5	f [Hz]	34.0	-	-
	T_n [s]	0.55	-	-
6	f [Hz]	34.0	-	56.0
	T_n [s]	0.95	-	0.4
7	f [Hz]	33.75	-	55.0
	T_n [s]	0.68	-	0.69
8	f [Hz]	34.0	-	55.5
	T_n [s]	0.66	-	0.68
9	f [Hz]	34.0	-	-
	T_n [s]	0.66	-	-
10	f [Hz]	34.0	-	55.5
	T_n [s]	1.03	-	0.35

Table 5.3.: Modal Decays - Lorentzian fit, Living Room Lab, Neuman.BERLIN KH 805, with furniture.

Mic Position	Mode	100	001	110
1	f [Hz]	34.5	-	56.5
	T_n [s]	1.53	-	0.5
2	f [Hz]	34.5	46.75	57.0
	T_n [s]	1.52	0.67	0.67
3	f [Hz]	34.75	-	-
	T_n [s]	1.46	-	-
4	f [Hz]	34.5	-	56.5
	T_n [s]	1.59	-	0.45
5	f [Hz]	34.5	47.5	57.25
	T_n [s]	1.51	0.61	0.75
6	f [Hz]	34.5	-	-
	T_n [s]	1.46	-	-
7	f [Hz]	34.5	46.75	56.5
	T_n [s]	1.58	0.67	0.61
8	f [Hz]	34.5	-	56.5
	T_n [s]	1.58	-	0.52
9	f [Hz]	34.5	47.0	-
	T_n [s]	1.56	0.68	-
10	f [Hz]	34.5	-	56.5
	T_n [s]	1.54	-	0.65

Table 5.4.: Modal Decays - Manual estimation, Living Room Lab, Neuman.BERLIN KH 805, Without furniture.

Mic Position	Mode	100	001	110
1	f [Hz]	34.0	-	55.0
	T_n [s]	1.47	-	0.4
2	f [Hz]	34.0	-	55.5
	T_n [s]	1.37	-	0.59
3	f [Hz]	34.0	-	56.0
	T_n [s]	1.49	-	0.42
4	f [Hz]	34.0	-	55.25
	T_n [s]	1.37	-	0.36
5	f [Hz]	34.0	-	-
	T_n [s]	1.37	-	-
6	f [Hz]	34.0	-	56.0
	T_n [s]	1.47	-	0.37
7	f [Hz]	34.0	-	55.0
	T_n [s]	1.49	-	0.46
8	f [Hz]	34.0	-	55.25
	T_n [s]	1.59	-	0.47
9	f [Hz]	34.0	-	-
	T_n [s]	1.53	-	-
10	f [Hz]	34.0	-	55.5
	T_n [s]	1.53	-	0.63

Table 5.5.: Modal Decays - Manual estimation, Living Room Lab, Neuman.BERLIN KH 805, with furniture.

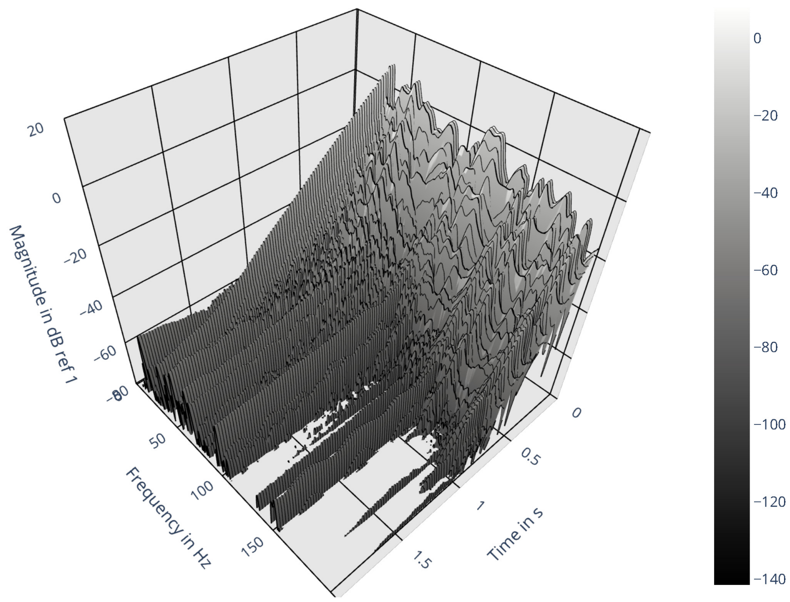

Figure 5.36.: Living Room Lab spectral decays - KH 805, without furniture, Gauss window, α=3.5, T_r =0.1, R=0.6, T_d =0.2.

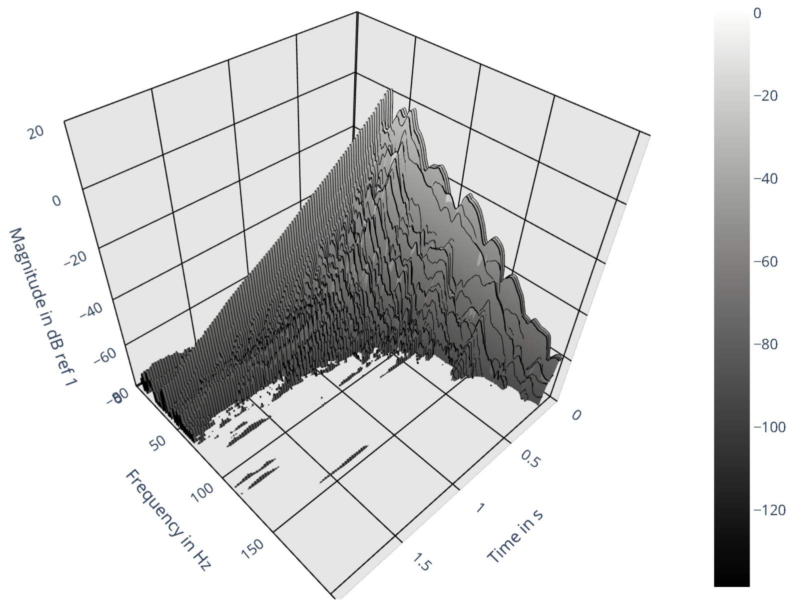

Figure 5.37.: Living Room Lab spectral decays - KH 805, with furniture, Gauss window, α=3.5, T_r =0.1, R=0.6, T_d =0.2.

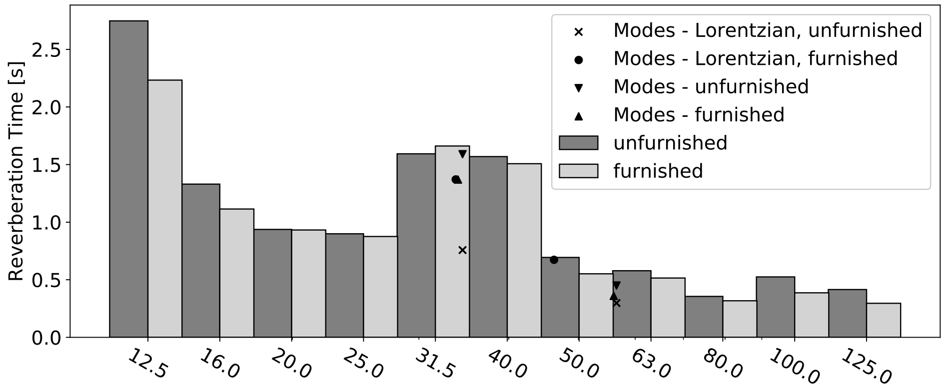

Figure 5.38.: Living Room lab RT (T_{30}) and modal decays. With and without furniture. KH 805.

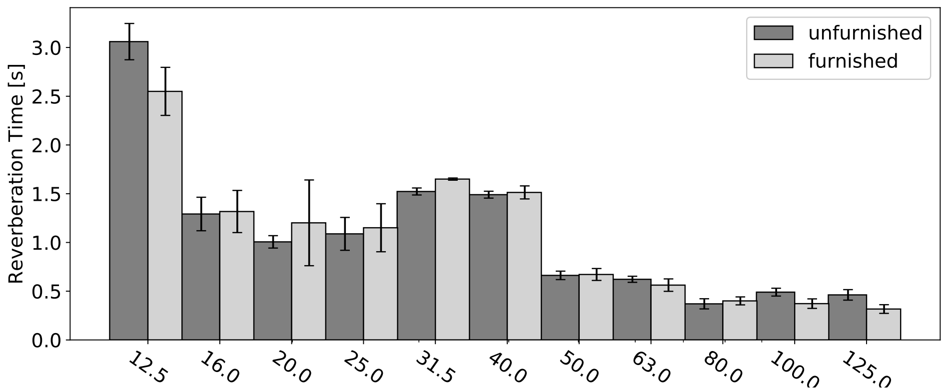

Figure 5.39.: Living Room lab averaged RT (T_{30}). With and without furniture. KH 805.

Genelec 7050 B.

Exciting the room using the *Genelec 7050B* proved to be slightly more efficient than the *KH 805*. This can be related to the fact that the *KH 805* was mounted on the ceiling of the room, very close to a very absorptive large surface. Despite that fact, most of the remarks made for the previous case, still apply here.

In more detail, the magnitude response shown in figure 5.40, is now showing two very prominent modes, the f_{100} =34.5 Hz and the f_{001} =47.0 Hz. The introduction of furniture has a more subtle effect than in the previous case, due to the fact that the room is more efficiently excited. Furniture does have an effect on the magnitude of these modes, but their half-width, which according to equation (3.7) is inversely proportional to the modal RT, stays unaffected.

This can be more clearly observed by examining the values of the modal reverberation times, presented at tables 5.6 and 5.7, for the unfurnished and the furnished room respectively. For the same reasons as before, a manual investigation of the modal half-widths was conducted, the results of which are presented in tables 5.8 and 5.9. Similarly, the resulting modal RT of the first mode, correspond very well with the value of the reverberation time in the 31.5 Hz frequency band.

The phase response in figure 5.41, doesn't reveal any strong non-linearities and the introduction of furniture has very little effect, as expected. The impulse response, presented in figure 5.42, shows an exponential decay form the steady state condition to the noise floor, whereas there is no visible effect on the curve's slope by the introduction of furniture.

The waterfall plots in figures 5.43 and 5.44, were generated using a rectangular window, apodized on both sides through the *Gauss* function, of $\alpha = 0.3$. The rise time was T_r=0.1 s, the flat portion was R=0.6 s and the decay time was T_d=0.2 s. The mode at f_{100}=34.5 Hz is once again, decaying very slowly and dominates the entire frequency band. In these figures however, the decay of the second mode at f_{010}=47 Hz is also visible, both in the unfurnished and the furnished room. Furniture in this case, has a much more subtle effect, while the additional damping actually makes the decay of the second mode more visible in figure 5.44.

The same remarks, as in the case were the room was excited with the *KH*805, can be made for the reverberation times presented in figures 5.45 and 5.46. In this case though, due to the better room excitation, the effect of the additional damping is much less visible between the furnished and the unfurnished room.

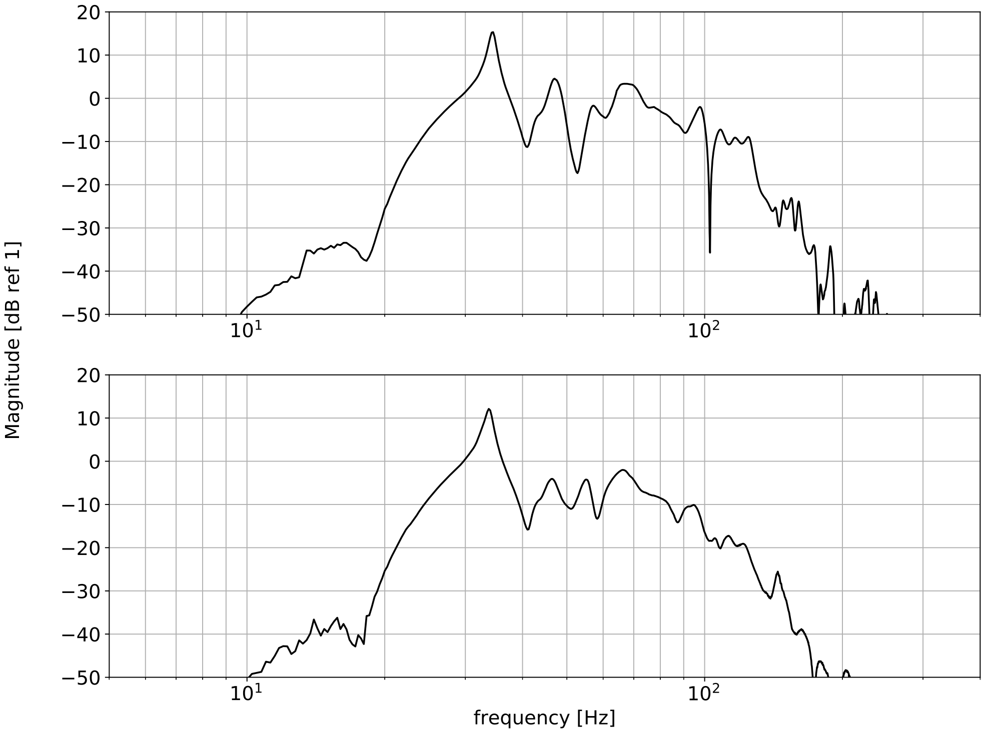

Figure 5.40.: Living Room Lab TF magnitude. Genelec 7050B. Top without furniture, bottom with furniture.

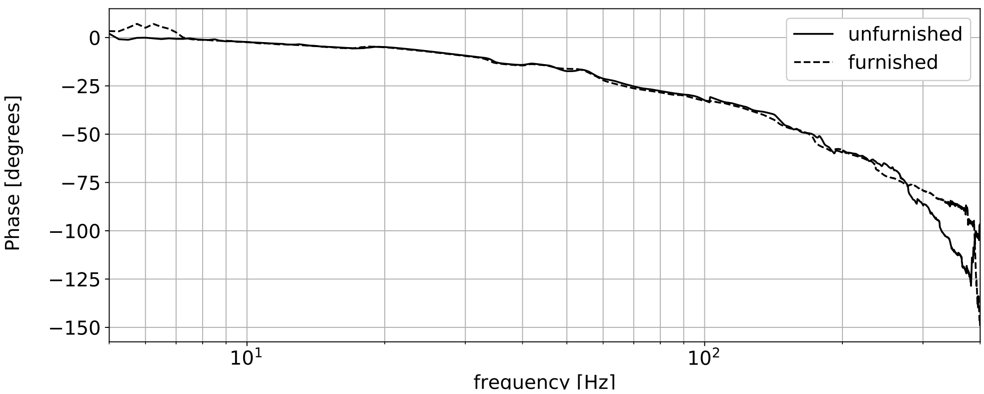

Figure 5.41.: Living Room Lab TF phase. Genelec 7050B.

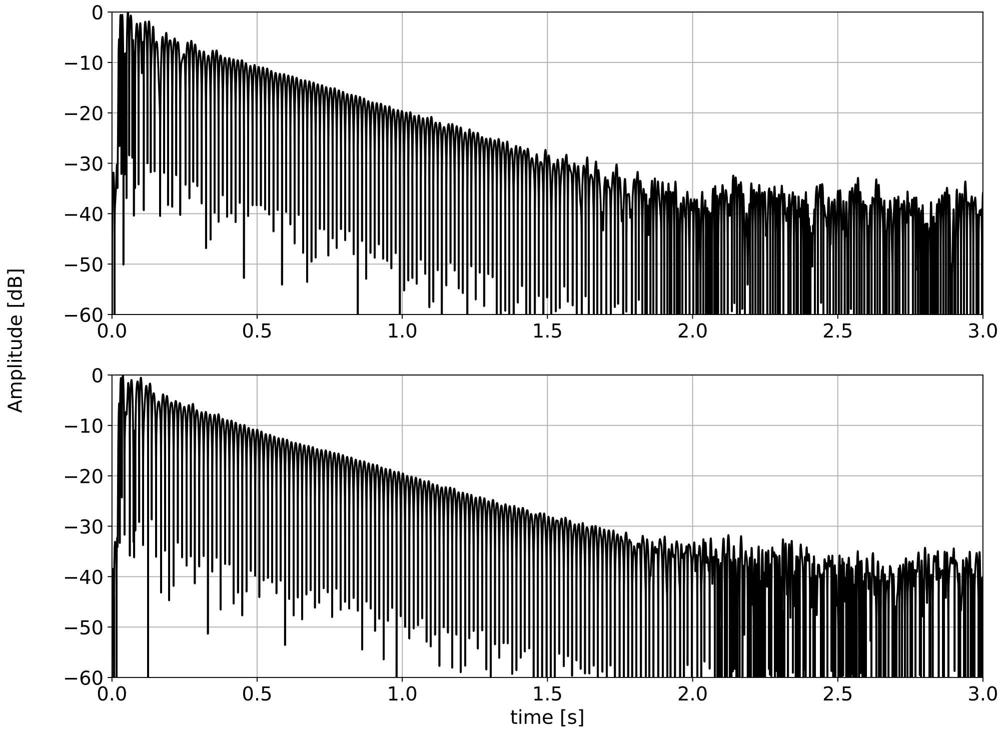

Figure 5.42.: Living Room Lab IR. Genelec 7050B. Top without furniture, bottom with furniture.

Mic Position	Mode	100	001	110
1	f [Hz]	34.5	46.75	56.5
	T_n [s]	0.49	0.68	0.74
2	f [Hz]	34.75	-	57.0
	T_n [s]	0.59	-	0.32
3	f [Hz]	34.5	-	56.5
	T_n [s]	0.53	-	0.59
4	f [Hz]	34.5	47.0	-
	T_n [s]	0.66	0.68	-
5	f [Hz]	34.5	-	-
	T_n [s]	0.72	-	-
6	f [Hz]	34.5	-	-
	T_n [s]	0.72	-	-
7	f [Hz]	34.5	-	-
	T_n [s]	0.46	-	-
8	f [Hz]	34.5	46.75	57.0
	T_n [s]	0.51	0.64	0.5
9	f [Hz]	34.5	46.75	-
	T_n [s]	0.37	0.36	-
10	f [Hz]	34.5	-	-
	T_n [s]	0.52	-	-

Table 5.6.: Modal Decays - Lorentzian fit, Living Room Lab, Genelec 7050B, Without furniture.

Mic Position	Mode	100	001	110
1	f [Hz]	33.75	-	-
	T_n [s]	0.75	-	-
2	f [Hz]	33.75	-	55.5
	T_n [s]	0.76	-	0.65
3	f [Hz]	34.0	-	55.25
	T_n [s]	0.9	-	0.62
4	f [Hz]	33.75	46.5	-
	T_n [s]	0.77	0.67	-
5	f [Hz]	33.75	-	55.5
	T_n [s]	0.82	-	0.41
6	f [Hz]	33.75	-	-
	T_n [s]	0.83	-	-
7	f [Hz]	33.75	-	-
	T_n [s]	0.78	-	-
8	f [Hz]	33.75	-	-
	T_n [s]	0.73	-	-
9	f [Hz]	33.75	-	-
	T_n [s]	0.73	-	-
10	f [Hz]	34.0	-	55.75
	T_n [s]	0.69	-	0.4

Table 5.7.: Modal Decays - Lorentzian fit, Living Room Lab, Genelec 7050B, With furniture.

Mic Position	Mode	100	001	110
1	f [Hz]	34.5	46.75	56.5
	T_n [s]	1.67	0.76	0.66
2	f [Hz]	34.5	-	57.0
	T_n [s]	1.68	-	0.41
3	f [Hz]	34.5	-	56.25
	T_n [s]	1.69	-	0.69
4	f [Hz]	34.5	47.0	-
	T_n [s]	1.67	0.78	-
5	f [Hz]	34.5	-	-
	T_n [s]	1.69	-	-
6	f [Hz]	34.5	- -	-
	T_n [s]	1.72	- -	-
7	f [Hz]	34.5	- -	-
	T_n [s]	1.68	- -	-
8	f [Hz]	34.5	47.0	57.0
	T_n [s]	1.69	0.7	0.68
9	f [Hz]	34.5	47.0	57.75
	T_n [s]	1.51	0.72	0.45
10	f [Hz]	34.5	-	-
	T_n [s]	1.57	-	-

Table 5.8.: Modal Decays - Manual estimation, Living Room Lab, Genelec 7050B, Without furniture.

Mic Position	Mode	100	001	110
1	f [Hz]	33.75	-	55.25
	T_n [s]	1.49	-	0.55
2	f [Hz]	33.75	-	55.75
	T_n [s]	1.52	-	0.39
3	f [Hz]	34.0	-	55.25
	T_n [s]	1.5	-	0.6
4	f [Hz]	33.75	46.5	55.25
	T_n [s]	1.51	0.63	0.69
5	f [Hz]	33.75	-	55.25
	T_n [s]	1.52	-	0.42
6	f [Hz]	33.75	-	-
	T_n [s]	1.52	-	-
7	f [Hz]	33.75	-	-
	T_n [s]	1.5	-	-
8	f [Hz]	33.75	-	55.75
	T_n [s]	1.53	-	0.64
9	f [Hz]	33.75	-	56.0
	T_n [s]	1.57	-	0.46
10	f [Hz]	34.0	-	55.75
	T_n [s]	1.5	-	0.42

Table 5.9.: Modal Decays - Manual estimation, Living Room Lab, Genelec 7050B, With furniture.

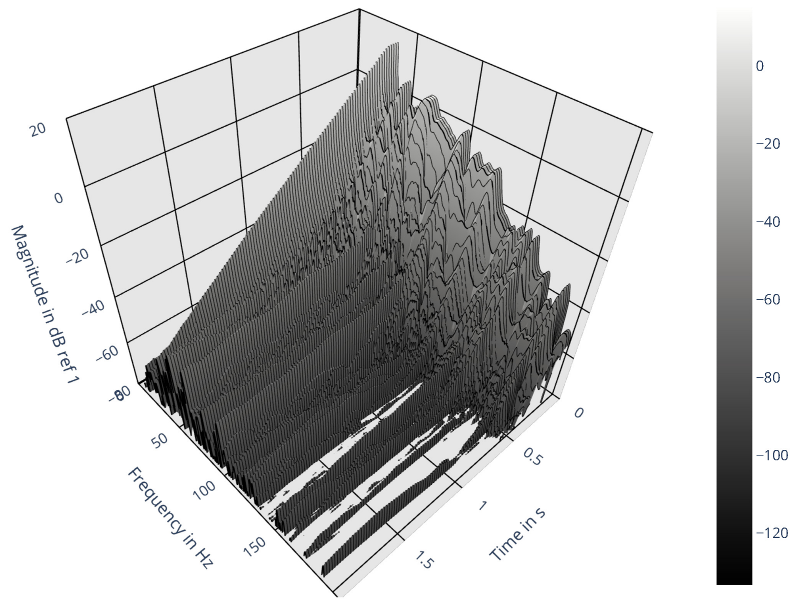

Figure 5.43.: Living Room Lab spectral decays - Genelec 7050B, without furniture, Gauss window, α=3.5, T_r =0.1, R=0.6, T_d =0.2.

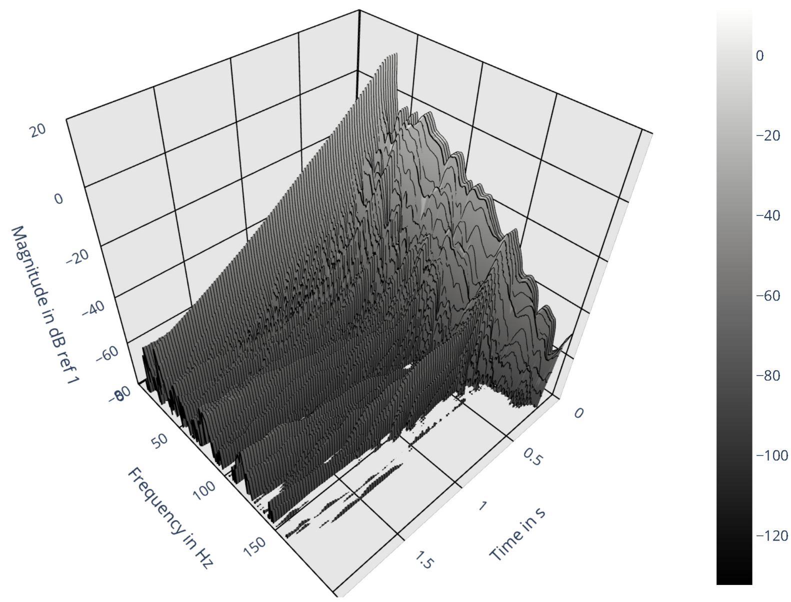

Figure 5.44.: Living Room Lab spectral decays - Genelec 7050B, with furniture, Gauss window, α=3.5, T_r =0.1, R=0.6, T_d =0.2.

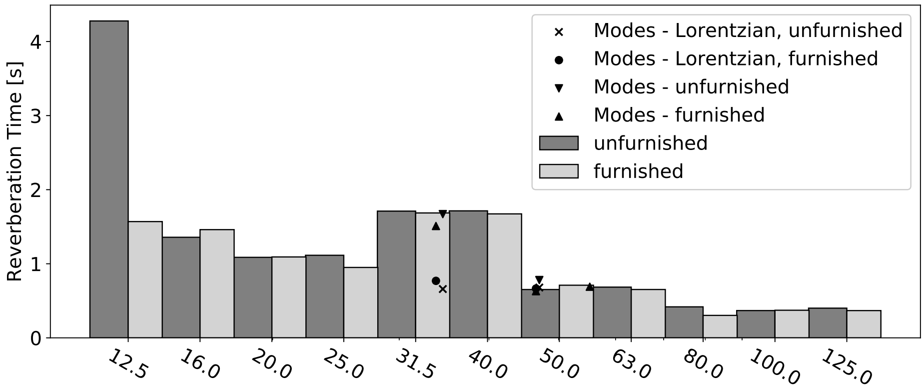

Figure 5.45.: Living Room lab RT (T_{30}) and modal decays. With and without furniture. Genelec 7050B.

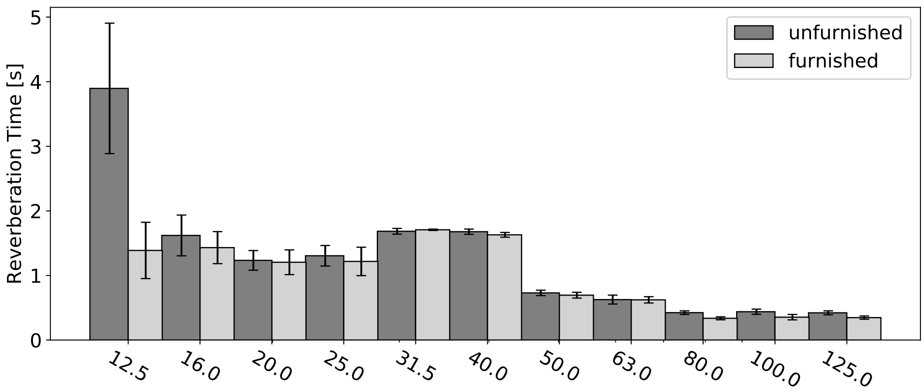

Figure 5.46.: Living Room lab averaged RT (T_{30}). With and without furniture. Genelec 7050B.

5.3.2. Audio Lab.

The *Audio Lab* has a similar response as the *Living Room Lab*, but with significantly more damping. This can be easily observed in the frequency response function of figure 5.47, where a similar result as in figure 5.40 is observed, but with the half-widths of the modes heavily flattened and their peaks significantly reduced. The phase response in figure 5.48 shows small non-linearities relating to the frequencies where anti-resonances occur. Comparing the IR in figure 5.49, with the corresponding IR of the *Living Room Lab*, it's possible to determine that the sound field of the *Audio Lab* decays much faster and that there is more than one slope, contributing to the behavior of it's decay. The effect of the additional damping can be observed by examining the waterfall plot in figure 5.50, were it's possible to see that the entire spectrum decays homogeneously. The fact that no single mode plays a significant role in determining the sound field, can further be motivated by looking at the RT graphs presented in figure 5.51 and comparing with figures 5.38,5.45 where the reverberation time does not increase suddenly in the 31.5 and 40.0 Hz third-octave band. Due to the excess damping, the calculation of the modal reverberation times was not possible.

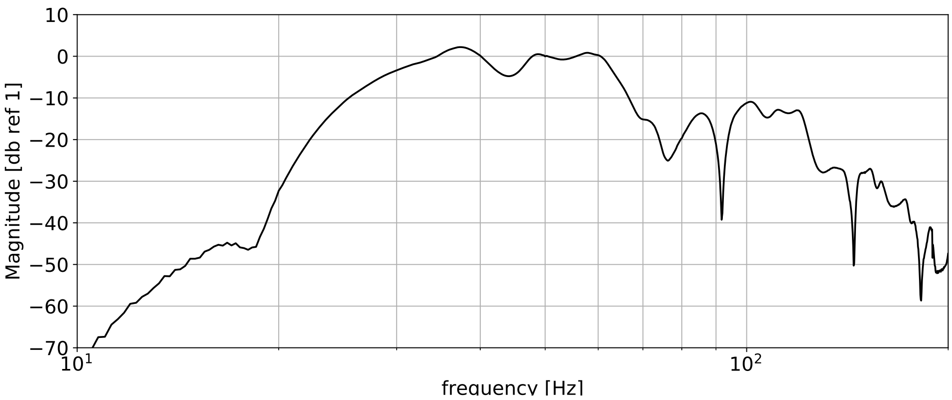

Figure 5.47.: Audio Lab TF magnitude. Genelec 7050B.

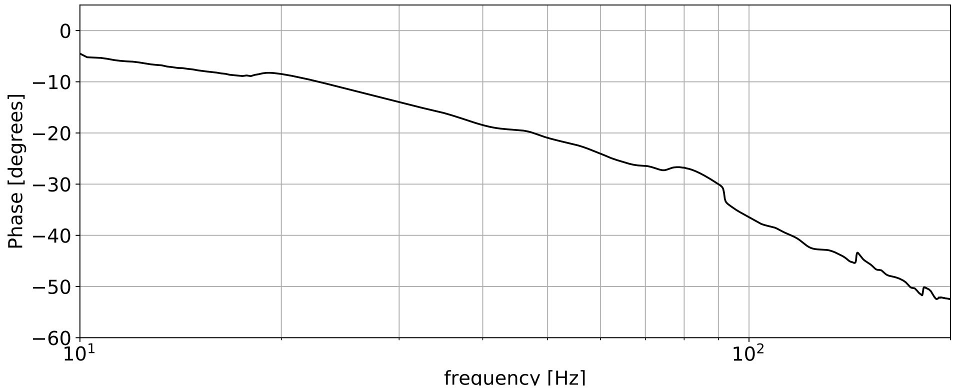

Figure 5.48.: Audio Lab TF phase. Genelec 7050B.

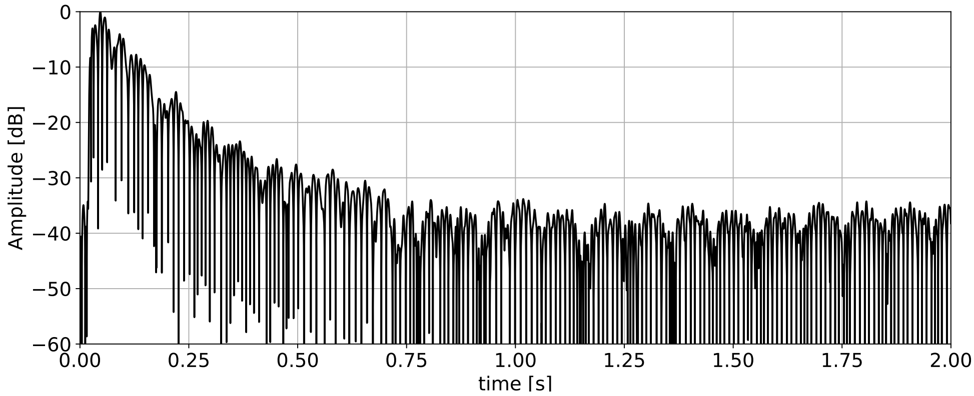

Figure 5.49.: Audio Lab IR. Genelec 7050B.

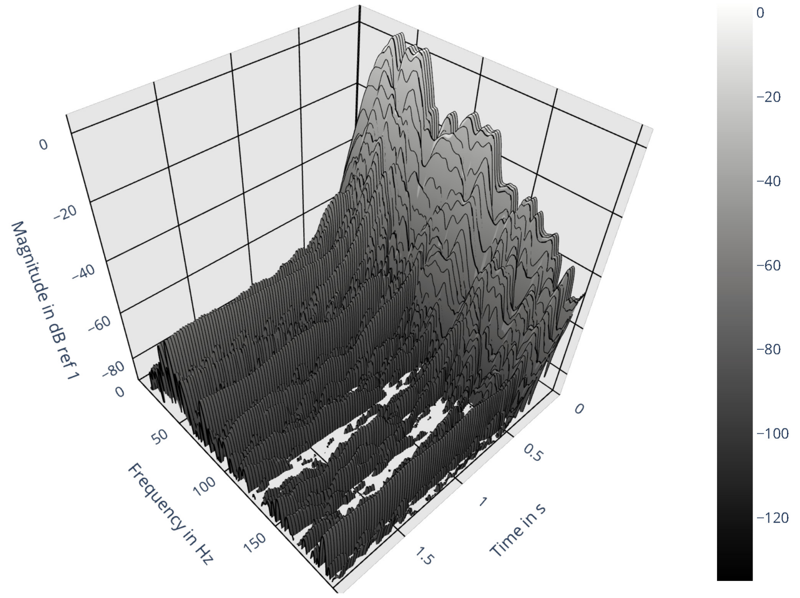

Figure 5.50.: Audio Lab spectral decays - Genelec 7050B, Gauss window, α=3.5, T_r =0.1, R=0.2, T_d =0.1.

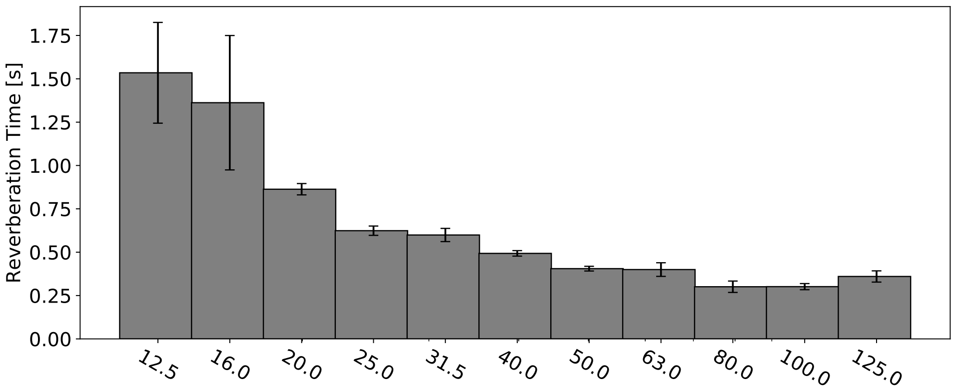

Figure 5.51.: Audio lab averaged RT (T_{30}). With and without furniture. Genelec 7050B.

5.4. Reduction Index.

The reduction index of the wall with the mounted window, that separates the two rooms, is presented in figure 5.52. The results presented in this plot were calculated using the *Genelec 7050B* sub-woofer, for the frequency range of 12.5−100 Hz and the *B&K Type 4295* for the 100 Hz to 10 kHz region. Due to the preexisting construction of the two rooms, as described in section 2.1.1, it is safe to assume that there is no flanking transmission and that all the sound is transmitted through either the intermediate wall, or the window that is mounted on it. This can be observed by comparing the plot with the reduction indices given by the manufacturer for both the wall and the window, presented in figures 2.3 and 2.7 respectively. The RI of figure 5.52 is very similar to both the graphs provided by the manufacturer, laying between the two, in terms of levels. More specifically the RI decreases with frequency, except for two deeps located at 125 Hz and 3150 Hz. The first deep at 3150 Hz can be attributed to the double wall resonance of the intermediate wall. The second deep at 125 Hz, corresponds to the frequency where the window resonates as a moving mass. Below the 31.5 Hz the RI increases, since the stiffness region of the construction is reached.

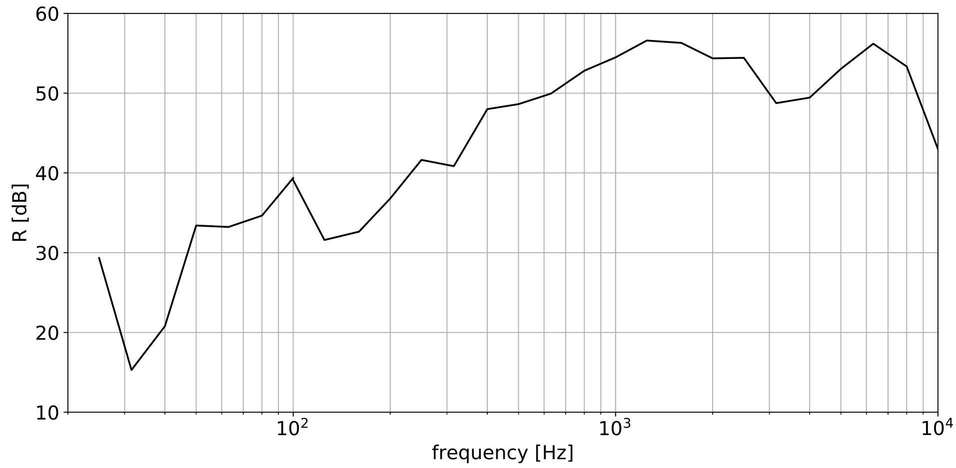

Figure 5.52.: Reduction index of the window-wall between the two rooms.

6. Conclusion.

The purpose of this project was the investigation of the acoustical properties of two listening test laboratories, related to the research projects that would take place in these facilities. In that regard, the construction of the two rooms was described and the methodology for evaluating the sound field of small rooms, in the diffuse field as well as the low frequency region was examined. The data for using this methodology were acquired though impulse response measurements, in the extraction of which, two different measurement techniques were employed. Furthermore, the properties of the electro-acoustic equipment used in the rooms, and in the measurement procedure were documented and finally, the sound reduction index for the main transmission path between the two rooms was calculated.

All the methods employed in this project, relied on the systems examined being linear and time invariant, allowing the extraction of an impulse response, that would theoretically reveal the entirety of it's characteristics. In that regard, impulse responses were extracted using both the H1 estimator and the deconvolution method. Both methods were deemed capable of producing accurate results, that fully described the systems, though having a few differences. More specifically the use of sinus sweep signals for excitation in the deconvolution method, provided better signal to noise ratio, shorter time of measurement and a smoother frequency response function than the H1 estimator. This made it very useful in the low frequency region, where the more smooth frequency response, improved the results of the methods applied, in the characterization of the modes. Furthermore, the short measurement duration, made the measurement of the transfer function of a large amount of loudspeakers, in varying angles, possible. On the other hand the H1 estimator, uses noise signals for excitation and the method of acquiring the IR does not require the use of filters. This can be crucial in applications that require the measured IR to include as little information, not relating to the system, as possible. Finally, the coherence function that can be calculated with this method, provides additional information on the room behavior, that was useful when examining the rooms' IRs, in the diffuse field.

The methodology used in order to characterize sound field of the rooms, included apart form the aforementioned IR extraction, the calculation of the reverberation time, the modal reverberation time as well as presentation of the spectral decays of the rooms, in waterfall plots. The reverse integration method was followed for the estimation of RT, which proved to be consistent for both excitation signals and most of the frequency region. The IR provided with information about the decay of the sound field that, was used in the estimation of the reverberation time, while the frequency response function gave important information about it's modal behavior. This was especially important in the low frequency region, where individual modes have a greater effect in the sound field of the room. Further insight, on the effect each mode had on the sound field, was given by examining the waterfall plots of room spectral decays. In this presentation, it was possible to determine which modes were decaying similarly with the frequency band they were in and which had a slower decay rate. The later would greatly affect the sound field and introduce inaccuracies in the calculation of the reverberation time. The calculation of the modal reverberation time, using the half-width of the mode, would provide with a more accurate decay measure of the sound field in very low frequencies. This method, has significant limitations, when the room in question is very damped, or the examined mode has a small half-width. In these cases the *Lorentzian* fit should be avoided. An indication of the later was revealed by examining the waterfall plots, in the region of the 31.5 Hz $3^{rd}-$octave band, where the decay of the sound field depended entirely on the first mode. However, the resulting modal RT was almost three times smaller. This ambiguity was taken into account and estimations of the modal half-widths were extracted by hand, verifying this limitation of the method.

Two rooms were examined using the aforementioned methodology, while the properties of the *Living Room Lab*, were investigated both prior and after furnishing the room. The *Living Room Lab* had quite high and varying reverberation time across the frequency spectrum when empty, with one very prominent mode at 34.5 Hz. The introduction of furniture significantly improved the RT for the frequency bands above 150 Hz, while below that, it had little to no effect. The modes of the room and their decays show spacial variation, while the introduction of the furniture has little to no effect on them. The resulting value for RT, it's small variation across the spectrum, as well as the few prominent low frequency modes, are typical characteristics of small household spaces and therefore, fulfill the design criteria for the *Living Room Lab*. The *Audio Lab* had significantly less fluctuation of the RT values across the whole spectrum and the decay of it's low frequency modes, showed great spacial variation. Examining it's waterfall plots, revealed very homogeneous decay of the sound field. These findings point to a more "dry" room that would have little effect on the sound reproduced in it, fulfilling it's design purpose.

Finally, the measured reduction index, for the intermediate wall, showed similar characteristics as the ones provided by the manufacturers. By taking into consideration this result, as well as the preexisting construction, it's safe to assume, that flanking transmission between the two rooms can be ignored.

In conclusion, the two labs have met their design criteria and the findings presented here, should provide researchers with a useful set of information about them, while the developed methodology can be easily used, in order to include any future changes of the rooms, in their documentation.

Bibliography

[1] Patrik Andersson. Sound and vibration measurements (svm) - lab 4: Signal analysis task, 2005 - 2018. Available at: http://www.ta.chalmers.se/content/protected/courses/svm/SVM_Lab4_instructions.pdf.

[2] John D. Bunton and Richard H. Small. Cumulative Spectra, Tone Bursts, and Apodization. *Journal of the Audio Engineering Society*, 30(6):386–395, jun 1982.

[3] INTERNATIONAL ELECTROTECHNICAL COMMISSION. IEC 61260:1995 - Electroacoustics - Octave-band and fractional-octave-band filters. 1995.

[4] *Genelec*. Genelec 7050b operating manual, 2005. Available at: https://www.genelec.com/sites/default/files/media/Studio%20monitors/7000%20Series%20Studio%20Monitors/7050B/om7050b.pdf.

[5] *Genelec*. Genelec 8030a operating manual, 2007. Available at: https://www.genelec.com/sites/default/files/media/Previous%20models/2-way%20loudspeakers/8030A/genelec_8030a_opman03-11.pdf.

[6] *Genelec*. Genelec 8020c operating manual, 2013. Available at: https://www.genelec.com/sites/default/files/media/Studio%20monitors/8000%20Series%20Studio%20Monitors/8020C/genelec_8020c_op.man_.pdf.

[7] National Instruments. Ni cDAQ™-9178 specifications, 2013. Available at: http://www.ni.com/pdf/manuals/374046a.pdf.

[8] National Instruments. Ni 9234 datasheet, 2015. Available at: http://www.ni.com/pdf/manuals/374238a_02.pdf.

[9] National Instruments. Ni 9260 datasheet, 2016. Available at: http://www.ni.com/pdf/manuals/376926a_02.pdf.

[10] INTERNATIONAL ELECTROTECHNICAL COMMISSION. IEC 60268-5:2003 - Sound system equipment – Part 5: Loudspeakers, 2003.

[11] Brüel & Kjær. Falcon™ range 1\2″ microphone preamplifier - type 2669 product data. Available at: https://www.bksv.com/media/doc/bp1422.pdf.

[12] Brüel & Kjær. 1\2" free-field microphone - type 4190 product data, 2009. Available at: https://www.bksv.com/-/media/literature/Product-Data/bp2211.ashx.

[13] Brüel & Kjær. *omnisource*^{TM} type 4295 product data, 2013. Available at: https://www.bksv.com/-/media/literature/Product-Data/bp1689.ashx.

[14] Brüel & Kjær. Power amplifier type 2735 product data, 2014. Available at: https://www.bksv.com/-/media/literature/Product-Data/bp2502.ashx.

[15] Brüel & Kjær. Sound calibrator type 4231 product data, 2014. Available at: https://www.bksv.com/-/media/literature/Product-Data/bp1311.ashx.

[16] Brüel & Kjær. Signal conditioner type 1708 product data, 2016. Available at: https://www.bksv.com/-/media/literature/Product-Data/bp2559.ashx.

[17] Heinrich Kuttruff. *Room Acoustics*. CRC Press, 6 edition, 2016.

[18] Swen Müller and Paulo Massarani. Transfer-Function Measurement with Sweeps. *Journal of the Audio Engineering Society*, 49(6):443–471, 2001.

[19] NEUMANN.BERLIN. Kh 805 operating manual, 2015. Available at: https://en-de.neumann.com/file-finder?product=KH%20805&category=monitors.

[20] NEUMANN.BERLIN. Kh 80 dsp instruction manual, 2017. Available at: https://en-de.neumann.com/file-finder?product=KH%2080%20DSP%20A%20G&category=monitors.

[21] Division of Applied Acoustics at Chalmers University of Technology. nidaqmxaio, 2018. https://github.com/AppliedAcousticsChalmers/nidaqmxAio.

[22] Andrea Prato, Federico Casassa, and Alessandro Schiavi. Reverberation time measurements in non-diffuse acoustic field by the modal reverberation time. *Applied Acoustics*, 110:160–169, 2016.

[23] M R Schroeder. New method of measuring reverberation time, 1965.

[24] EUROPEAN STANDARD. EN ISO 3382-2:Acoustics - Measurement of room acoustic parameters - Part 2: Reverberation time in ordinary rooms (ISO 3382-2:2008) Acoustique. *Euro code SS-EN-1191-2*, 2008.

[25] EUROPEAN STANDARD. EN ISO 10140-4:Acoustics - Laboratory measurement of sound insulation of building elements - Part 4: Measurement procedures and requirements (ISO 10140-4:2010), 2010.

Appendices

A. Equipment settings.

The various settings for the equipment used in measurements as well as the settings for the loudspeakers mounted on the ceiling of the *Living Room Lab* are presented in tables A.1 through A.5.

Parameter	Value
LS Sensitivity (dBu for 100 db SPL at 1 m)	0
ROLL-OFF -6 dB	off
ROLL-OFF -4 dB	off
ROLL-OFF -2 dB	off
PHASE -270^o	off
PHASE -90^o	off
PHASE -180^o	off
LFE BANDWIDTH	120 Hz
LFE +10 dB	off
Input	FRONT LEFT

Table A.1.: Loudspeaker settings: Genelec 7050B.

Parameter	Value
TREBLE TILT -2Db	OFF
BASS ROLL-OFF -6dB 85 Hz	OFF
BASS TILT -4 dB	OFF
BASS TILT -2 dB	OFF
BASS TILT -6 dB	OFF
Volume Knob	MAX

Table A.2.: Loudspeaker settings: Genelec 8030A and 8020B.

Parameter	Value
BASS MANAGEMENT	ACTIVE
LS Output Level (dB SPL at 1 m for 0 dBu)	100
LS Input Gain (dBu)	0
RIGHT CHANNEL INPUT MODE	RIGHT
SUBWOOFER PHASE (degrees)	0\0
INPUT GROUND LIFT	LIFTED
LOW CUT (GAIN dB)	0
PARAMETRIC EQUALIZER	OFF
Input	RIGHT \ LFE

Table A.3.: Loudspeaker settings: KH 805.

Parameter	Value
LOCAL CONTROL	ON
ACOUSTICAL CONTROL	ON
OUTPUT LEVEL (dB SPL at 1 m for 0 dBu)	100
INPUT GAIN	-15

Table A.4.: Loudspeaker settings: KH 80 DSP.

Parameter	Value
Power Amplifier Gain switch (dB)	20
Input	Input CH1
Output	Output CH1

Table A.5.: Amplifier settings: B&K Type 2735 2 x 35 Watt Measurement Power Amplifier.

B. Loudspeaker mounting and serial numbers.

A detailed schematic of the loudspeakers mounted on the ceiling of the *Living Room Lab* is displayed in figure B.1, along with the number that corresponds to each loudspeaker. Each loudspeaker is assigned in a ceiling quadrant, noted as **Q1**, **Q2**, **Q3** and **Q4** in figures B.1, B.2 and table B.1. All the loudspeakers in each quadrant are grouped into one 8 channel **D-Sub** cable, that is connected to the breakout box of the control room. The channel that corresponds to each loudspeaker can be found in table B.1. The output of the breakout box that corresponds to each quadrant is displayed in figure B.2, along with the outputs that are connected to four *D-Sub* cables reaching inside the lab. Finally, the length and name of each **D-Sub** connected to the breakout box are presented in table B.2.

The serial numbers for the 25 measured *Neuman.Berlin KH 80 DSP* are presented in table B.3 along with the calibration file that was used for each one of them.

The serial numbers for the 21 measured *Genelec 8020B* are presented in table B.4, along with their corresponding calibration files, the quadrant of the ceiling they are mounted on and the channel they are connected at the breakout box of the control room.

Ceiling Quardant	Q1	Q2	Q3	Q4
Channel	LS	LS	LS	LS
1	1	13	4	17
2	2	14	5	18
3	3	15	6	19
4	10	16	7	20
5	11	-	8	-
6	12	-	9	-
7	-	-	-	-
8	B1	B2	B3	B4

Table B.1.: Living Room Lab - Loudpeaker numbering and breakout box channels.

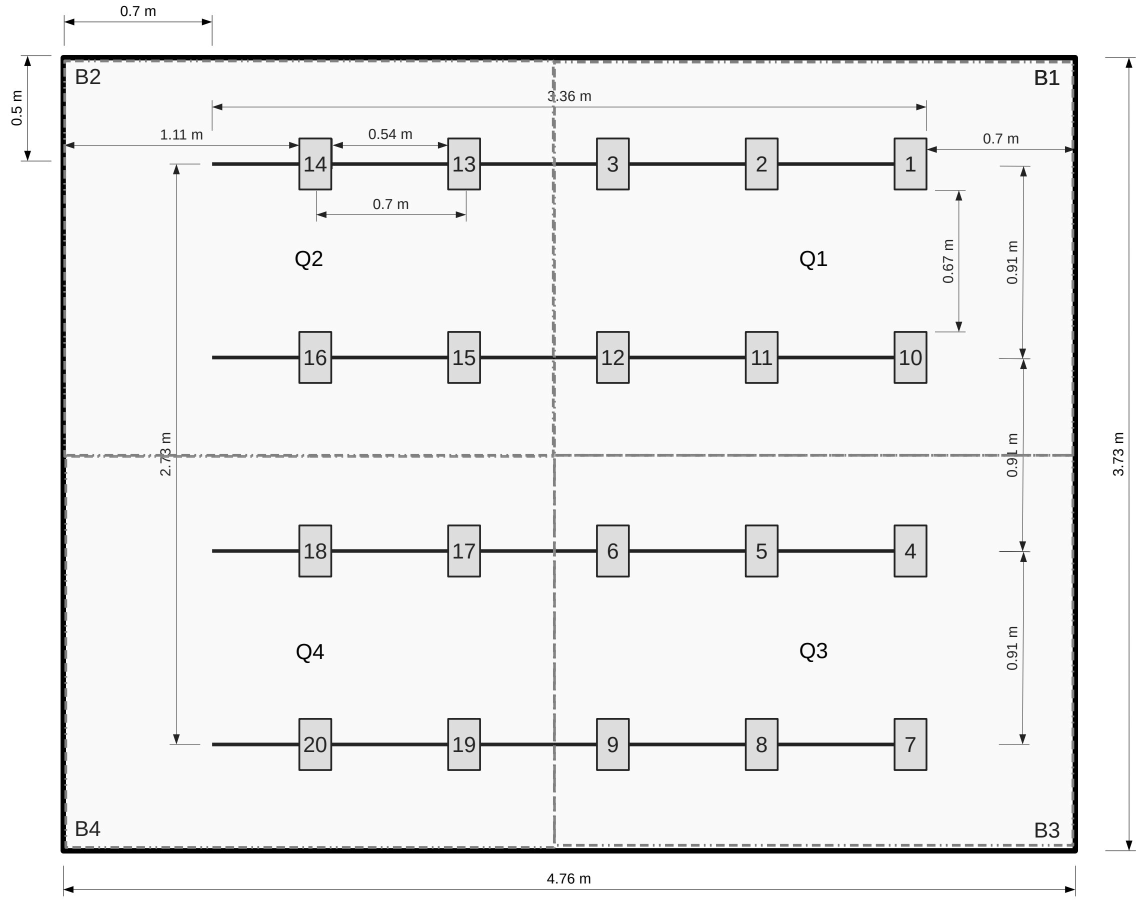

Figure B.1.: Loudspeaker grid mounted on the ceiling of the Living Room Lab.

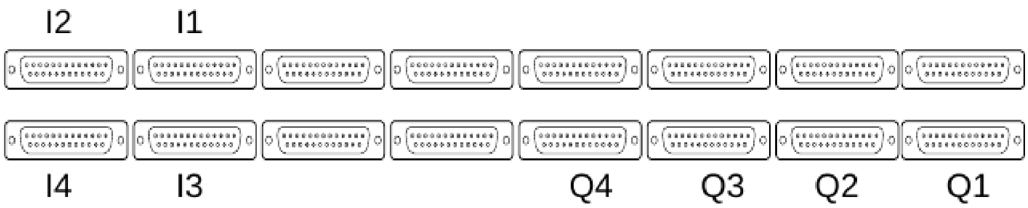

Figure B.2.: Living Room Lab - Control Room breakout box grouping

D-Sub Name	Cable Number	Cable Length [m]
Q1	3	7
Q2	7	13.2
Q3	10	5
Q4	4	7
I1	8	2
I2	1	7
I3	9	2
I4	4	7

Table B.2.: Living Room Lab - Cable lengths.

LS	S/N	Calibration File
1	3188328006	anechoic_DB1_Cal.[npy/mat]
2	3248339459	anechoic_DB1_Cal.[npy/mat]
3	3248339506	anechoic_DB1_Cal.[npy/mat]
4	3297189693	anechoic_DB1_Cal.[npy/mat]
5	3297189695	anechoic_DB1_Cal.[npy/mat]
6	3297191079	anechoic_DB1_Cal.[npy/mat]
7	3297191080	anechoic_DB1_Cal.[npy/mat]
8	3297192133	anechoic_DB1_Cal.[npy/mat]
9	3327195332	anechoic_DB1_Cal.[npy/mat]
10	3248339533	anechoic_DB2_Cal.[npy/mat]
11	3297189689	anechoic_DB2_Cal.[npy/mat]
12	3297189784	anechoic_DB2_Cal.[npy/mat]
13	3297189787	anechoic_DB2_Cal.[npy/mat]
14	3297191081	anechoic_DB2_Cal.[npy/mat]
15	3297191082	anechoic_DB2_Cal.[npy/mat]
16	3297191145	anechoic_DB2_Cal.[npy/mat]
17	3297191305	anechoic_DB2_Cal.[npy/mat]
18	3297191306	anechoic_DB2_Cal.[npy/mat]
19	3297192146	anechoic_DB2_Cal.[npy/mat]
20	3297192147	anechoic_DB2_Cal.[npy/mat]
21	3297193044	anechoic_DB2_Cal.[npy/mat]
22	3248339522	anechoic_DB3_Cal.[npy/mat]
23	3297189744	anechoic_DB3_Cal.[npy/mat]
24	3297192124	anechoic_DB3_Cal.[npy/mat]
25	3297191291	anechoic_DB6_Cal.[npy/mat]

Table B.3.: Neuman.BERLIN KH 80 DSP, serial numbers and corresponding calibration files.

LS	Mounted on	Channel	S/N	Calibration File
1	Q1	1	PM6024954Dec10	anechoic_DB5_Cal.[npy/mat]
2	Q1	2	PM6024950Dec10	anechoic_DB5_Cal.[npy/mat]
3	Q1	3	PM6024937Dec10	anechoic_DB5_Cal.[npy/mat]
4	Q3	1	PM6024963Dec10	anechoic_DB5_Cal.[npy/mat]
5	Q3	2	PM6051966Jul12	anechoic_DB4_Cal.[npy/mat]
6	Q3	3	PM6024951Dec10	anechoic_DB4_Cal.[npy/mat]
7	Q3	4	PM6024936Dec10	anechoic_DB5_Cal.[npy/mat]
8	Q3	5	PM6051963Jul12	anechoic_DB5_Cal.[npy/mat]
9	Q3	6	PM6051962Jul12	anechoic_DB4_Cal.[npy/mat]
10	Q1	4	PM6051967Jul12	anechoic_DB4_Cal.[npy/mat]
11	Q1	5	PM6051951Jul12	anechoic_DB4_Cal.[npy/mat]
12	Q1	6	PM6024958Dec10	anechoic_DB5_Cal.[npy/mat]
13	Q2	1	PM6024959Dec10	anechoic_DB6_Cal.[npy/mat]
14	Q2	2	PM6024947Dec10	anechoic_DB6_Cal.[npy/mat]
15	Q2	3	PM6024953Dec10	anechoic_DB6_Cal.[npy/mat]
16	Q2	4	PM6024955Dec10	anechoic_DB6_Cal.[npy/mat]
17	Q4	1	PM6051950Jul12	anechoic_DB6_Cal.[npy/mat]
18	Q4	2	PM6024952Dec10	anechoic_DB6_Cal.[npy/mat]
19	Q4	3	PM6024956Dec10	anechoic_DB6_Cal.[npy/mat]
20	Q4	4	PM6024962Dec10	anechoic_DB6_Cal.[npy/mat]
21	-	-	PM6024946Dec10	anechoic_DB4_Cal.[npy/mat]

Table B.4.: Neuman.BERLIN KH 80 DSP, serial numbers and corresponding calibration files.

C. Measurement files.

The data collected for this project, as well as all the analytical results of the applied methodology, are stored in the *Division of applied acoustics, Department of Civil and Environmental Engineering of Chalmers University of Technology*. All the files are saved in both *numpy.ndarray* format, with the *".npy"* extension, or as *Matlab* files with the *".mat"* extension. The directories and the filenames have been named in a way that relates to their content. More specifically:

- **rooma** - refers to the *Living Room Lab*.
- **roomb** - refers to the *Audio Lab*.
- **ls** - means that a linear or logarithmic sweep signal was used.
- **wn** - means that a white noise signal was used.
- **Gsub** - stands for *Genelec 7050B*.
- **Bsub** - stands for *Neuman.BERLIN KH 805*.
- **Omni** - stands for *B&K Type 4295*.
- **micx** - specifies the microphone position used in the measurement.
- **Cal** - signifies that the file is a calibration file.
- **RT** - stands for reverberation time.
- **IR** - stands for measurements related to impulse response extraction.
- **TF** - signifies a directory containing the calculated transfer function results, related to the data of it's parent directory.
- **RAC** - signifies a directory containing the calculated reverberation time results, related to the data of it's parent directory.
- **Hpb** - signifies a directory containing the calculated modal reverberation time results, calculated using the half power bandwidth, related to the data of it's parent directory.

- **Graphs** - signifies a directory containing ".html" graphs of the results in it's parent directory, that can be viewed using a web browser.

- **config_files** - signifies a directory containing ".txt" files with the parameters used by the measurement system, when acquiring the data present on it's parent directory.

Therefore, the file "rooma_wnBsub_mic3_180825-1339_TF_191028-2107.npy", will correspond to a transfer function calculation, conducted on 19-10-28 at 21:07 using the data file "rooma_wnBsub_mic3_180825-1339.npy". This data file refers to the *Living Room Lab*, excited using white noise and the *KH 805* sub-woofer, on microphone position 3 on 18-08-25 at 13:39.

Note that the microphone position, is specified using "mic3" right before the time stamp, for the measurement of the impulse response and the reduction index measurements. In the RI case though, the position of the two microphones is specified as "ax_bx" with "ax" referring to the receiving room and "bx" referring to the sending room.

The directivity measurement: "ls_KH80DSP_3297189784_10_180928-1626.npy" stands for the measurement of the *KH 80 DSP* loudspeaker, with a serial number of *3297189784*, measured using a sinus sweep signal on a 10 degrees angle, on 18-09-28 at 16:26. Note that this is a file with raw data, the transfer function data relating to it are found in the "TF" sub-directory and will be named:

"ls_KH80DSP_3297189784_10_180928-1626_TF_191113-2006.npy".

The "/LoudSpeakers/Directivity/LS_Database/" directory, "DBx" refers to the calibration file used in the measurement.

While all the calibration files reside in the directory "calibration_files", a copy of each has been put inside the directory with the raw data that has been acquired using it, for convenience.